INTRAMOLECULAR INTERACTIONS OF MARCKS AND ITS RELATIONSHIP TO TUMOR NECROSIS FACTOR-ALPHA AND RHEUMATOID ARTHRITIS

By

IMAN MOHAMMAD ASHRAF AL-NAGGAR

A DISSERTATION PRESENTED TO THE GRADUATE SCHOOL
OF THE UNIVERSITY OF FLORIDA IN PARTIAL FULFILLMENT
OF THE REQUIREMENTS FOR THE DEGREE OF
DOCTOR OF PHILOSOPHY

UNIVERSITY OF FLORIDA

2008

I dedicate this work to Allah (God Almighty) in partial fulfillment of His mandate to seek Knowledge; to my husband, mother, father, grandmother, grandfather and siblings, whose love and support kept me going; to the Bubb, Edison and Long Labs who provided a great scientific atmosphere for me to flourish; and finally, to all my children, born (Salma) and yet to come, whom I love greatly.

ACKNOWLEDGMENTS

I would like to begin by thanking God for giving me this great opportunity to learn and for putting in my path wonderful people who have helped me and shown me the way. I want to thank all those people, and will try my best to remember them all here.

I want to start with my loving husband, Mr. Ahmad M. Mahmoud. To put it simply, this would not have been possible without his love and support. Support is such a small word to describe everything Ahmad has done for me over the last 5 years. Ahmad spent hours walking around the ARB and the College of Medicine looking for information about a graduate program I could attend at UF. He would drop me off each morning and pick me up every evening, take me to eat when I was hungry, take me back to the lab at 2 and 3 and 4 am when I had crazy experiments running late. Ahmad didn't care whether or not I cooked, cleaned or did laundry because I had so much studying and lab work to do and would go grocery shopping because I hated to. He traveled with me to conferences and took care of our daughter and me. Ahmad always sincerely asked me whether there was anything he could do for me. He also came with me to lab parties where he didn't know anyone and felt out of place because it made me happy. He endured lots of stubbornness and hard headedness and still forgave me and made me feel loved. He was wonderful to my family when they came to visit because I needed them, regardless of how busy he was and he understood that every year I wanted to spend the holidays visiting my family rather than taking that road trip of his dreams. He always made me feel like the more important graduate student even when he was in an equally challenging program, and, when he was drowning in failing experiments, he still found a way to convince me not to give up and that mine would work someday. Ahmad forced me to socialize when I felt the least social, forcing me on a trip when I didn't want to because he knew I needed it. Support was all those dinners of pasta, Ragu and frozen meatballs he put together for us while I wrote this thing.

Support was everything nice, every kind word and gesture he did for me during my most trying years yet. All that said, I thank my husband Ahmad for his support. I would not have made it this far without him.

I would like to thank my parents, Dr. Ashraf Al-Naggar and Ms. Wafaa Badawy for pushing me towards graduate school. They have always known what's best for me and have always insisted that I do it, regardless of what I wanted. I have finally understood that they were right all along, and that they knew better. They realized my potential long before I did and I am very glad they did not allow me to waste it. They have gone to great measures to ensure that I had everything I needed to help me survive graduate school and not to have to worry about anything else along the way. They bought me a beautiful house and ensured my comfort. They visited me whenever they could. I am lucky to have them as parents: very hardworking, smart, selfless and dedicated, they set a wonderful example for my siblings and me. I really appreciate everything they have done for me and pray that I will always be the daughter they want me to be. I would like to thank my grandparents Dr. Wadie Badawy and Ms. Haneya Shokri for valuing education beyond any limits and pushing me and everyone they know to pursue higher levels of education. I also thank them for their unconditional love and endless prayers that have kept me on track.

I would like to thank Dr. Michael R. Bubb and Dr. Arthur S. Edison for agreeing to mentor me and doing a fantastic job at it! They are both great scientists and I am in awe of their critical thinking. I really could not hope for better teachers: kind, smart, knowledgeable, patient, supportive, understanding, loving and caring. I am inspired by their hard work and dedication to science and education. I am humbled by their modesty and humanity. I am honored by their

friendship. Not only am I a far better scientist than I thought I could become in 5 years, I am a better human being for having known them and worked with them. I thank them for everything!

I would like to thank my committee members for their guidance and great ideas: Dr. Sally Litherland, Dr. Eric Sobel and Dr. Shannon Holliday. I have been fortunate to have a diverse, knowledgeable committee that had answers to all my questions, solutions to my problems, and great advice and encouragement when I needed them most.

I would like to thank Dr. Minoru Satoh for all his help and problem solving in my ELISA experiments, and for always being there when I needed him. Dr. Satoh is a very smart and knowledgeable person from whom I was lucky to get help. His kindness and giving know no boundaries. Although he was not officially a member of my committee, he gave me the full support one can expect from a committee member. I thank him for all his help.

I would like to thank Dr. Joanna Long for being a great friend and inspiration. Dr. Long has shown me that it is possible to be both a strong, smart, successful scientist and a great mother of four! She is a genuinely wonderful person and I truly am in awe of her.

I would like to thank all the people in the Bubb, Edison and Long Labs that have helped me throughout my years in graduate school, as well as make my long hours in the lab enjoyable: Dr. Elena Yarmola, Dr. Hazel Tapp, Dr. Cherian Zachariah, Dr. Jiahong Shao, Vijay Antharam Aaron Dossey, Omjoy Ganesh, Ramadan Ajredini, Terry Green, Mini Samuel-Landtiser, Fatma Kaplan, Heather Cornell, Seth McNeil, and too many undergraduates to list. I especially thank Minh Q. Vo, Reuben Judd and Alejandro Sanchez for their help and friendship and wish them great luck in their future. I would like to thank Zoe Fisher, Firas Kobeissy and Nichole Giordani for great study groups and treasured friendships.

I would like to thank Mary Handlogten from Dr. Weiner's Lab for teaching me how to use the RT-PCR and being there when I had questions and being a great friend.

I would like to thank Alfred Chung for making all the challenging peptides I needed for my assays. I would like to thank Scott McMillen, Scott McClung and Stan Stevens for their help with mass spectrometry. I would like to thank everyone else who helped me in any way with my experiments; I hope they can forgive me for not mentioning them by name.

I would also like to thank all the staff that has assisted me greatly at UF (Department of Biochemistry and Molecular Biology and the Interdisciplinary Program in Biomedical Sciences) and at the Malcom Randall Veterans Affairs Medical Center: Joyce Conners, Susan Gardner, Valerie Cloud-Driver, Elise Feagle, Pat Jones, Bradley Moore, Denise Mesa, Terry Ricki, Shelley Jenkins, Shyra Bailey and many more.

I would like to thank my sister, Sarah Al-Naggar, who always made time for me in the midst of her busy Harvard Law School graduate education. She was always there for me when I needed her and she is the best friend I have ever had and I hope she always will be.

I would like to thank Dr. Wayne McCormack, Dr. Richard Condit, Dr. Susan Frost and Dr. Linda Bloom for all their help, guidance and advice.

I would like to thank my friends who have made my years in Gainesville less lonely by providing me with a family away from my family. The El-Mahdawi Family (Uncle Ahmed, Auntie Fouz, Lamia, Ahmed, Wafaa, Omar and Fouz), the Enani Family (Auntie Mona, Hanan, Mahmoud and Eman) and the Dietrich Family (Rick, Chris, Todd, Larrett, Ricky, William and Michael) have taken me and my husband and eventually my baby Salma in and made us feel loved and cared for.

Finally, I would like to thank the University of Florida and the College of Medicine for providing such a rich and truly interdisciplinary graduate program in which I am very lucky to have been a part.

TABLE OF CONTENTS

LIST OF TABLES

LIST OF FIGURES

LIST OF ABBREVIATIONS

Ab	Antibody
ANOVA	Analysis Of Variance
AP	Alkaline Phosphatase
AspN	Endoproteinase Asp-N
ATP	Adenosine 5'-Triphosphate
BSA	Bovine Serum Albumin
Ca^{2+}	Calcium
$CaCl_2$	Calcium Chloride
CaM	Calmodulin
CCL-2	Chemokine (C-C Motif) Ligand 2
Cdk5	Cyclin-Dependent Kinase-5
cDNA	Complimentary Deoxyribonucleic Acid
Ct	Threshold cycle
C-term.	MARCKS C-Terminus Protein
Da	Dalton
DEAE	Diethylaminoethyl
DFP	Diisopropylfluorophosphate
DMSO	Dimethyl Sulfoxide
DNA	Deoxyribonucleic Acid
DNase I	Deoxyribonuclease I
DTT	Dithiothreitol
ED	Effector Domain
EDC	1-Ethyl-3-(3-Dimethylaminopropyl) Carbodiimide Hydrochloride
EDTA	Ethylenediaminetetraacetic Acid

EGTA	Ethylene Glycol Tetraacetic Acid
ELISA	Enzyme-Linked Immunosorbent Assay
ERK	Externally Regulated Kinases
ESI	Electrospray Ionization
GluC	Endoproteinase Glu-C
HAP	Hydroxy Apatite
HCl	Hydrogen Chloride
HPLC	High Pressure/Performance Liquid Chromatography
IgG	Immunoglobulin G
IL-17	Interleukin-17
IL-1β	Interleukin-1 Beta
IPTG	Isopropyl β-D-1-Thiogalactopyranoside
IRB	Institutional Review Board
JRA	Juvenile Rheumatoid Arthritis
KCl	Potassium Chloride
K_d	Dissociation Constant
kDA	kiloDalton
Kl	Dissociation Constant of Labeled PSD
Ku	Dissociation Constant of Unlabeled PSD
LC	Liquid Chromatography
LPA	Lysophosphatidic Acid
LPS	Lipopolysaccharide
mAb	Monoclonal Antibody
MALDI	Matrix-Assisted Laser Desorption/Ionization
MAP	Mitogen-Activated Protein Kinase

MARCKS	Myristoylated Alanine Rich C Kinase Substrate
MCP-1	Monocyte Chemotactic Protein-1
MCTD	Multiple Connective Tissue Disorder
MES	2-(*N*-morpholino) Ethanesulfonic Acid
$MgCl_2$	Magnesium Chloride
MH2	MARCKS Homology 2 Domain
MIANS	2-(4-Maleimidoanilino) Naphthalene-6-Sulfonic Acid
MRI	Magnetic Resonance Imaging
mRNA	Messenger Ribonucleic Acid
MS	Mass Spectrometry
MTX	Methotrexate
MW	Molecular Weight
NaN_3	Sodium Azide
NFκB	Nuclear Factor Kappa B
N-term.	MARCKS N-Terminus Protein
OD	Optical Density
PAGE	Polyacrylamide Gel Electrophoresis
PBS	Phosphate Buffered Saline
PCR	Polymerase Chain Reaction
pI	Isoelectric Point
PIP_2	Phosphotidylinositol 4,5-Bisphosphate
PMA	Phorbol 12-Myristate 13-Acetate
PMSF	Phenylmethanesulphonylfluoride or Phenylmethylsulphonyl Fluoride
Pred	Prednisone
PRK1	PKC-Related Kinase 1

PSD	Phosphorylation Site Domain
R	Correlation
RA	Rheumatoid Arthritis
RASF	Rheumatoid Arthritis Synovial Fibroblasts
Rh-PSD	Tetramethylrhodamine-5-Maleimide-Labeled PSD
RIPA	Radio-Immunoprecipitation Assay
RNA	Ribonucleic Acid
RNase	Ribonuclease
RT	Room Temperature
RT-PCR	Reverse Transcriptase-Polymerase Chain Reaction
Sav-HRP	Streptavidin-Horseradish Peroxidase
SDS	Sodium Dodecyl Sulphate
SDS-PAGE	Sodium Dodecyl Sulphate-Polyacrylamide Gel Electrophoresis
SLE	Systemic Lupus Erythematosus
SOC	Super Optimal Broth, C=catabolite repression
TBS	Tris-Buffered Saline
TNF-α	Tumor Necrosis Factor-Alpha
TNFR1/2	Tumor Necrsosis Factor Receptor 1 or 2
TPKII	Tau Protein Kinase II
Tris	Tris Hydroxymethylaminoethane
Und	Undetermined
UV	Ultraviolet

Abstract of Dissertation Presented to the Graduate School
of the University of Florida in Partial Fulfillment of the
Requirements for the Degree of Doctor of Philosophy

INTRAMOLECULAR INTERACTIONS OF MARCKS AND ITS RELATIONSHIP TO TUMOR NECROSIS FACTOR-ALPHA AND RHEUMATOID ARTHRITIS

By

Iman Mohammad Ashraf Al-Naggar

May 2008

Chair: Michael R. Bubb
Cochair: Arthur S. Edison
Major: Medical Sciences--Biochemistry and Molecular Biology

The myristoylated alanine-rich C kinase substrate, MARCKS, is a natively unfolded protein that plays important roles in multiple cellular processes, e.g., regulation of brain development, regulation of the actin cytoskeleton, control of lipid second messengers (e.g., phosphatidylinositol bisphosphate, PIP_2), cellular migration and adhesion, endo-, exo- and phago-cytosis, neurosecretion, maintenance of dendritic spine morphology, regulation of growth cone adhesion and pathfinding, regulation of airway mucin secretion, neurite initiation and myoblast migration.

MARCKS contains a central effector domain called the Phosphorylation Site Domain (PSD), which is the site of interaction with its binding partners such as F-actin and Ca^{2+}-calmodulin, as well as its site of phosphorylation by protein kinase C (PKC). In our experiments using a non-myristoylated recombinant MARCKS protein, we found that the protein repeatedly failed to bind to and bundle F-actin filaments and binds Ca^{2+}-calmodulin with lower affinity than reported in the literature. We have shown that intramolecular interactions occurring between the basic PSD of MARCKS and its acidic termini are masking the PSD, thus making it unavailable to interact with its binding partners. Charge neutralization assays suggest that these interactions

may be ionic in nature, which is further supported by the unique charge distribution of the protein. We hypothesize that post-translational modifications known to occur at the termini flanking the PSD may disrupt these intramolecular interactions, activating the protein *in vivo*. A series of fluorescence anisotropy and native PAGE experiments using constructs of MARCKS missing either end of the protein have shown that such intramolecular interactions may occur with either end of the molecule. Mass spectrometric analysis has narrowed these possible sites of interaction on the protein.

In addition, we wished to elucidate the utility of MARCKS as a marker for diagnosis and prognosis in rheumatoid arthritis (RA). The striking upregulation in MARCKS expression previously reported following TNF-α stimulation of immune cells and the important role this cytokine plays in RA, where the most successful therapy today is TNF-α blockade, prompted us to wonder whether MARCKS has a causal role in this disease.

Finally, we wanted to look at the role MARCKS plays in the TNF-α signal transduction pathway. Microarray evidence suggests that MARCKS may play an essential role in TNF-α induced apoptosis.

CHAPTER 1
INTRODUCTION

MARCKS

The myristoylated, alanine-rich C kinase substrate, MARCKS, was first characterized in rat cerebral cortex synaptosomes and in quiescent 3T3 cells as a major substrate for Protein Kinase C, PKC [1, 2]. In humans, it is composed of 332 amino acids (MW 31.6 kDa) and in mice it has only 309 amino acids (MW. 29.6 kDa). MARCKS is also found in *Xenopus laevis*, chicken, rats, cows, monkeys and in Pacific electric rays. MARCKS is a ubiquitously expressed protein, highest in brain, spleen, and lung, moderate in testis, pancreas, adrenal, kidney, and liver, and lowest in heart and skeletal muscle [3]. It is a very acidic protein (pI 4.2-4.7), composed mainly of alanines, glutamic acids, glycines, prolines and serines.

MARCKS contains three highly conserved regions: an N-terminal myristoylation consensus sequence, an MH2 domain (MARCKS homology 2 domain) close to the N-terminus which resembles the cytoplasmic tail of the cation-independent mannose-6-phosphate receptor, whose function is unknown and is the only site of intron-splicing, and a central, highly basic phosphorylation site domain. This latter domain, composed of 25 amino acids of which 13 are positively charged (12 Lysines and 1 Arginine), contains two actin-binding sites [4], a Ca^{2+}-calmodulin binding domain [5], as well as 4 serine residues that are substrates for phosphorylation by PKC [6], Protein kinase C-Related Kinase (PRK1, [7]) and Rho-associated kinase [8] and plays a major role in phospholipid binding [9]. The PSD was also found to be ADP-ribosylated [10, 11].

The structure of MARCKS is best described as “natively unfolded” [12]. Uversky [13] has defined natively unfolded proteins as being “extremely flexible, essentially noncompact (extended), and [having] little or no ordered secondary structure under physiological conditions.”

The extent to which MARCKS is flexible is unknown. These proteins are described as having large net charges at neutral pH, a low content of hydrophobic amino acid residues [14, 15], and are enriched in E, K, R, G, Q, S, P and A residues [16]. The intrinsic disorder of proteins is believed to allow greater plasticity, which allows them to interact efficiently with several targets and thus mediate crosstalk between different cellular processes and signal transduction pathways. Their increased sensitivity to proteases allows their fast turnover and thus increased regulation. MARCKS is an acidic protein, with only 6 phenylalanines, 5 of which are in the PSD and anchor MARCKS to the plasma membrane, no tyrosine or tryptophan residues, and is made of almost 30% alanine residues and 20% acidic residues (51 glutamic acids and 8 aspartic acids in murine MARCKS, which give MARCKS its acidic nature) that are equally distributed in the protein, but completely absent from its effector domain, 34 prolines, 32 glycines, 30 serines and 23 lysines (12 of which are in the PSD, which has a charge of +13). It was shown by electron microscopy that it is a rod-shaped, elongated molecule with dimensions of about 4.5nm x 36nm [17] and this was confirmed by CD studies, which showed little or no helix although sequence analysis showed α-helical propensity [18]. The protein was found to barely form any secondary and absolutely no tertiary structure in solution, or when bound to Ca^{2+}-calmodulin [18, 19] or membrane-bound [20, 21]. Following phosphorylation by PKC in the PSD, both full-length MARCKS [17, 20] and its PSD [22] have been found to become a little more compact, but still unstructured. The lack of structure in MARCKS has been the rationale for studies employing a peptide that corresponds to the effector domain of MARCKS.

MARCKS exists both in a membrane-bound and cytosolic form. MARCKS binds reversibly to the inner leaflet of the plasma membrane. This interaction involves both the myristoyl group (a co-translational lipid modification which adds myristic acid, a C_{14} saturated

fatty acid to the N-terminal glycine of MARCKS via an amide bond to the amino group of the glycine), which inserts itself into the hydrophobic core of the lipid bilayer and the electrostatic interaction of its basic domain, the PSD, with acidic phospholipids, namely PIP_2 [23-25]. Finally, penetration of the side chains of the five phenylalanine residues found in the PSD into the hydrophobic core of the bilayer also aids in anchoring MARCKS to the plasma membrane [26]. None of the above-mentioned interactions on its own, however, is sufficient to successfully anchor MARCKS to the plasma membrane. This has been named the myristoyl/electrostatic switch model. Phosphorylation of the PSD (as by PKC; [27]) and actin or Ca^{2+}-calmodulin binding all cause MARCKS to localize to the cytosol.

MARCKS Functions

MARCKS has unusual biochemical properties, which make it able to interact with various molecules, and so many functions have been proposed for MARCKS. It was found to bind and crosslink F-actin filaments [17] and so is thought to be an actin crosslinking protein. Accordingly, roles in remodeling of the actin cytoskeleton and affecting cytoskeletal processes such as endocytosis [28, 29], exocytosis [30, 31], phagocytosis and macropinocytosis [32, 33] control of cell morphology, motility, adhesion, protrusive activity and cortical actin formation in embryonic cells [34] have been suggested. MARCKS phosphorylation leads to cortical F-actin disassembly and potentiation of secretion in chromaffin cells [35]. MARCKS has also been implicated in inhibition of adherence to extracellular matrix proteins affecting cell migration [36], regulation of integrin-mediated muscle cell spreading [37, 38], and inbition of myoblast migration [39-41]. Actin binding is prevented by both phosphorylation of the PSD and Ca^{2+}-calmodulin binding. It binds Ca^{2+}-calmodulin and this interaction is abolished by phosphorylation of MARCKS by PKC [5], and is thus thought to play a PKC-dependent role in regulating the availability of Ca^{2+}-calmodulin for other processes [42]. MARCKS also binds and

sequesters PIP_2 with high affinity, reversibly inhibiting phospholipase C [25, 43-48] and is hypothesized to play a role in the regulation of PIP_2 availability and regulation and activation of phospholipase D [49-51]. It was also shown to play a role in tumor suppression [52-56], learning and synaptic plasticity [57], and neurosecretion [58]. MARCKS also regulates growth cone adhesion and pathfinding [59], plays a role in mucin secretion in human airway epithelial cells [60-63], is involved in neurite initiation and maintaining of dendritic spine morphology [64-67], Knockout studies of MARCKS in mice show that MARCKS plays a vital role in the normal developmental processes of neurulation, hemisphere fusion, forebrain commissure formation, and formation of cortical and retinal laminations, regulation of brain development and postnatal survival [68], as well as the pathophysiology of mood disorders [69].

MARCKS is also involved in inflammation and neuropathic pain where it is a substrate of Rho-kinase [70]. It was reported that MARCKS is the major protein produced in response to treatment of neutrophils and macrophages with the cytokine TNF-α, i.e. 90% of protein synthesized by these cells in response to this inflammatory cytokine is MARCKS [71]. It also stimulates MARCKS synthesis in the human promyelocytic leukemia cell line HL-60 and the human myeloid leukemia cell line U937 [72]. Harlan et al. identified promoter regions within the MARCKS gene which contained multiple transcription initiation sites, including a potential NFκB transcription start site, which is shown to be activated by TNF-α [73, 74]. The specific role MARCKS plays as a TNF-α effector has not been elucidated. However, changes in the actin cytoskeleton and cell morphology following cell treatment with TNF-α [75, 76], are very similar to effects of MARCKS on the actin cytoskeleton and hence it is probable that MARCKS plays a role in mediating these effects. This becomes important, as TNF-α seems to serve as a mediator in various pathologies such as septic shock, cancer, AIDS, transplantation rejection, multiple

sclerosis, diabetes, rheumatoid arthritis, trauma, malaria, meningitis, ischemia-reperfusion injury, and adult respiratory distress syndrome. In rheumatoid arthritis, TNF-α blockade has recently emerged as one of the most potent therapies. Similar effects on MARCKS protein levels are observed with lipopolysaccharide (LPS) treatment of BV-2 microglial cells, and this effect is inhibited by treating cells with inhibitors of NFκB, a transcription factor downstream of both TNF-α and LPS [77]. This suggests that MARCKS synthesis is tightly regulated. However, to our surprise, prior published results show that this up-regulation of MARCKS mRNA synthesis is not apparent in microarray data of cells following TNF-α treatment (Table 1-1), suggesting that TNF-α might employ a mechanism other than increasing transcription to achieve high protein levels in the cell or that the pathway may be important only in selected cell types such as monocytes and macrophages. These could range from stabilizing MARCKS mRNA, to stabilizing the protein itself through either binding by other molecules or inhibition/down-regulation of degradation pathways. The MARCKS mRNA has a half life of 14 hours in quiescent fibroblasts and this is reduced to 2 hours upon stimulation of cells with phorbol esters that activate PKC or with growth factors [78, 79]. In fact, it has been shown that the 3`-untranslated region of the MARCKS mRNA contains CU-rich *cis*-elements that destabilize the MARCKS transcript [80]. This instability is reversed by binding by the mRNA binding proteins of the Hu family, HuD and HuR. In contrast to fibroblasts, in neuron cells that have high levels of HuD and HuR, the MARCKS transcript is well stabilized and its half life does not change upon PKC activation.

Major Post-Translational Modifications

MARCKS Phosphorylation

Initially, MARCKS was believed to be substrate to phosphorylation by protein kinase C only [42, 81]. Phosphorylation by PKC in the PSD of MARCKS regulates many aspects of

MARCKS interactions: it abrogates its binding to the plasma membrane [82, 83] and PIP_2 [9], making it dislocate to the cytosol, it prevents it from binding to F-actin [17] and Ca^{2+}-calmodulin [5] and it protects it from cleavage by an unidentified cysteine protease [84] and by the cysteine protease Cathepsin B [85]. It is clear that phosphorylation of MARCKS by PKC in the PSD is one of the most important post-translational modification for regulation of the functions of this protein.

Palmer et al. [7] showed that the PKC-related kinase (PRK1) also phosphorylates MARCKS at serines 152, 156 and 163, which correspond to the PKC-phosphorylated sites of MARCKS, giving it an extra form of regulation in different cell signaling pathways.

Later it was shown that MARCKS can be a substrate for other kinases. Taniguchi et al. [86] showed it to be an *in vivo* substrate of proline-directed protein kinases, such as mitogen-activated protein (MAP) kinase or Cyclin-dependent kinase-5 (Cdk5) (which are abundant in brain and phosphorylate similar sequences) using a reverse-phase capillary high performance liquid chromatography separation of lysyl endoprotease digested calf brain MARCKS followed by electrospray mass spectroscopy (LC/MS) determination of fragment sizes and phosphorylation and Edman degradation to determine sites of phosphorylation. Of seven phosphorylated serine residues they identified (bovine MARCKS Ser 27, 46, 81, 100, 117, 134 and 158), only one was in the PSD of MARCKS, while the other six were N-terminal to the PSD and all were followed by a proline residue. Using the more powerful electrospray ionization/ion trap mass spectrometry, they later identified two more phosphorylation sites on the C-terminus of MARCKS in rat brain (Ser291 and Ser299) that are also thought to be substrates for proline-directed kinases because they are also immediately followed by prolines [87] and speculated that, although the C-terminus has no known function, it is regulated by phosphoryltion. Yamamoto et

al. [88] found MARCKS to be phosphorylated by cdc2 kinase and tau protein kinase II (TPKII) in cytosolic fractions of rat brains. Phosphorylation sites were found to be completely different from PKC phosphorylation sites and occurred on both serine and threonine residues on MARCKS, and phosphorylation increased binding to CaM. Finally, Manenti et al. [89] found that MARCKS was phosphorylated *in vitro* by Cdk2 and Cdk4, and to a lesser degree, Cdk1. They determined the phosphorylation sites using electrospray MS after digestion of the protein, and found Ser27 and Thr150 to be phosphorylated by cyclin E-Cdk2. When MARCKS was first phosphorylated by PKC, the initial rate of phosphorylation by Cdk2 was improved without modifying the number of sites concerned.

Schönwaβer et al. [90] showed that although MARCKS is phosphorylated at Ser-113 (in mouse, equivalent to Ser-116 in human and cow MARCKS) *in vitro* by p42 MAP kinase, it is not phosphorylated by MAP kinase *in vivo* in permeabilized Swiss 3T3 cells after stimulation with platelet-derived growth factor or PMA even though p42 MAP kinase was shown to be active in these cells, and that PKC activation induced MARCKS phosphorylation at the PKC sites. Ohmitsu et al. [91] showed that MARCKS is phosphorylated by MAP kinase on Ser-113 in rat hippocampal neurons following stimulation of the glutamate receptor, in addition to phosphorylation by PKC on the PKC sites (Ser 152, 156, 163), which was transient. They also showed that phosphorylation of MARCKS at Ser113 by MAP Kinase reduced its CaM binding ability to 75% of control, while binding of F-actin was abolished by this phosphorylation, to an extent comparable to that of PKC phosphorylation of the PSD, suggesting that MAP kinase can functionally regulate the properties of MARCKS, especially in its interaction with F-actin. Hasegawa et al. [92] showed that MARCKS is phosphorylated in rat microglia by ERKs (ERK-1

and ERK-2, members of the MAPK family of kinases) following stimulation by the amyloid β protein.

In addition to phosphorylation with PKC, MAP kinases and Cdk's, MARCKS was found to be a substrate of Rho-kinase in human neuronal cells in response to stimulation with lysophosphatidic acid (LPA) [8]. Serine 159, which also corresponds to a PKC phosphorylation site, was found to be a substrate for Rho-associated kinase both *in vitro* and *in vivo* in these human neuronal teratoma cells, NT-2. The same residue, Ser159 was also found to be a substrate for protein kinase A (PKA) *in vitro* in these cells. These phosphorylation sites were recognized using a phosphorylation site-specific antibody against Ser159-phospho-MARCKS (pS159-Mar-Ab). This provides additional regulation of MARCKS by a different signal transduction pathway, which doesn't involve PKC activation, the Rho/Rho-kinase pathway.

MARCKS Proteolysis

Because of its important cellular functions, the regulation of MARCKS concentrations in cells is important. The MARCKS gene is under multiple modes of transcriptional control, including cytokine-and transformation-dependent, cell-specific, and developmental regulation. In general, MARCKS protein concentrations are reported to closely parallel its mRNA levels, which in turn can be regulated at the level of gene transcription by several factors. For example, as described previously, it was reported that TNF-α and LPS can cause dramatic increases in the levels of MARCKS mRNA and protein in neutrophils, macrophages, and related cells [71, 72]. MARCKS expression is also severely decreased in cells transformed with a variety of oncogenes [55, 56, 93, 94]. For example, in v-*src*-transformed murine fibroblasts, MARCKS transcription is down-regulated by 68% compared with untransformed cells, and inhibition of v-*src*-tyrosine kinase activity restores MARCKS mRNA levels to normal, suggesting that the reduced MARCKS mRNA levels are a direct effect of v-*src* activity [55]. MARCKS is also tightly

transcriptionally regulated during mouse development [95] and this was shown to be under control of CBF/NF-Y/CP-1-like and Sp1-like transcription factors in *Xenopus laevis* [96].

In addition to transcriptional regulation of MARCKS levels, specific proteolytic cleavage by multiple kinases may play a role in this regulation. Spizz et al. [84] first described cleavage of MARCKS by an unknown cysteine protease into two major fragments between asaparagine 147 and glutamate 148 (3 amino acids N-terminal to the PSD) in human foreskin fibroblasts. They found, however, that only unphosphorylated MARCKS was a substrate for this protease and that PKC-phosphorylation of the PSD protected MARCKS from this cleavage. This could be a mechanism for strict regulation of MARCKS protein levels in these cells. A year later, Spizz et al. [85] described another cysteine protease that cleaved MARCKS in a pH-dependent manner and fragments associated with lysosomal fractions, suggesting it was a lysosomal cathepsin, and was identified as Cathepsin B in human fibroblasts. Manenti et al. [97] showed that the same cleavage of MARCKS between Asn147 and Glu148 also occurs in bovine brain, and might be a general mechanism for down-regulation of MARCKS activity. More interestingly, Braun et al. [98] have found that macrophages contain a protease which specifically cleaves human MARCKS expressed in a cell-free system or in *E. coli* between Lys-6 and Thr-7, and that this cleavage is myristoylation dependent, i.e. unmyristoylated MARCKS is not recognized or cleaved by these proteases. This cleavage of the N-terminus of MARCKS represents an important mechanism of demyristoylation of MARCKS, which in turn regulates it association with the plasma membrane and binding to other proteins, as Matsubara et al. [99] have demonstrated that the myristoyl group plays a role in calmodulin binding to MARCKS. Finally, it was shown by Dulong et al. [100] both *in vitro* and *in vivo* in myoblasts that the Ca^{2+}-dependent cysteine protease calpain cleaves MARCKS and this cleavage is dependent on the

phosphorylation of MARCKS by PKC. Interestingly, they showed that calpain cleavage of MARCKS before myoblast fusion was required for the process to occur, inferring that cleavage of MARCKS may lead to physiologically active fragments rather than just down-regulate the protein.

Tumor Necrosis Factor

Tumor necrosis factor (TNF, TNF-α, cachectin) is a pleiotropic pro-inflammatory cytokine that exerts multiple biologic effects. It is synthesized as a 26-kDa type II transmembrane precursor that is displayed on the plasma membrane, with the N-terminus in the cytoplasm and the C-terminus exposed to the extracellular space. The TNF precursor is proteolytically cleaved by TNF alpha converting enzyme (TACE) to yield a biologically active 17-kDa mature TNF [101]. Mature TNF monomers self associate to form a homotrimer [102]. TNF mediates its effect through two different but structurally homologous TNF receptors: TNFR1 and TNFR2 (both are type I transmembrane glycoproteins). These TNF receptors are present on all types of cells except red blood cells [103]. TNFR1 is considered to be responsible for most biologic actions of TNF [104, 105].

TNF is produced by numerous immune cells (macrophages/monocytes, natural killer cells, Kupffer cells, B cells, T cells, basophils, eosinophils, glial cells, mast cells) as well as non-immune cells (astrocytes, granulose cells, osteoblasts, cardiac myocytes, fibroblasts, keratinocytes, neurons, neutrophils, T cells, retinal pigment epithelial cells, smooth muscle cells, spermatogenic cells, tumor cells). It is produced in response to an assortment of activating stimuli including LPS, antibodies to LFA-3, calcium ionophores, C5a, CD44, CD45, enterotoxin, GM-CSF, hypoxia, IL-1, leukotrienes, mellitin, MIP-1α, nitric oxide, oxygen radicals, parasites, phorbol esters, synthetic lipid A, TNF, toxic shock toxin-1, viruses and irradiation [106].

TNF has many functions, including promoting synthesis of: adhesion molecules, proinflammatory cytokines, chemokines, MMPs, RANK ligand expression, promotion of angiogenesis, activation of cells (T-cells, B-cells, macrophages), and antiviral and antitumor effects [107]. At the signaling level, TNF induces several responses including the activation of phospholipases (A_2 and C) and acidic sphingomyelinases which in turn generate second messengers such as diacylglycerol and ceramide [108]. TNF also activates three MAP Kinase cascades, JUN N-terminal Kinase (JNK), caspase cascades, and several transcription factors such as NFκB.

TNF is a potent modulator of the actin cytoskeleton in various cell types. It induces F-actin depolymerization and actin synthesis in epithelial cells and results in vascular leakiness [109, 110]. In human umbilical vein endothelial cells (HUVECs), TNF induces the transient increase in F-actin, the reorganization of the actin cytoskeleton, formation of membrane ruffles, filopodia and actin stress fibers leading to cell retraction and formation of intercellular gaps[111]. These effects were found to be mediated by members of the Rho family of small GTPases, Rho, Rac and Cdc42 in endothelial cells. In macrophages, where TNF stimulates many responses including migration, TNF was shown to decrease levels of F-actin and inhibit Cdc42-mediated filopodium extension[75].

In mouse fibroblasts, TNF triggers Cdc42 activation leading to filopodia and lamellipodia formation, which then disappear, leaving only stress fibers behind [112]. TNF affects chemotaxis and motility in macrophages [113], fibroblasts [114], Langerhans cells [115], epidermal keratinocytes [116], and neutrophils [76, 117]. In glomerular epithelial cells, TNF induces actin polymerization and redistribution and focal adhesions, through phosphorylation of vinculin, paxillin and focal adhesion kinase, affecting how these cells contact the glomerular

capillary basement membrane [118]. In pulmonary endothelial cells, TNF-induced apoptosis was shown to require rearrangement of the actin cytoskeleton, which was mediated by Rho-kinase [119]. In contrast, TNF was found to elicit antiapoptotic effects in opossum kidney cells via redistribution of the actin cytoskeleton through inhibition of caspase-3; this was governed by the phosphatidylinositol-3 kinase, Cdc42/Rac1, and phospholipase-γ1 [120]. TNF induces signaling events in lung endothelial cells that result in cytoskeletal changes and increases in EC permeability; these changes are mediated through phosphorylation of ERM proteins (ezrin, radixin, and moesin) by protein kinase C (PKC) [121]. In mouse embryonic fibroblasts, the WD-repeat protein factor associated with nSMase activity (FAN), a member of the family of TNF receptor adaptor proteins that are coupled to specific signaling cascades, was found to be essential for TNF-induced actin cytoskeletal changes, reorganization and filopodium formation, and that this required the presence of the PH domain which localizes FAN to the plasma membrane by binding specifically to phosphatidylinositol-4,5-bisphosphate (PIP_2) [122].

Rheumatoid Arthritis

RA is an immunologically mediated chronic inflammatory disease of unknown etiology. It is characterized by synovial cell proliferation and inflammation with destruction of adjacent articular tissue [123]. RA has a prevalence of 1% worldwide; it is believed to be the most common, potentially treatable cause of disability in the Western world [124]. The consequences of RA can vary from hardly any impairment to severe disease with continuing high disease activity and progressive joint destruction resulting in severe loss of function and increased mortality [125-127]. It can be rapidly destructive, with 60% of patients having erosions of joints seen on radiographs within 2 years of disease onset [128, 129]. RA patients suffer from a loss of functional ability leading to an inability to work, causing an economic burden to society [128].

As early as 1953, patients with RA were shown to have an approximate 10-year premature mortality [130].

Despite extensive research, the cause of RA is unknown. It is believed that it is multifactorial, with genetic and environmental factors playing important roles. The prevailing view is that RA is mediated by antigen-activated T cells that infiltrate the synovial membrane [131, 132], which leads to a series of inflammatory processes, resulting in vascular and synovial cell proliferation with resorption of cartilage and bone. Non-immunologic pathways also probably contribute to tissue injury and destruction in established RA [131]. Degradation of articular extracellular matrix components is a hallmark of RA and is largely mediated by matrix metalloproteinases (MMPs). RA is strongly associated with MHC class II allele HLA-DR4, and to a lesser extent to HLA-DR-a and DR14. Activated T cells, macrophages, and fibroblasts produce proinflammatory cytokines that play a key role in synovitis and tissue destruction in RA. TNF and IL-1 are two of the main cytokines that enhance synovial proliferation and stimulate secretion of MMPs, other inflammatory cytokines, and adhesion molecules [133].

There is no good early definition of RA. RA is usually defined by the ACR criteria [134], but it is well known that these criteria are not optimal to distinguish early RA from undifferentiated (and sometimes self-limited) poly-arthritis and early manifestations of other auto-immune diseases such as post-viral arthropathies, early spondyloarthropathy, and other, self-limiting arthrides that may satisfy the 1987 ACR RA criteria [135]. Current classification criteria, which rely on the presence of clinical signs and symptoms and laboratory and radiographic findings, lack the ability to differentiate RA from similar rheumatic conditions, especially in elderly persons [136]. Patients in the early stages of disease and those who have mild RA may not be correctly identified using these criteria.

Immunologic events in RA occur many years before the onset of clinical disease. Rheumatoid Factor has been shown in patients years before the onset of symptoms [137]. Similarly, anti-cyclic citrullinated peptide antibodies precede disease by 14 years and precede the detection of RF by an average 2.8 years [138]. Increases in highly sensitive C-reactive protein (CRP) have been shown before onset of clinical disease in patients with or without serologic abnormalities [139]. When serologic events occur in the presence of the appropriate genetic environment, disease activation would seem even more likely. In addition, environmental factors are important, particularly heavy smoking, which is associated with an increased risk of development of seropositive RA [140, 141]. These data support the hypothesis that the activation of RA is multifactorial with autoimmune and genetic factors important, most likely in conjunction with appropriate environmental stimuli. Complementary to the serologic changes detected before clinically manifest disease, imaging and arthroscopy detect synovitis in clinically normal joints. Ultrasound and MRI are able to show the presence of synovitis in patients with early RA in joints with a normal clinical examination [142-144].

As described, disease may predate symptoms by many years. There is considerable evidence that radiographic damage, loss of function [145], and loss of bone mineral density [146, 147], occur early in the disease process. In early RA (<6 months of symptoms), 40% of patients have erosive disease at presentation [148]. Even in an early synovitis clinic that attracts patients at the earliest stages of disease, 25% of patients have radiographic erosions at presentation [149]. New imaging techniques show bone changes occur even earlier than was first thought. Bone edema, the MRI precursor to erosions, can be seen in patients after only 4 weeks of symptoms [150]. Ultrasound can show erosions before they are evident on plain radiography [144].

Not only does damage occur early, but also reversibility of functional loss may be lost with time. Patients treated less than 2 years from disease onset showed a significant improvement in function, using the Health Assessment Questionnaire, after intervention compared with patients treated beyond this time point in a study of 440 patients [151]. In a review of 11 different studies, Anderson et al [152] showed that disease duration was paramount in predicting response to DMARD therapy. Of patients, 53% presenting with less than 1 year's disease duration showed a response, whereas later groups showed diminished responses with time. Similarly, in a study of 448 RA patients, the patients who presented with less than 5 years' disease duration maintained a lower mortality ratio over 21.5 years of follow up compared with late presenters [153].

A commonsense approach to the management of a persistent, progressive, damaging condition such as RA would seem to be intervention before the onset of damage, at a stage when disease still may be reversible. Such a phase of disease has been described as a "window of opportunity" for intervention, a period in early-stage RA during which the progression rate of joint damage is set, and therapeutic interventions can exert maximum effects [154]. Unfortunately, due to the lack of a sensitive and specific marker for early RA, this "window" is often missed.

With better understanding of the pathogenesis of autoimmune diseases and advancing developments in biopharmaceutical technology, biologic therapeutic agents have been introduced. These agents target specific components of the immune response considered central to the etiology of RA. Although traditional DMARDs generally slow joint damage progression, the prevention of joint damage has become a revolutionary possibility, particularly with the biologics inhibiting TNF. These TNF inhibitors suppress disease activity directly and

powerfully and lower the disease burden significantly from the moment that treatment is started [155-157].

Due to its pleiotropic effects, TNF has been an attractive therapeutic candidate and is felt to play a central role in the pathogenesis of RA. A number of lines of evidence that support this hypothesis are:

- The biologic activity of TNF can account for the pathologic processes contributing to RA (e.g., cell recruitment and activation, synovial lining cell proliferation, increased prostaglandin, and matrix-degrading metalloproteinase activity as well as bone and cartilage destruction) [158];
- TNF and TNF receptors are upregulated in rheumatoid synovium [159, 160];
- Anti-TNF downregulates IL-1 and other proinflammatory cytokines in vitro [161];
- When TNF is overexpressed in a transgenic mouse model, it results in the development of a form of erosive arthritis similar to RA [162].
- Animal models of arthritis are ameliorated by anti-TNF [163].
- TNF blockade results in great clinical benefit in RA [164-170].

It has been shown that a brief intervention early in the course of RA can "reset" radiologic progression rates during subsequent years independent of consequent therapy [171]. In addition, delayed treatment trials have shown that a delay of only 3 to 9 months in starting DMARD therapy has a significant negative impact on radiographic outcome 2 years later [172, 173]. Both these observations support the "window of opportunity" hypothesis. Because the TNF inhibitors have been proved to stop joint damage progression in severe progressive RA, the achievements of these agents in early RA are currently of great interest. Currently, there are three anti-TNF agents available for clinical use: infliximab, a chimeric anti TNF mAb; etanercept, a soluble TNF-receptor construct; and adalimumab, a human anti-TNF mAb. However, as expected for blocking an important immune cytokine, side effects are a concern and include a risk of increased infection (in particular TB and opportunistic infections), drug-induced SLE,

lymphomas autoantibody formation, demyelinating disease, injection site reactions, cytopenias and congestive heart failure [107, 174, 175].

Apoptosis

Apoptosis is the normal physiologic mechanism by which cells commit suicide, also known as programmed cell death. It has evolved in multicellular organisms to allow for the elimination of cells in normal and pathologic settings. Apoptosis is crucial for normal development and tissue homeostasis and is subject to genetic control [176, 177]. Abnormalities in this important mechanism are associated with various disease states such as cancer [178, 179], autoimmunity [180, 181], and degenerative disorders [182, 183]. Apoptosis can be triggered by intracellular and extracellular events, and signaling occurs through different independent pathways, which converge on the activation of a family of cysteine proteases (caspases), which subsequently cleave myriad cellular substrates. Caspases can be activated directly by engagement of cell surface receptors ("death receptors") such as Fas/CD95 or TNFR1, or by signals in response to intracellular damage or stress that are transmitted to the Bcl-2 family. In addition to caspases, there are three major functional groups of molecules involved in triggering and affecting the apoptotic process: adaptor proteins (physically link cell death effectors and regulators by forming bridges between caspases and upstream regulators of apoptosis, controlling the activation of initiator caspases), members of the tumor necrosis factor receptor superfamily, and members of the Bcl-2 family of proteins. As described previously, TNF is a potent proinflammatory cytokine that can induce apoptosis [184]. TNF also elicits antiapoptotic cell signals, leading to suppression of apoptosis, which is mostly dependent on nuclear factor-κB (NF- κB), and to inflammatory response [185-190]. It has also been shown that TNF activates cell survival signaling cascades that result in the inhibition of apoptosis independently of NF- κB [191, 192]. Whether members of the TNFR superfamily will trigger proliferation, survival,

differentiation, or death depends on the cell type and the other signals that the cell receives [193-195].

TNF can induce apoptosis by ligating the TNFR1. Once this receptor is ligated, its death domain (DD) motif recruits several adaptor proteins via homotypic domain interactions. These interactions allow caspase aggregation and activation [196-198], which are also mediated by another domain found in adaptor molecules, the Death Effector Domain (DED). Initiator caspases (e.g., caspases 8 and 10) are first activated and start an avalanche of increasing caspase activity by processing and activating effector caspases (e.g., caspases 3 and 6) [199]. Caspases then carry out cell killing by cleaving and inactivating certain vital cellular proteins such as DNA repair enzymes, lamin, gelsolin, MDM2 (inhibitor of p53), and protein kinase Cδ [199, 200], or by directly or indirectly activating enzymes that go on to play further roles in apoptosis [201].

Table 1-1. MARCKS does not appear to be upregulated by TNF-α in microarray data.

#	Cell type	Effect of TNF-α on MARCKS mRNA Transcription	Reference
1	Primary RA synovial fibroblasts (RASFs)	Insignificant Change	[202]
2	Cultured primary human synoviocytes	Insignificant Change	[203]
3	HeLa cells	Showed results for genes upregulated ≥2.5 fold—No MARCKS data	[204]
4	Coronary artery endothelial cells and smooth muscle	Showed results for differentially expressed genes—No MARCKS data	[205]
5	Hearts of TNF- α overexpressing transgenic mice	Showed results for top 50 upregulated genes—No MARCKS data	[206]
6	Human umbilical vein endothelial cells (HUVECs)	Significant Increase in MARCKS mRNA expression	[207]
7	Human keratinocytes	Showed results for differentially expressed genes—No MARCKS data	[116]

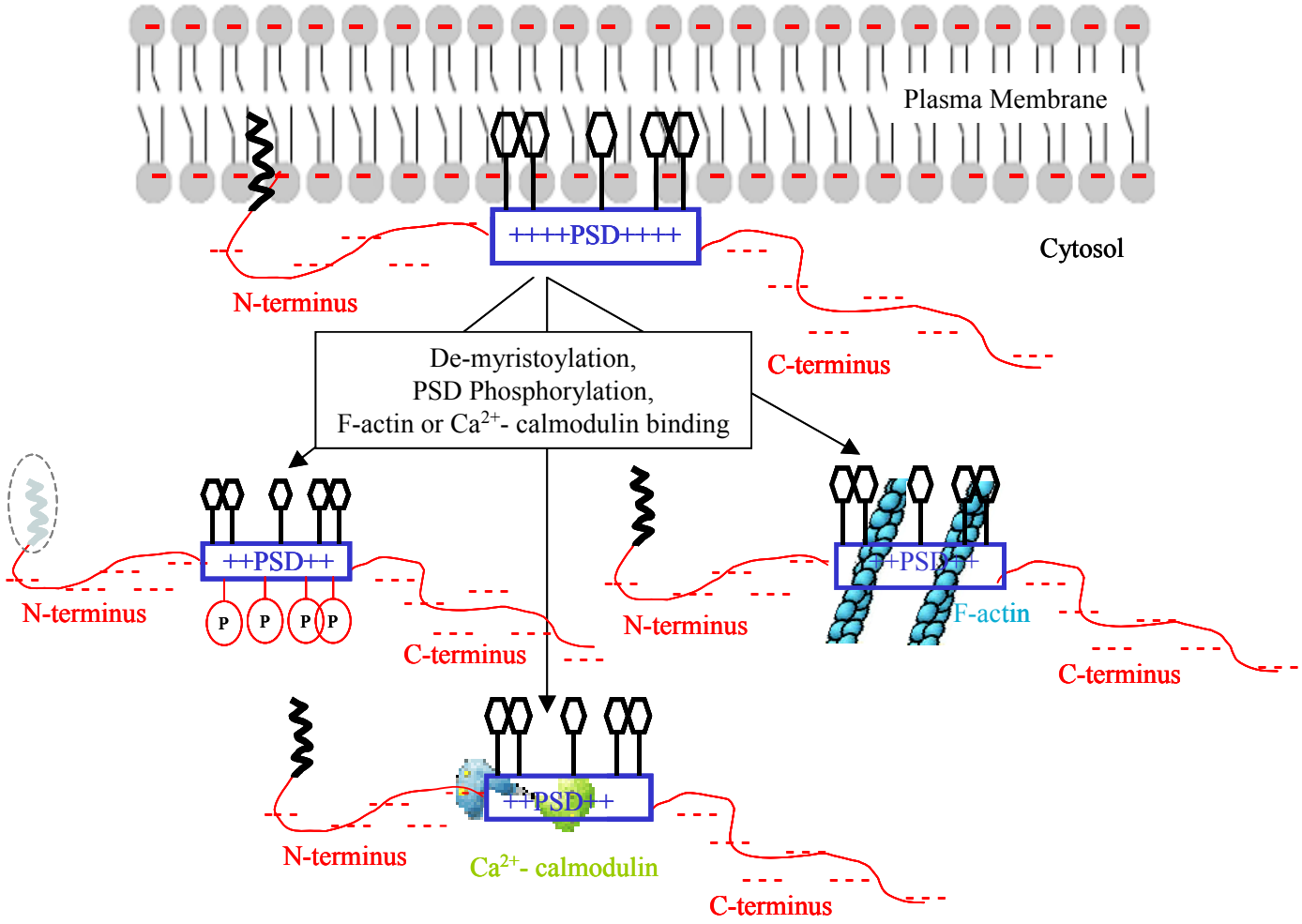

Figure 1-1. MARCKS cycles between the plasma membrane and the cytosol. MARCKS binds to the inner leaf of the plasma membrane via its N-terminal myristoyl group and its PSD. Upon PSD phosphorylation, de-myristoylation, F-actin or Ca2+-calmodulin binding, this interaction is abolished and MARCKS translocates to the cytoplasm. Sticks with hexagon heads represent phenylalanine residues in the PSD.

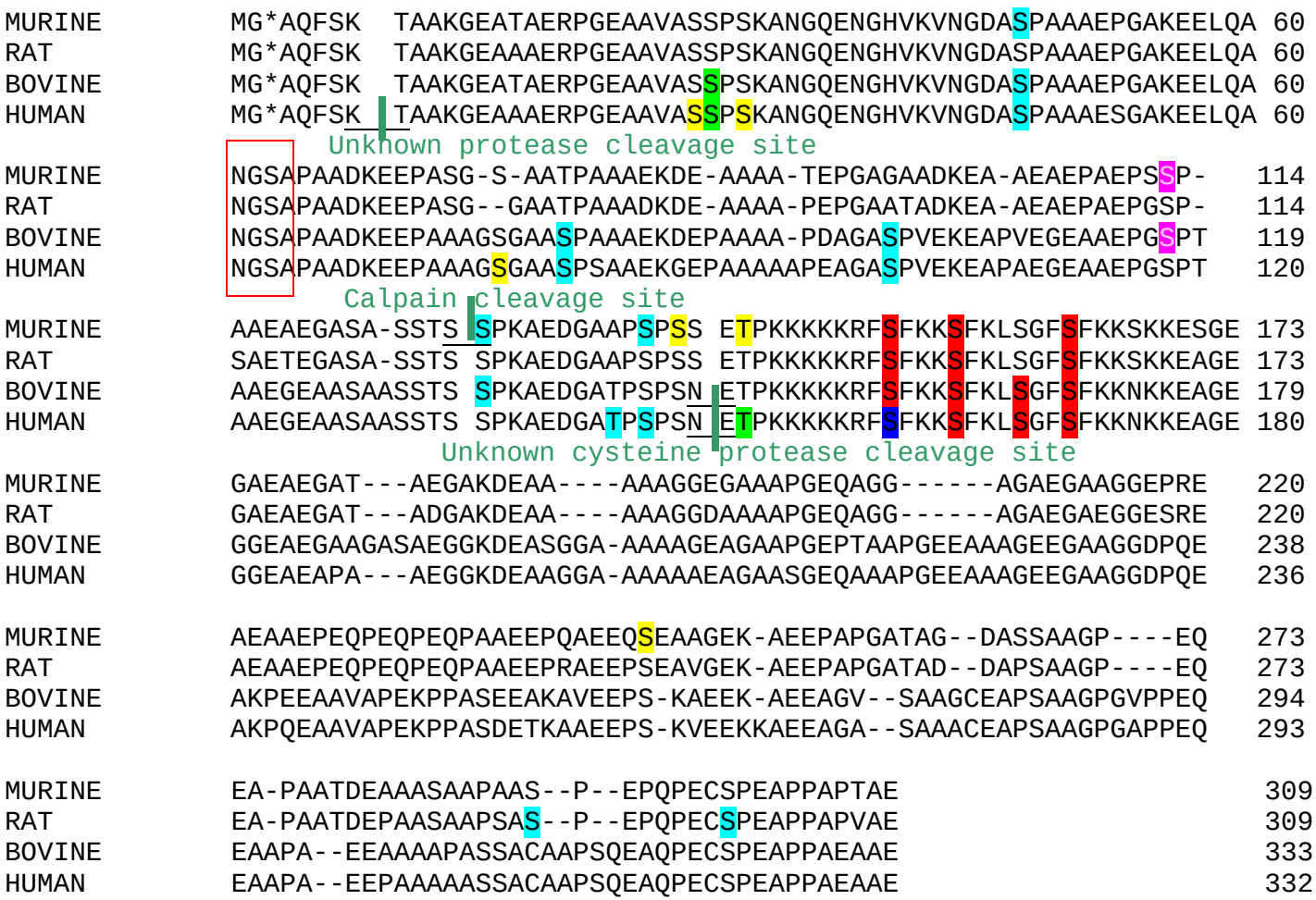

Figure1-2. Known post-translational modifications of MARCKS. Myristoylated residues are marked by an asterisk, cleavage sites are underlined and residues separated by a green vertical bar, residues experimentally shown to be phosphorylated are highlighted in yellow, and the N-glycosylation consensus sequence is boxed in red. The PSD is also reported to be ADP-ribosylated, but the exact position of this PTM is unknown. Ser27 and Thr150 highlighted in green are phosphorylated by E-Cdk2, Ser113 in pink by p42MAP Kinase, Ser in red are phosphorylated by PKC and PRK1; Ser159 in blue is also phosphorylated by PKA and RhoA Kinase. Serines in cyan are phosphorylated by proline-directed protein kinases.

CHAPTER 2
INVESTIGATING INTRAMOLECULAR INTERACTIONS OF MARCKS

Introduction

MARCKS is a highly acidic protein (pI 4.2-4.6, [71, 208, 209]) with a central extremely basic domain (pI 11.61) called the Phosphorylation Site Domain (PSD). The PSD is composed of 25 amino acids, 13 of which are positively charged (12 lysines and 1 arginine) and does not contain any acidic residues. In contrast, the rest of the protein is 21% acidic with 51 glutamic acids and 8 aspartic acids out of 309 amino acids in murine MARCKS.

In this chapter, we will test the hypothesis that intramolecular interactions occur between the phosphorylation site domain (PSD, also known as effector domain, ED) of MARCKS and the rest of the protein. This hypothesis is based on our observation that recombinant, full length non-myristoylated MARCKS does not bind F-actin and Ca^{2+}-calmodulin *in vitro* as previously reported, [5, 17] and on the fact that MARCKS is an unstructured protein with a unique charge distribution (Figure 2-1). Why is the PSD unavailable to interact with MARCKS binding proteins in an unfolded, unstructured protein? While this could simply be due to continued failure to produce active protein over the past few years using various different purification protocols, it is most likely more complicated than that.

We hypothesize that ionic interactions between the acidic termini of MARCKS and the oppositely charged PSD, which is the site of most known interactions of MARCKS, mask the PSD thus making it unavailable to interact with MARCKS binding partners such as actin and calmodulin (Figure 2-2). Various experiments done in our lab have shown that a synthetic rhodamine-labeled PSD peptide can bind to the full-length protein, and competition assays suggest a single binding site for the PSD on the protein [210].

We will test our hypothesis in two ways; first, we will do a chemical neutralization of acidic charges on MARCKS (pulished work: Tapp H, Al-Naggar IM et al. *JBC* (2005) **280**: 9946-9956); then, we will make truncations of the protein which will be missing either terminus but retain the full PSD; We will then test whether either of these modifications will render the protein more active in biochemical binding assays.

Neutralization of Acidic Residues on MARCKS

Neutralization of acidic residues on MARCKS was done as previously described [211] using 1-Ethyl-3-(3-Dimethylaminopropyl) carbodiimide Hydrochloride (EDC, MW 191.7, Figure 2-3, A), to crosslink the negatively charged carboxyl groups on acidic residues to ethanolamine, resulting in a loss of negative charge on those residues (Figure 2-3, B). EDC is a heterobifunctional cross-linker that possesses two different reactive groups (a carboxyl and amine functional groups) that allow for sequential (two-stage) conjugations, helping to minimize undesirable polymerization or self-conjugation. EDC couples carboxyls to primary amines or hydrazides resulting in the formation of amide or hydrazone bonds (Figure 2-3, D). Carboxy termini of proteins can be targeted, as well as glutamic and aspartic acid side-chains. In the presence of excess cross-linker, polymerization is likely to occur because all proteins contain carboxyls and amines. The bond that results is a peptide bond, so reversal of the conjugation is impossible without destroying the protein [212-214].

EDC reacts with carboxylic acid groups and activates the carboxyl group to form an active *O*-acylisourea intermediate, allowing it to be coupled to the amino group in the reaction mixture (ethanolamine was used in our experiments). An EDC by-product is released as a soluble urea derivative after displacement by the nucleophile. The *O*-acylisourea intermediate is unstable in aqueous solutions, making it ineffective in two-step conjugation procedures without increasing the stability of the intermediate using N-hydroxysuccinimide. This intermediate reacts with a

primary amine to form an amide derivative. Inability to react with an amine results in hydrolysis of the intermediate, regeneration of the carboxyls, and the release of an N-unsubstituted urea. The cross-linking reaction is usually performed between pH 4.5 to 5 and requires only a few minutes for many applications. However, the yield of the reaction is similar at pH from 4.5 to 7.5.

In this experiment, we performed a simple charge neutralization protocol, whereby negative residues on MARCKS (namely glutamic and aspartic acids, found only on either terminus on MARCKS and not in the PSD) were chemically modified to neutral amides. Once modified in that manner, MARCKS was used to perform biochemical assays, including actin polymerization assays, high speed pelleting assays, actin bundling assays, binding assays and fluorescence anisotropy assays with reported MARCKS binding partners, F-actin and Ca^{2+}-calmodulin, which we have so far been unsuccessful at reproducing in our lab with full length non-myristoylated MARCKS.

Neutralization of the acidic residues on the termini of MARCKS is expected to prevent hypothesized ionic intramolecular interactions with the basic PSD of MARCKS, which is the known site of interaction between MARCKS and its binding partners such as actin and calmodulin. We believe that these interactions mask the PSD and make it unavailable to interact with these proteins, and therefore expect that neutralizing the charges responsible for these interactions while leaving the PSD intact would make the latter available to interact with actin and calmodulin and would produce positive results in our biochemical assays that measure interactions and binding.

Methods

Preparation of EDC-modified MARCKS

As previously described for modification of the acidic residues of caldesmon, [211] MARCKS (28 μM) in 100 mM MES, 400 mM ethanolamine pH 5.5 was incubated for 10 minutes at room temperature. Freshly prepared EDC in water (200 mM) was added to give varying final EDC concentrations (0 mM, 4 mM, 12 mM and 20 mM). Reactions were incubated at room temperature for 1 hour, then stopped by addition of ß-mercaptoethanol (100 mM), and then dialyzed into 5 mM Tris-HCl, 5 mM ß-mercaptoethanol, pH 7.9. Aliquots of treated MARCKS from each reaction mixture were run on 12% SDS-PAGE to confirm modification by EDC as detected by an expected shift in electrophoretic mobility. Unmodified MARCKS runs anomalously as an ~80 kDa protein because of its unusual pI, and modification of the acidic residues shifts it towards its expected position at 30 kDa [211]. Modification of the acidic but not basic residues was confirmed by amino acid analysis.

Actin-binding assays

Time course of actin polymerization. The effect of EDC-treated MARCKS on the rate of actin polymerization was determined using a time-course of actin polymerization assay. Three μM 4% pyrenyl-actin (in G-buffer; 5 mM Tris, 0.1 mM $CaCl_2$, 0.01 mM NaN_3, 0.2 mM ATP, 0.2 mM DTT, pH7.9) and 6 μM EDC-treated MARCKS (in 10 mM Tris, 5 mM β-mercaptoethanol, pH7.9) were used. Actin polymerization was initiated by the addition of 195 μM $MgCl_2$ to a final Mg^{2+} of 200 μM and pyrenyl-actin fluorescence intensity was immediately measured at 21°C in a Photon Technology International (South Brunswick, NJ) photon-counting spectrofluorimeter with excitation at 366 nm and emission at 386 nm. MARCKS buffer alone (10 mM Tris, 5 mM β-mercaptoethanol, pH7.9) was used as a control.

Time course of actin depolymerization. The effect of EDC-treated MARCKS on the rate of actin depolymerization was measured in a time course of actin filament depolymerization assay by dilution of 10% pyrenyl-labeled F-actin (10 μM) polymerized with 2 mM $MgCl_2$ to 0.1 μM in F-buffer (5 mM Tris, 2 mM $MgCl_2$, 0.125 mM EGTA, 40 mM KCl, 0.1 mM $CaCl_2$, 0.01 mM NaN_3, 0.2 mM ATP, 0.2 mM DTT, pH7.9) in the absence or presence of 2 μM EDC-treated MARCKS (0, 4, 12 and 20 mM EDC-treated). Pyrenyl-actin fluorescence intensity was followed at 21°C in a Photon Technology International (South Brunswick, NJ) photon-counting spectrofluorimeter with excitation at 366 nm and emission at 386 nm.

High speed F-actin binding. To find out whether EDC-treated MARCKS binds to F-actin, a high speed F-actin binding assay was performed. In this assay, G-actin was allowed to polymerize to F-actin, then 10 μM F-actin was incubated for 1 hour with 6 μM EDC-treated MARCKS (0, 4, 12 or 20 mM EDC-treated MARCKS). Reactions were then centrifuged at high speed (65,000 rpm) for 1 hour at 12°C to allow F-actin and anything bound to it to pellet. Supernatants were loaded onto a 12% SDS gel and stained with SYPRO Ruby protein stain (Molecular Probes).

MIANS-calmodulin binding assay

To determine whether EDC-treated MARCKS bound more efficiently to calmodulin, we performed a MIANS-calmodulin binding assay. MIANS-calmodulin is a fluorescently labeled calmodulin whose fluorescence increases upon binding to other molecules. To calmodulin equilibration buffer (10 mM Tris, 50 mM KCl, 0.6 mM $CaCl_2$, pH 7.9) increasing concentrations of EDC-treated MARCKS (0, 0.2, 0.5, 1, 3, 6 μM, etc…) were added to 0.2 μM spinach MIANS-calmodulin, until a plateau in MIANS-calmodulin fluorescence was reached. Samples were excited at 322 nm and emission read at 438 nm in a Photon Technology International

(South Brunswick, NJ) photon-counting spectrofluorimeter. For negative controls, MARCKS is replaced with MARCKS buffer (10 mM Tris, 40 mM KCl, 5 mM β-mercaptoethanol, pH7.9).

Results

Neutralizing charges on MARCKS by EDC causes a shift in MARCKS motility on SDS-PAGE: 30kDa MARCKS runs anomalously as a 65-87kDa protein on an SDS gel due to its highly negative charge, which prevents binding of SDS molecules due to same charge repulsion, so MARCKS does not run based only on its mass as it is supposed to in SDS-PAGE. This charge neutralization was shown by amino acid analysis to be very mild, i.e. only a few amino acids were actually neutralized overall, e.g, at the highest EDC concentration used, only 6 amino acids were shown to be neutralized. However, this modification still seems to have a great effect on MARCKS activation making it more reactive with its binding partners (F-actin and calmodulin) in our biochemical assays.

EDC neutralization of MARCKS increased the rate of actin polymerization, especially at 20 mM EDC treatment (Figure 2-4). Neutralized MARCKS also had the greatest effect on the rate of actin depolymerization, slowing it down at 20 mM EDC (Figure 2-5), an effect attributed to the barbed end capping activity of MARCKS. In an actin high speed pelleting assay, only 12 and 20 mM EDC-treated MARCKS pelleted with F-actin following centrifugation (Figure 2-6), meaning that MARCKS can only bind the negatively charged binding site on F-actin if it loses some of its negative charges. The binding of MARCKS to MIANS-calmodulin was also very much enhanced by the EDC-charge neutralization of MARCKS (Figure 2-7). All these effects were consistent with the hypothesis that EDC-neutralized MARCKS would behave like a peptide that corresponds to the PSD.

MARCKS Truncations

Deleting either end of MARCKS is the second way we will test our hypothesis that the MARCKS termini are somehow interacting with the PSD. In addition, the EDC negative charge neutralization experiment does not provide us with any information about which one of the termini of MARCKS actually interacts with and blocks the PSD, or whether they both do. In order to answer this question, we made truncations of MARCKS where deleted either terminus at a time while leaving the PSD intact (Figures 2-8 and 2-9). We then purified the resulting truncated proteins, MARCKS N-terminus and MARCKS C-terminus, and used them for assays routinely performed to test for MARCKS-protein interactions (i.e., polymerization assays, high speed pelleting assays, actin bundling assays, binding assays and fluorescence anisotropy assays with known MARCKS binding partners, F-actin and Ca^{2+}-calmodulin).

Either one or both of the acidic termini of the protein could be interacting with the PSD and rendering it inactive (Figure 2-2). If the former is true, deleting one terminus would make one of our constructs active. If the latter is true, deleting only one terminus may only weakly activate the protein, if at all, suggesting that more complicated post-translational modifications exist intracellularly that lead to the activation of MARCKS.

Methods

Generating truncations of MARCKS

Cloning. Primers containing NdeI and BamHI restriction sites were designed to amplify the entire N-terminus of MARCKS starting at the beginning of MARCKS up to and including the PSD (Fwd Primer: agg gaa ttc cat atg ggt gcc cag ttc tcc, Rev Primer: cgc gga tcc tta gcc cga ctc ctt ctt gct). A primer set was also designed to amplify the C-terminus of MARCKS, starting 4 residues before the PSD, including the PSD and ending at the STOP codon of MARCKS (Fwd Primer: agg gaa ttc cat atg agc agc gag acc ccg, Rev Primer: tta gga tcc tgg agc tta ctc ggc cgt).

PCR was carried out using as a template the complete murine MARCKS sequence in a pET19b vector (Novagen) using Roche's High Fidelity Taq Polymerase and PCR reagents and the following parameters: an initial denaturation of 95°C for 10 minutes, 30 cycles of 94°C for 1 min (denaturation), 55°C for 1 min (annealing), 72°C for 1 min (extension), and a final extension at 72°C for 10 minutes. Either 20% sterile glycerol or 10% DMSO was also required for the success of the PCR reaction with both primer sets. The resulting PCR fragment was TA cloned into a TOPO pCR2.1 vector (Invitrogen), double digested with NdeI and BamHI (New England Biolabs) and cloned into the NdeI and BamHI sites of pET9a vector (Novagen, Figure 2-10) under control of the T7 promoter using T4 DNA Ligase (New England Biolabs). Ligations were carried out overnight in a 16°C water bath and were then transformed into *E. coli* Nova Blue competent cells (Novagen) using a heat shock protocol (add 1µl of purified plasmid to 20µl of competent cells, place on ice for 30 min, heat shock at 42°C for 45 seconds and place back on ice for 5 minutes, add 80µl of fresh SOC media, shake for 1 hour at 37°C) and plated on Kanamycin-containing LB agar plates. Colonies were picked the following day, grown in 10 mL LB in a shaker at 37°C for 16 hours, plasmid DNA isolated using Qiagen's Plasmid Miniprep Kit and sent for DNA sequencing for sequence verification. Correct constructs were then transformed into *E. coli* BL21(DE3) expression cells using the heat shock protocol described above, and grown in large scale in LB to an optical density at 600 nm of 0.5-0.6 at 37°C and induced for 3 hours by addition of 1 mM IPTG. After 3 hours, cells were spun down and frozen at -80°C and proteins were subsequently purified.

Purification. Frozen cells were resuspended in resuspension buffer (5 mL buffer for every 500 mL of cell culture pellet, 10 mM Tris, 5 mM β-mercaptoethanol, 2 mM EDTA, 100 µM EGTA, pH 7.9 and protease inhibitors 0.1 mM PMSF and 1 mM DFP). Resuspended cells were

sonicated four times for 30 seconds each with 30-second intervals on ice, heated to 85°C for 10 min, and centrifuged at 38,000 rpm for 1 hour. The supernatant was loaded onto a DEAE anion exchange column and fractions collected with a 0-400 mM KCl gradient in 5 mM Tris buffer, pH 7.9. Fractions containing protein were identified by running a 12% SDS gel. Fractions containing our protein of interest were pooled, dialyzed into 25 mM Sodium Phosphate buffer, pH6.2 and loaded onto an HAP column. Proteins were eluted from the HAP column with a step gradient of 100, 200 and 300 mM Sodium Phosphate buffer, pH 6.2. Fractions containing protein were identified by running a 12% SDS gel and UV scans between 240 and 300nm (look for phenylalanine peaks between 258nm and 263nm). Fractions containing protein were then dialyzed into MARCKS gel filtration buffer (5 mM Tris, 40 mM KCl, 5 mM β-mercaptoethanol, pH7.9) and loaded onto a 100 cm Sephacryl HR300 gel filtration column. Purity of eluted MARCKS truncation was confirmed by SDS-page, amino acid analysis and UV absorption. UV scans are particularly useful with MARCKS and its truncations, because phenylalanine (Phe, F) is the only aromatic amino acid in the protein (MARCKS contains no tyrosines or tryptophans), and in pure MARCKS there is characteristic phenylalanine fine structure in the 240-300nm region of the UV spectrum, and lack of absorbance at 280nm. If further purification was needed, the protein was then loaded onto a Mono-Q anion exchange column, and eluted with a 100-400 KCl gradient in the presence of 10 mM Tris, pH7.9.

Testing activity of MARCKS truncations

Low speed actin bundling. This assay tests whether the PSD on MARCKS truncations is available to bundle F-actin. In this assay, G-actin was allowed to polymerize to F-actin (1% pyrenyl-labeled) by addition of 2 mM $MgCl_2$, then 3 μM F-actin was incubated overnight with 3 or 6 μM of either MARCKS trucation or PSD as a positive control. Pyrene fluorescence was measured before and after a low speed centrifugation at 14,000 rpm for 15 minutes at room

temperature in a tabletop microcentrifuge. Pyrenyl-actin fluorescence intensity was followed at 21°C in a Photon Technology International (South Brunswick, NJ) photon-counting spectrofluorimeter with excitation at 366nm and emission at 386nm.

Actin-binding in native gels. To look for interactions between actin and MARCKS truncations, we mixed 4 μM actin with MARCKS (5 μM), MARCKS C-terminus (5 μM), and MARCKS N-terminus (14 μM). Samples were incubated for 30 minutes at room temperature, mixed with native sample buffer and loaded on a 7% Tris-Tricine native gel (25 mM Tris-Tricine, 0.1 mM $CaCl_2$, 0.01 mM NaN_3, 0.2 mM ATP and 0.2 mM DTT, pH 8.3). Gel electrophoresis was carried at a constant 100V.

F-actin high speed pelleting assay. Previously described.

Time course of actin polymerization. Previously described.

Results

By deleting either end of MARCKS separately, we expected to activate the PSD by unmasking it, and making it interact with F-actin and calmodulin. However, this would not be the case if both ends of MARCKS were interacting with and masking the PSD. All our actin-binding and interaction biochemical assays were negative with MARCKS truncations, indicating the presence of PSD-interacting sites at either end of MARCKS or an incorrect hypothesis. Neither N- nor C-terminus of MARCKS bundled F-actin in a low speed bundling assay whereas PSD did successfully (Figure 2-11). Neither the N- nor C-terminus formed complexes with actin in a native gel (Figure 2-12). Neither protein pelleted with F-actin in an F-actin high speed pelleting assay (Figure 2-13). Both MARCKS truncation proteins only slightly slowed down the rate of actin polymerization (Figure 2-14). In this same assay, lower concentrations of PSD slowed down the rate of actin polymerization while higher concentrations greatly increased the rate of actin polymerization.

Conclusions

The EDC charge neutralization experiments which activated MARCKS in all our biochemical assays provide strong evidence that there is an intramolecular interaction between the PSD of MARCKS and the rest of the protein, and that this interaction has a large ionic component to it.

The negative results obtained from experiments performed with the MARCKS truncation proteins suggest that there is more than one binding site for the PSD on MARCKS and that they are found at both N-terminus and C-terminus.

*GAQFSKTAAKGEATAERPGEAAVASSPSKANGQENGHVKVNGDASPAAAEPGAKEEL
QANGSAPAADKEEPASGSAATPAAAEKDEAAAATEPGAGAADKEAAEAEPAEPSSPAA
EAEGASASSTSSPKAEDGAAPSPSSETP***KKKKKRFSpFKKSpFKLSpGFSpFKKSKK***ESGEG
AEAEGATAEGAKDEAAAAAGGEGAAAPGEQAGGAGAEGAAGGEPREAEAAEPEQPEQ
PEQPAAEEPQAEEQSEAAGEKAEEPAPGATAGDASSAAGPEQEAPAATDEAAASAAPA
ASPEPQPECSPEAPPAPTAE

Figure 2-1. Amino acid sequence of murine MARCKS (Accession # NP_032564). Acidic residues are shown in red, basic residues shown in blue, PSD is in italic, potentially phosphorylated residues in the PSD are followed by a lower case green p, the myristoylation sequence is underlined, and the myristoylated residue is marked by an asterisk.

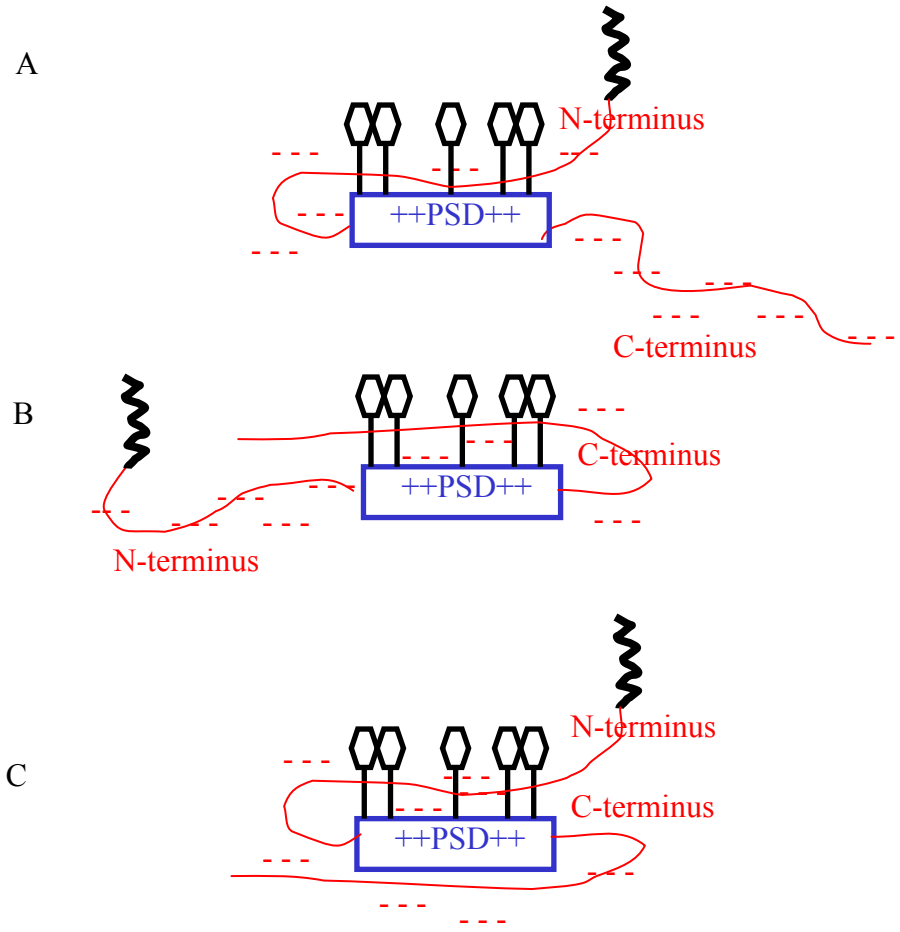

Figure 2-2. The basic PSD of MARCKS may be masked by interacting with the acidic termini of MARCKS. A) PSD interacting with the N-terminus only. B) PSD interacting with the C-terminus only. C) PSD interacting with both the N- and C-termini of MARCKS simultaneously. Sticks with hexagon heads represent phenylalanine residues in the PSD.

A

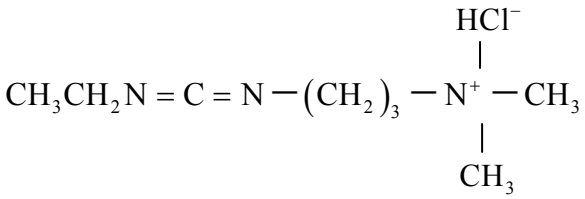

B

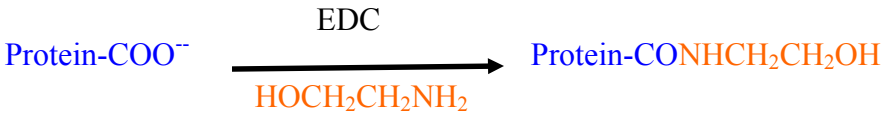

C

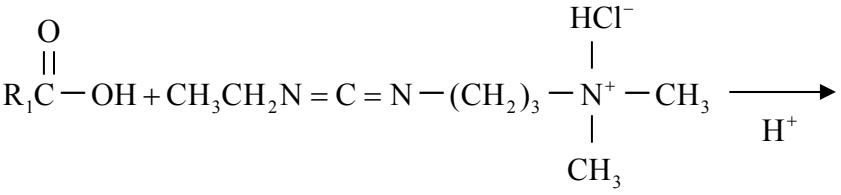

D

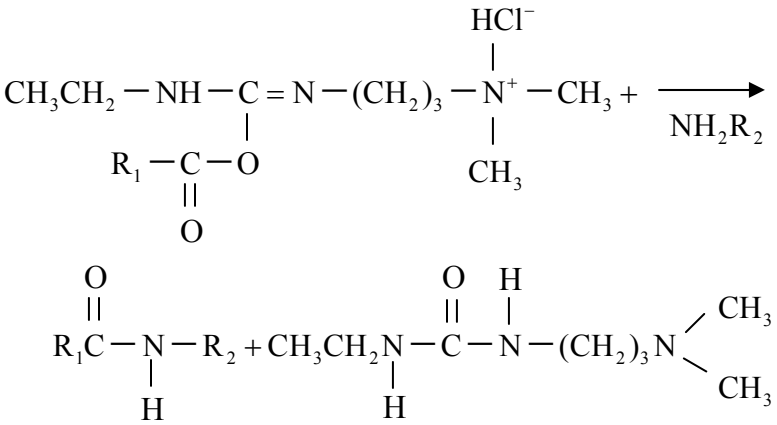

Figure 2-3. EDC coupling reaction for negative charge neutralization on MARCKS. A) Structure of 1-Ethyl-3-(3-Dimethylaminopropyl) Carbodiimide Hydrochloride. (MW 191.7 Da), B) EDC coupling reaction in the presence of excess ethanolamine ($HOCH_2CH_2NH_2$). The specific nucleophile (NH_2R_2) provided in excess in our reaction is ethanolamine, and results in the covalent modification hereby illustrated, C) EDC reacts with carboxylic acid group and activates the carboxyl group, allowing it to be coupled to the amino group in the reaction mixture, D) EDC is released as a soluble urea derivative after displacement by the nucleophile.

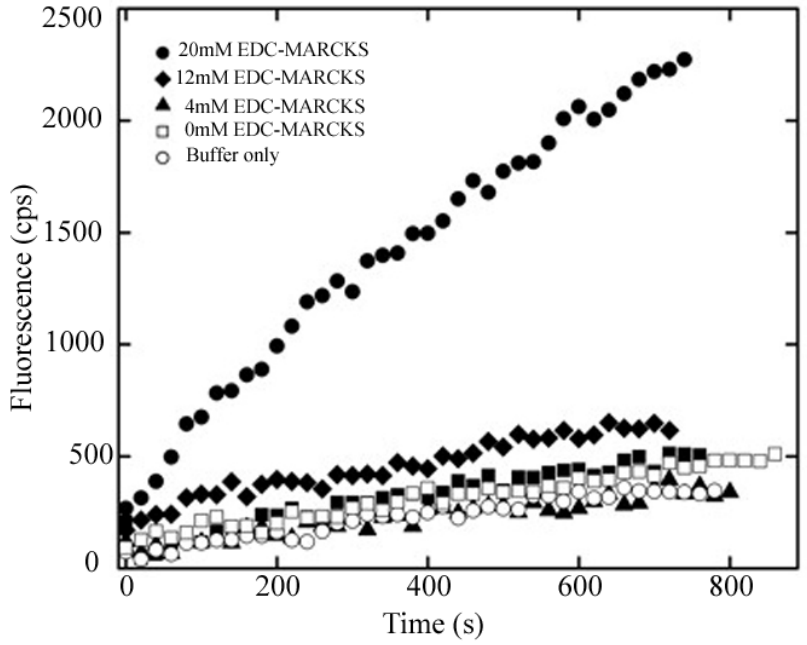

Figure 2-4. Effect of EDC neutralization of negative charges on MARCKS on actin polymerization. Untreated, 0 mM EDC and 4 m EDC-treated MARCKS do not accelerate the rate of actin polymerization as the PSD would alone. At 12 mM EDC treatment a slight acceleration in actin polymerization is observed and much more at 20 mM EDC treatment.

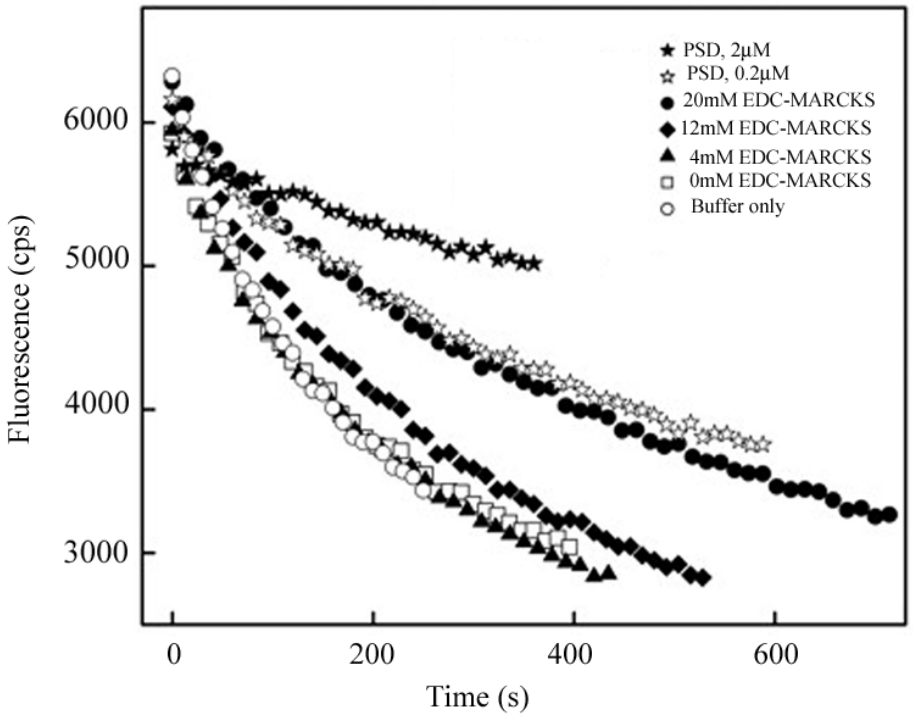

Figure 2-5. Effect of EDC neutralization of negative charges on MARCKS on actin depolymerization. 2 μM of 0 EDC and 4 m EDC-treated MARCKS do not affect the rate of actin depolymerization as the PSD does at both 0.2 and 2 μM. At 12 mM EDC treatment a slight slowing in actin polymerization is observed and much more at 20 mM EDC treatment. At 2 μM, 20 mM EDC-treated MARCKS affects depolymerization similarly to 0.2 μM PSD.

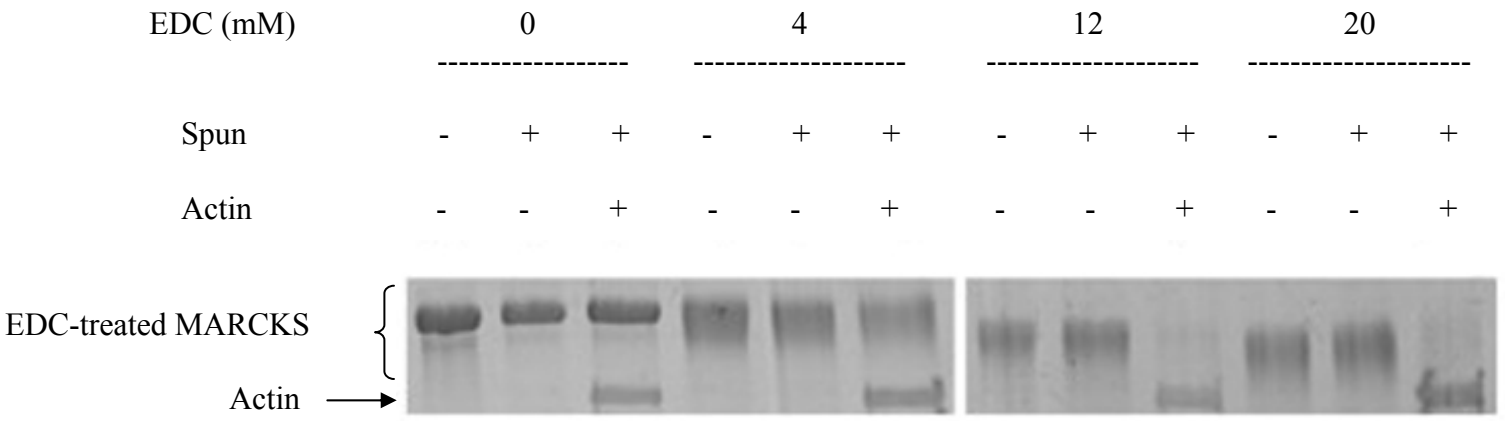

Figure 2-6. Effect of EDC neutralization of negative charges on MARCKS on F-actin binding. Increasing concentrations of EDC (4, 12 and 20 mM) in the presence of ethanolamine were used to neutralize some acidic residues on MARCKS by conjugating them with ethanolamine. At 0 and 4 mM EDC, MARCKS does not bind to and pellet with F-actin in a high speed F-actin pelleting assay. However, at 12 and 20 mM EDC, MARCKS disappears from the supernatant and pellets with F-actin.

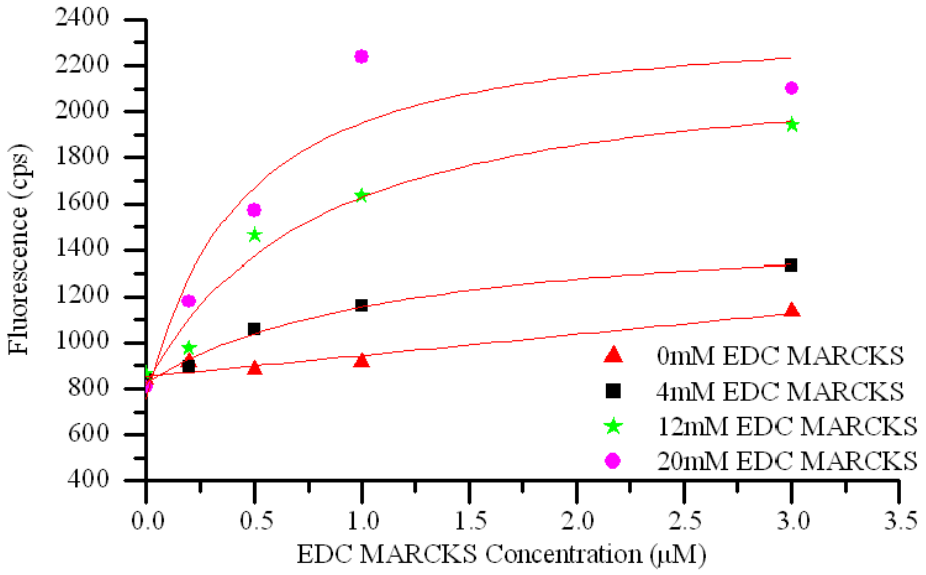

Figure 2-7 Effect of EDC neutralization of negative charges on MARCKS on calmodulin binding. Without EDC charge neutralization, MARCKS binds minimally to MIANS-labeled calmodulin. However, EDC treated MARCKS binds to MIANS-calmodulin increasingly with increasing EDC concentrations used to neutralize the charges.

A

GAQFSKTAAKGEATAERPGEAAVASSPSKANGQENGHVKVNGDASPAAAEPGAKEEL
QANGSAPAADKEEPASGSAATPAAAEKDEAAAATEPGAGAADKEAAEAEPAEPSSPAA
EAEGASASSTSSPKAEDGAAPSPSSETP***KKKKKRFSFKKSFKLSGFSFKKSKK***

B

SETP***KKKKKRFSFKKSFKLSGFSFKKSKK***ESGEGAEAEGATAEGAKDEAAAAAGGEGA
AAPGEQAGGAGAEGAAGGEPREAEAAEPEQPEQPEQPAAEEPQAEEQSEAAGEKAEEP
APGATAGDASSAAGPEQEAPAATDEAAASAAPAASPEPQPECSPEAPPAPTAE

Figure 2-8. Amino acid sequence of MARCKS truncation proteins. A) MARCKS N-terminus + PSD. B) MARCKS C-terminus + PSD.

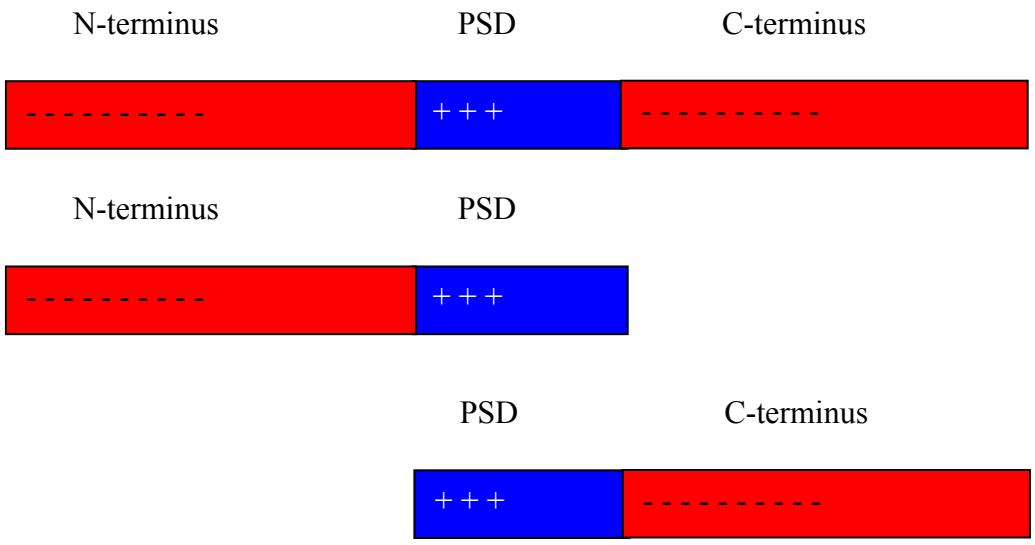

Figure 2-9. Schematic diagram of MARCKS truncations. A) Full length MARCKS. B) PSD+MARCKS N-terminus protein. C) PSD+MARCKS C-terminus protein.

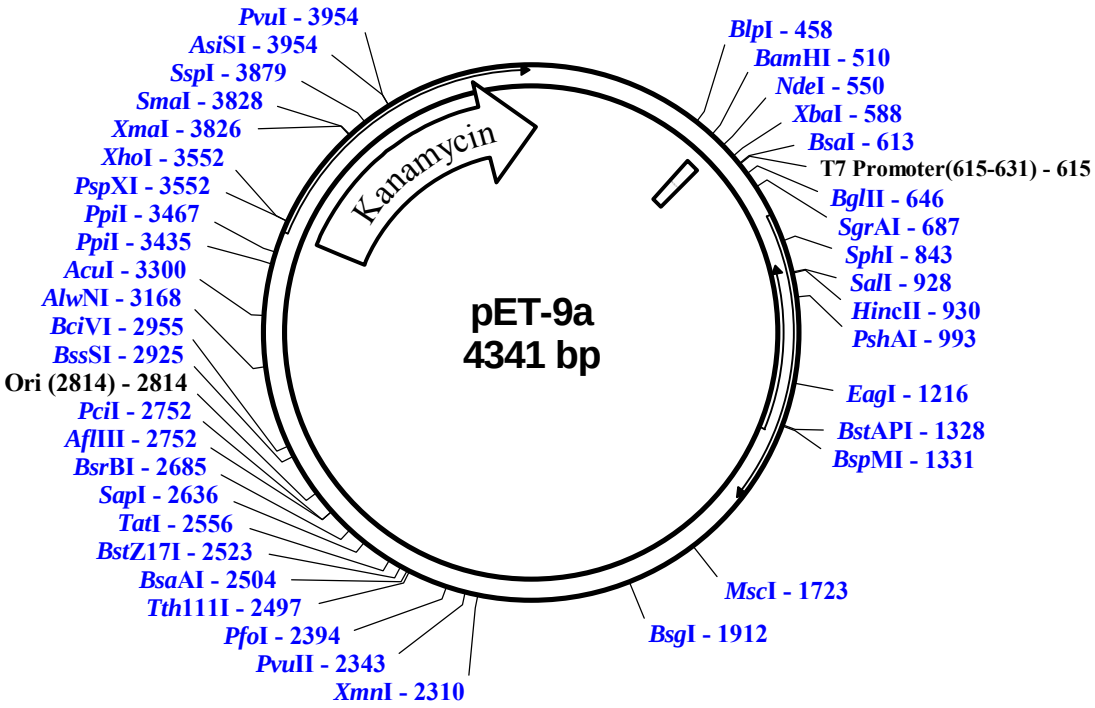

Figure 2-10. Novagen's pET-9a bacterial expression vector. MARCKS N-and C-terminus truncations were cloned using the NdeI and BamHI restriction sites under the control of the T7 promoter.

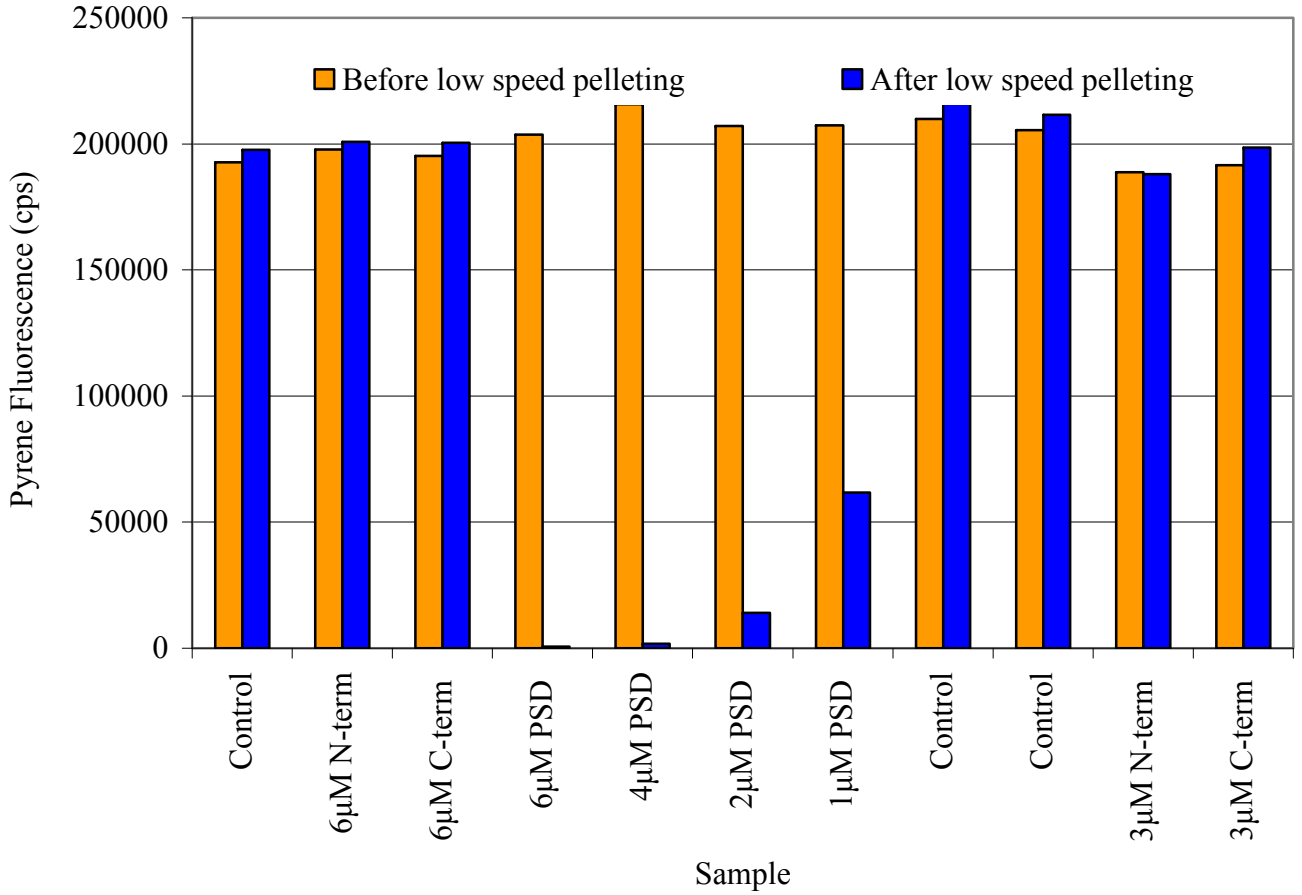

Figure 2-11.Effect of MARCKS truncations and PSD on F-actin bundling. Fluorescence of pyrenyl actin is measured in the supernatants before and after a low speed spin. The PSD shows a dose-dependent effect on F-actin bundling at 1, 2, 4 and 6 μM, but neither N- nor C-termini show any bundling at 3 or 6 μM concentrations.

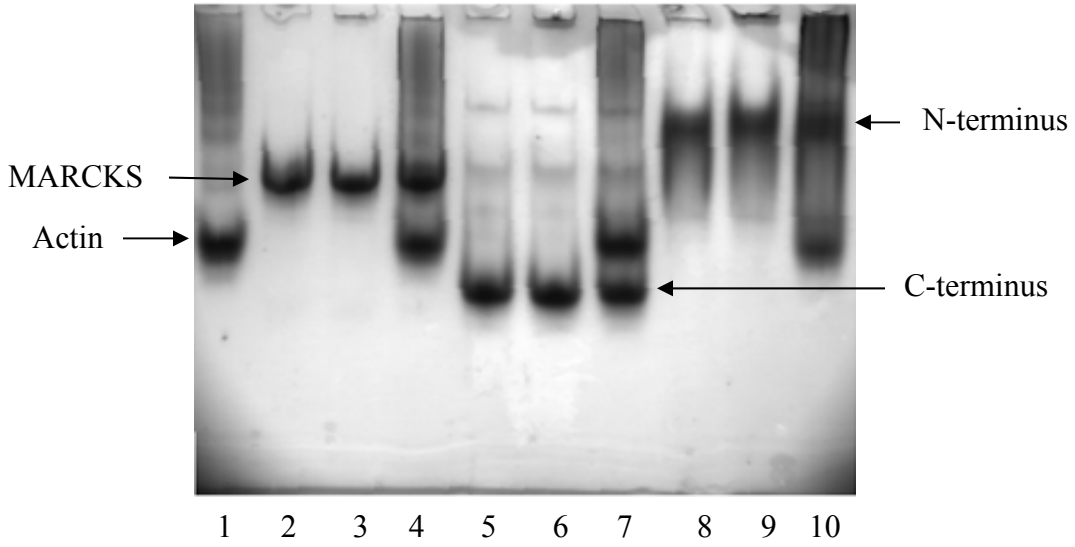

Figure 2-12. Coomassie stained native gel of MARCKS proteins with actin and rhodamine-labeled PSD. 1) Actin, 2) MARCKS, 3) MARCKS and Rh-PSD, 4) MARCKS and actin, 5) C-terminus, 6) C-terminus and Rh-PSD, 7) C-terminus and actin, 8) N-terminus, 9) N-terminus and Rh-PSD, 10) N-terminus and actin.

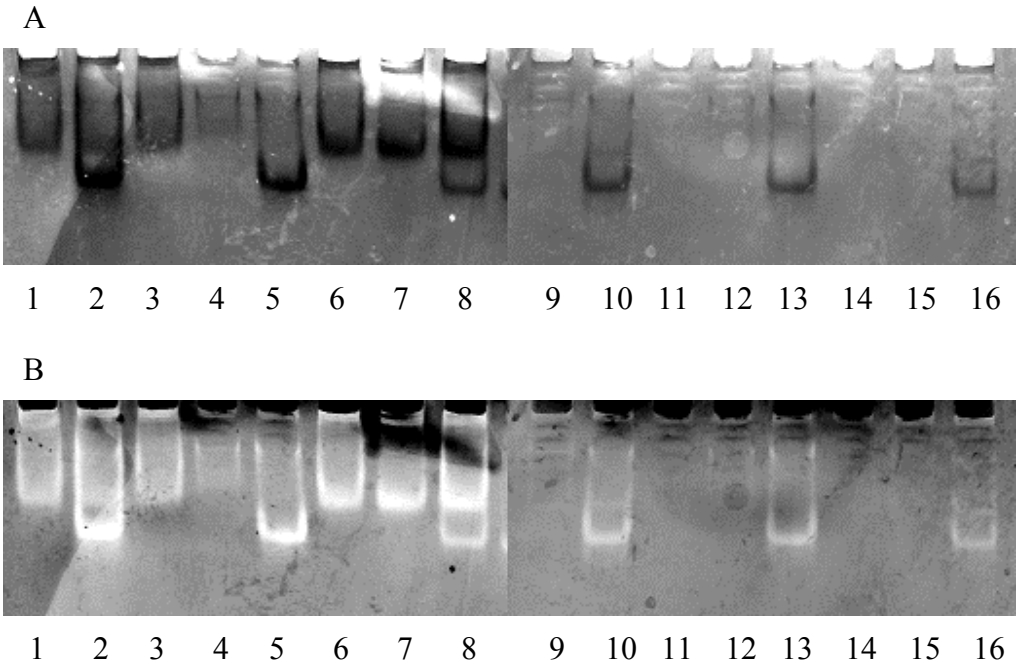

Figure 2-13. Actin high speed pelleting assay with MARCKS truncations. A, 1) 6μM N-term. + 3μM F-actin, 2) 6μM C-term. + 3μM F-actin, 3) 3μM F-actin, 4) 6μM N-term, 5) 6μM C-term., 6) 3μM F-actin, 7) 3μM N-term. + 3μM F-actin, 8) 3μM C-term. + 3μM F-actin, 9) 6μM N-term. + 3μM F-actin, 10) 6μM C-term. + 3μM F-actin, 11) 3μM F-actin, 12) 6μM N-term, 13) 6μM C-term., 14) 3μM F-actin, 15) 3μM N-term. + 3μM F-actin, 16) 3μM C-term. + 3μM F-actin. B, invert of A. In both A and B, 1-8, unspun samples, 9-16, samples after high-speed spin: 1 hour at 65,000rpm at 12°C. See text for details.

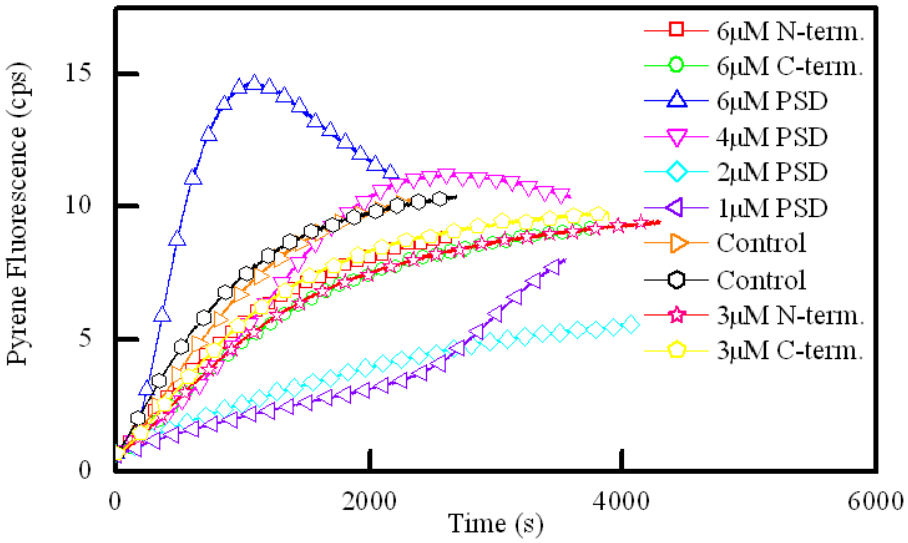

Figure 2-14. Effect of MARCKS truncations on the time course of actin polymerization. At 3 and 6 μM concentrations, both the N- and C-termini of MARCKS very slightly slow down the rate of actin polymerization. PSD is shown as a control.

CHAPTER 3
SEARCHING FOR AN INTERNAL BINDING SITE ON MARCKS

Introduction

Experiments described in Chapter 2 support our hypothesis that ionic intramolecular interactions are occurring within MARCKS molecules, rendering the protein inactive in our biochemical assays. The nature of these interactions is still unclear: are we looking at a single high affinity internal binding site for the PSD on the rest of the protein, or non-specific ionic interactions? In the former case, can such a binding site be identified? In the latter case, are these occurring with both ends of the protein or just one? Could there be more than one site of interaction for the PSD with each terminus of MARCKS?

We attempted to answer these questions using two approaches. In the first approach, we used mass spectrometry to sequence the PSD binding site on MARCKS. In the second approach, we employed a direct binding assay based on fluorescence anisotropy using the MARCKS truncations created and described in Chapter 2 and a rhodamine-labeled synthetic external PSD.

Mass Spectrometric Determination of Internal Binding Site of MARCKS

Mass Spectrometry

Mass spectrometry (MS) is an analytical technique that measures the mass-to-charge ratio of ions. MS has been an established technique in organic chemistry for many years. It is an enormously sensitive technique that requires very little material. Masses can be obtained with great accuracy, often with an error of less than one part in a million. Until recently, however, the very low volatility of proteins made mass spectrometry useless for the investigation of these molecules. This difficulty has been circumvented by the introduction of techniques for effectively dispersing proteins and other macromolecules into the gas phase (namely matrix-assisted laser desorption-ionization (MALDI) [215-217] and electrospray ionization (ESI) [218-

221]). Mass spectrometry allows one to determine the precise mass of intact proteins and of peptides derived from them by enzymatic or chemical cleavage. This information can then be used to search genomic databases, in which the masses of all proteins and of all their predicted peptide fragments have been tabulated. A match to a particular open reading frame can often be made knowing the mass of only a few peptides derived from a given protein. Mass spectrometry has permitted the development of peptide mass fingerprinting. Following two-dimensional gel electrophoresis, the sample of interest is extracted and chemically or enzymatically cleaved. The masses of the protein fragments are then determined by MS. Finally, the peptide masses, or fingerprint, are matched against the fingerprint found in databases of proteins that have been "electronically cleaved" by a computer simulating the same fragmentation technique used for the experimental sample. Mass spectrometry is also used to determine the sequence of amino acids of individual peptide fragments. Peptide sequencing is also important if proteins contain post-translational modifications, such as attached carbohydrates, phosphates, or methyl groups. In this case, the precise amino acids that are the sites of modifications can usually be determined. To obtain such peptide sequence information, two mass spectrometers are required in tandem. The first separates peptides obtained after digestion of the protein of interest and allows one to zoom in on one peptide at a time. This peptide is then further fragmented by collision with high-energy inert gas atoms (e.g., argon, xenon), which preferentially cleave the peptide bonds, generating a ladder of fragments, each differing by a single amino acid. The second mass spectrometer then separates these fragments and displays their masses. The amino acid sequence can be deduced from the differences in mass between the peptides. Post-translational modifications are identified when the amino acid to which they are attached show a characteristically increased mass.

Methods

Biotin-labeled PSD was synthesized at the University of Florida's Protein Core, having the following sequence KKKKKRFSFKKSFKLSGFSFKKSKKSK-biotin. Experiments to elucidate the internal binding site of the PSD on MARCKS were done by immobilizing the biotin-PSD on a streptavidin column, followed by addition of MARCKS to those columns either before or after digestion with an endoproteinase as described in detail in the following protocols. MARCKS fragments were then eluted from the column using a salt gradient, desalted and sent for mass spectrometric analysis.

AspN pre-column digest

Three milliliters of MARCKS (3 mL of 10 μM MARCKS =0.9 mg MARCKS (0.3 mg/mL) = 30 nmoles) were dialyzed into Asp-N digestion buffer (50 mM sodium phosphate buffer, pH 7.9). MARCKS was then digested with endoproteinase AspN (4 μg AspN, 1:225 ratio) overnight at 37°C in a waterbath. A 0.5 mL streptavidin column (Ultralink Immobilized Streptavidin Plus, Product #53117 Lot # HI106344) was equilibrated with 1X PBS and 0.75 mL of 1 mg/mL (220 nmoles) MARCKS PSD-EK-biotin (diluted in 100 mM MES, 50 mM NaCl, pH 4.9) were bound to the streptavidin column for 1 hour at room temperature on a rotator. The biotin-PSD column was equilibrated with 10 mM Tris, pH 7.9. The AspN digest was boiled for 10 minutes to inactivate AspN, and then kept on ice. It was then diluted 1:20 with 10 mM Tris, pH 7.9, no KCl before applying to biotin-PSD column. The AspN digested material was applied to the biotin PSD column and allowed to bind by reapplying flow through to the column at RT multiple times. The column was washed with 10 mM Tris, pH 7.9 (No KCl), followed by a 1 mL step gradient of 10 mM Tris, pH 7.9 with 50 mM KCl increments (50,100,150,200,250,300,400,500,1000 mM KCl). One milliliter fractions were collected. Fractions were desalted using a MacroSpin column packed with Vydac C18 with a loading

capacity of 300 µg (Catalog number SMM SS18V, Nest Group, Southborough, MA). The column was rinsed with acetonitrile, equilibrated

and washed with 0.1% TFA, and fragments eluted with 80% acetonitrile and 20% TFA. Fragments were then run on the QSTAR® XL Hybrid LC/MS/MS system (a high-performance, hybrid quadrupole time-of-flight mass spectrometer) mass spectrometer at the University of Florida's Protein core with an LC Packings HPLC to obtain sequence data.

Glu-C on column digest

Ten milliliters of MARCKS (10 mL of 6 µM MARCKS= 60 nmoles MARCKS) were dialyzed into 10 mM Tris-HCl, pH 7.9. A 1 mL streptavidin column (Ultralink Immobilized Streptavidin Plus, Product #53117 Lot # HI106344) was equilibrated with 1XPBS and 2 mL of 1 mg/mL (570 nmoles) MARCKS PSD-SK-biotin (diluted in 1XPBS) were bound to the streptavidin column for 1 hour at room temperature on a rotator. The streptavidin-biotin-PSD column was then equilibrated with 10 mM Tris-HCl, pH 7.9 and 10 mL MARCKS bound to the equilibrated column in 10 mM Tris-HCl, pH 7.9 on a rotator at 4ºC overnight. The resin was allowed to settle and the buffer to pass through, flow through collected and UV scan (240-300nm) showed it contained some MARCKS. The column was then equilibrated with endoproteinase GluC digestion buffer (25 mM ammonium bicarbonate, pH 8) and 100 µg GluC dissolved in 500 µL ammonium bicarbonate buffer, pH 8 added to the column. Digestion was allowed to take place at RT for 7 hours on a rotator. Following the digestion, the resin was allowed to settle for 30 minutes then a step gradient of 10 mM Tris, pH 7.9 with 50 mM KCl increments was carried out (1 mL of each salt concentration was added and fractions collected): 50, 100, 150, 200, 250, 300, 400, 1000 mM KCl. Fractions were boiled for 10 minutes to inactivate GluC then frozen at -80°C until sent for mass spec analysis. Fractions were desalted using a MacroSpin column packed with Vydac C18 with a loading capacity of 300 µg (Catalog

number SMM SS18V, Nest Group, Southborough, MA). The column was rinsed with acetonitrile, equilibrated and washed with 0.1% TFA, and fragments eluted with 80% acetonitrile and 20% TFA. Fragments were run on the QSTAR® XL Hybrid LC/MS/MS system (a high-performance, hybrid quadrupole time-of-flight mass spectrometer) mass spectrometer at the University of Florida's Protein core with the LC Packings HPLC to obtain sequence data.

Results

We used the observation that the intramolecular interaction between the PSD and MARCKS has a strong ionic component to elute MARCKS fragments from a biotinylated PSD immobilized on a streptavidin column using a KCl salt gradient. Resulting fragments were subjected to mass spectrometry to determine which fragments of MARCKS had the highest affinity to the PSD. When AspN was used to digest MARCKS, we obtained poor coverage of MARCKS (about 30%), mostly in the N-terminus of the protein. AspN generated MARCKS fragments that were too large for the mass spectrometer we were employing. AspN did not cut MARCKS often enough and generated larger fragments of MARCKS, especially at the C-terminus. The majority of the N-terminus seemed to come off in the washes (Figure 3-1), suggesting that it did not bind to the PSD. However, a few fragments at the N-terminus were not present and thus we cannot eliminate the possibility that those are interacting with the PSD. The fact that we were not seeing most fragments of the C-terminus could simply be due to the previously mentioned problem that AspN fragments of MARCKS were too large for detection by electrospray mass spectrometry and we may need to use MALDI-TOF which can tolerate larger fragment sizes, or that they were indeed binding to PSD. This problem was solved by using GluC instead of AspN in our digestion, since GluC cuts MARCKS about 50 times and generates fragments of optimal size for detection by electrospray LC- MS/MS. These fragments were then run onto a mass spectrometer (Table 3-1) and as expected we found most of the protein in the

flow through and washes (Figure 3-2, A and B), but some peptides did not elute below 200 mM KCl concentration (Figure 3-2, E). The sequence for these peptides could be obtained to 95% probability and we obtained nice spectra for these peptides. Only 3 fragments seemed to persist at the higher salt concentration (150 mM KCl), one of them located at the N-terminus of MARCKS and two at the C-terminus. Their sequences are: AAEAEPAEPSSPAAEAEG, AAAAAGGEGAAAPGEQAGGAGAEGAAGGEPREAE and AAASAAPAASPEPQPE. Interestingly, the identified N-terminus fragment was missing from the AspN washes (DKEAAEAEPAEPSSPAAEAEGASASSTSSPKAE) and may either mean that it was binding to PSD or that it was too large to detect (33 amino acids, monoisotopic MW 3159.4084Da).

Use of MARCKS Truncations to Determine PSD-Interacting Terminus

In order to narrow down the location of the PSD binding site on MARCKS, we decided to use our truncated MARCKS proteins (described in Chapter 2) in direct binding assays with a rhodamine-labeled synthetic PSD. We hypothesize that if a single binding site for the PSD was present on one of the termini of MARCKS or if PSD bound to multiple sites on a single terminus, then we would only see binding of our external PSD to that terminus. Similarly, if the PSD interacts with both termini of MARCKS, then we would observe interaction of our rhodamine-labeled PSD with both truncations of MARCKS.

In the first set of experiments, we used a technique based on the change in fluorescence anisotropy of the rhodamine-labeled PSD upon binding to other proteins, i.e. MARCKS truncations. In the second set of experiments, we used native gel electrophoresis to detect PSD-MARCKS truncations interactions.

Fluorescence Anisotropy Assays

Fluorescence anisotropy is a technique for measuring the binding interaction between two molecules and can be used to measure the binding or dissociation constants for the interaction. It

is based on the fact that when a fluorophore is excited by polarized light, it will also emit polarized light. However, if a molecule is moving, it will scramble the polarization of the light by radiating at a different direction from the incident light. The scrambling effect is greatest when the fluorophores are tumbling freely in solution and decreases with decreased rate of tumbling. We can measure protein interactions by labeling a protein (preferably a small protein or peptide) with a fluorophore; once that labeled protein binds to another protein or molecule forming a larger, more stable complex in solution, it will tumble more slowly, resulting in an increase in the polarization of the emitted light and reducing the scrambling effect. The extent of polarization is proportional to the amount of protein complex formed and that is also proportional to the amount of the binding partners in solution. Thus, we can titrate the amount of one of the proteins and generate a binding curve.

The anisotropy is defined as the ratio of the difference between the emission intensity parallel to the polarization of the electric vector of the exciting light and that perpendicular to that vector divided by the total intensity. Because the anisotropy of emission (A) is related to the correlation time of the fluorophore through the Perrin equation $A_0/A\text{-}1 = \tau/\tau_c$ where A_0, is the limiting anisotropy of the probe, which depends on the angle between the absorption and emission transition dipoles, and τ is the fluorescence lifetime, these measurements can be used to obtain hydrodynamic information concerning macromolecules and macromolecular complexes [222, 223].

For our anisotropy assays, we synthesized a tetramethylrhodamine-labeled PSD [4, 224, 225]. This peptide was used in both a direct binding assay with our truncated MARCKS proteins, which allowed us to calculate a binding constant for each of the proteins, and in a competition assay with unlabeled synthetic PSD as the competitor in the presence of our

MARCKS truncations [210]. The purpose of the competition assay was to determine the stoichiometry of the interaction between MARCKS truncation proteins and external PSD.

Direct binding anisotropy assay

In this assay, 0.15 μM Tetramethylrhodamine-5-maleimide-labeled PSD (Rh-PSD) was added to increasing concentrations of MARCKS truncation proteins (N-terminus or C-terminus) in MARCKS gel filtration buffer (10 mM Tris, 40 mM KCl, 5 mM β-mercaptoethanol, pH 7.9). Data were collected on a Photon Technology International (South Brunswick, NJ) spectrofluorimeter. Tetramethylrhodamine-5-maleimide-labeled PSD was excited with vertically polarized light at 546 nm. The horizontal and vertical components of the emitted light were detected at 568 nm.

Competition anisotropy assay

In this assay, a constant amount of Tetramethylrhodamine-5-maleimide-labeled PSD (0.2 μM) and a constant amount of either MARCKS truncation proteins (0.5 μM, chosen from direct binding anisotropy data) were added to increasing concentrations of unlabeled PSD (0-100 μM). Reactions were carried out in MARCKS gel filtration buffer (10 mM Tris, 40 mM KCl, 5mM β-mercaptoethanol, pH 7.9). Data were collected on a Photon Technology International (South Brunswick, NJ) spectrofluorimeter. Tetramethylrhodamine-5-maleimide-labeled PSD was excited with vertically polarized light at 546 nm. The horizontal and vertical components of the emitted light were detected at 568 nm.

Native Gel Electrophoresis with Fluorescently Labeled PSD

"Native" or "non-denaturing" gel electrophoresis is run in the absence of SDS or any denaturing agents. While in SDS-PAGE the electrophoretic mobility of proteins depends primarily on their molecular mass, in native PAGE the mobility depends on both the protein's charge and its hydrodynamic size [226-229].

The electric charge driving the electrophoresis is governed by the intrinsic charge on the protein at the pH of the running buffer. This charge depends on the amino acid composition of the protein as well as post-translational modifications.

Since the protein remains folded, its hydrodynamic size and mobility on the gel will also vary with its conformation (higher mobility for more compact conformations, lower for larger structures like oligomers). If native PAGE is carried out near neutral pH to avoid acid or alkaline denaturation, then it can be used to study conformation, self-association or aggregation, and the binding of other proteins or compounds.

For native gel electrophoresis of proteins, either polyacrylamide or agarose gels can be used. We used both types of gels to look for complex formation between the rhodamine-labeled PSD and MARCKS truncation proteins.

Native PAGE of rhodamine-labeled PSD and MARCKS truncations

To look for interactions between Rh-PSD and MARCKS proteins, we mixed 11 μM Rh-PSD with MARCKS (5 μM), MARCKS C-terminus (5 μM), and MARCKS N-terminus (14 μM). Samples were incubated for 30 minutes at room temperature, mixed with native sample buffer and loaded on a 7% Tris-Tricine native gel (25 mM Tris-Tricine, 0.1 mM $CaCl_2$, 0.01 mM NaN_3, 0.2 mM ATP and 0.2 mM DTT, pH 8.3) [230]. Gel electrophoresis was carried out at 100V constant. The gel was first visualized under UV to look for fluorescence of Rh-PSD then stained with Coomassie Brilliant Blue G-250 protein staining dye.

Native agarose gel electrophoresis of rhodamine-labeled PSD and MARCKS truncations

Samples were prepared exactly as described for Native PAGE and run in a 2% agarose gel made in Tris-Tricine native buffer (25 mM Tris-Tricine, 0.1 mM $CaCl_2$, 0.01 mM NaN_3, 0.2 mM ATP and 0.2 mM DTT, pH 8.3). Gel electrophoresis was carried out at a constant 100 V.

Results

Both the N-and C-termini of MARCKS bound with high affinity to an external rhodamine-labeled PSD (Figures 3-3 and 3-4), which is consistent with them being inactive in our actin-binding assays as shown in chapter 2. The N-terminus has a lower K_d than the C-terminus (0.07μM versus 0.28 μM). A competition assay with both rhodamine-labeled and unlabeled external PSD to determine specificity of the interaction showed that the N-terminus only has one binding site for the PSD, whereas it takes about 5 times more unlabeled PSD to compete off the labeled PSD off of the C-terminus, suggesting multiple binding sites for the PSD on the C-terminus (Figures 3-5 and 3-6). Some may be specific whereas others may be non-specific and their affinities for the PSD may vary. An overlay of direct binding and competition anisotropy data for the N-and C-termini of MARCKS is shown in Figure 3-7. Both agarose and polyacrylamide native gels suggest that the N-terminus interacts more strongly with the rhodamine-labeled PSD (Figures 3-8 and 3-9). The smear formed by Rh-PSD interacting with N-terminus was expected given that the N-terminus itself runs as a smear or forms a ladder on a native gel (Figure 3-10) further suggesting that it has the ability to form oligomers due to an intramolecular binding site that can become intermolecular.

Conclusions

The PSD can interact with multiple sites on MARCKS. Mass spectrometry has identified three possible sites, one at the N-terminus and two at the C-terminus. This is consistent with the data in Chapter 2 which showed that removing either end does not render MARCKS active and with binding and competition data showing that both N- and C-terminus of MARCKS can interact with external PSD.

It is important to note that our experiments were carried out in 40 mM KCl, which is about three times lower than the intracellular salt concentration. Under these conditions, the C-

terminus of MARCKS may not be interacting at all with its phosphorylation site domain, and the N-terminus, which has a higher affinity binding site for the PSD as shown in our assays may. This can easily be determined by repeating the binding and competition assays using 100-150 mM KCl, which is more physiological.

Specific proteolysis N-terminal to the PSD, post-translational modifications, changes in ionic strength or binding by other proteins are all mechanisms by which MARCKS may be activated *in vivo*. Interestingly, three cleavage sites for MARCKS have been described (Figure 1-2), all cutting the protein N-terminal to the PSD, and two of which would remove the PSD binding site we have identified at the N-terminus (residues 103-119 in murine MARCKS). One cut site is between Asn 147 and Glu 148 (found only in human and bovine MARCKS) and the other between Ser 126 and Ser127 (present in all species). In addition, serine residues in our identified PSD binding sites both at the N- and C-termini were reported to be phosphorylated: at the N-terminus binding site, residues 103-119, Ser 113 was reported to be phosphorylated. At the C-terminus, where we identified residues 189-222 and 282-297 as two potential PSD binding site, Ser 291 was reported to be phosphorylated in rat MARCKS. These post-translational modifications and proteolysis may account for the activity of MARCKS *in vivo* and MARCKS purified from brain compared to the recombinant, bacterially expressed protein we used in our actin and calmodulin-binding assays with little to no success.

Table 3-1. Mass spectrometry results of GluC MARCKS fragments bound to biotin-PSD.

Fraction	Peptide sequence	Best peptide identification probability	Best Mascot Ion score	Best Mascot identity score	Best X! Tandem - log(e) score	Calculated peptide mass (AMU)
FT	AAAATEPGAGAADKE	95.00%	59.50	55.50	6.510	1329.6288
FT	AAASAAPAASPEPQPE	95.00%	39.40	55.30	2.060	1464.6973
FT	AAGEKAEEPAPGATAGDASSAAGPEQE	95.00%	00.00	00.00	5.960	2469.1018
FT	AAVASSPSKANGQENGHVKVNGDASPAAAE	93.40%	00.00	00.00	2.820	2837.3193
FT	AEPAEPSSPAAE	95.00%	46.10	55.00	4.920	1155.517
FT	AEPAEPSSPAAEAE	95.00%	42.30	55.30	3.620	1355.5967
FT	ATAERPGE	95.00%	50.10	56.60	0.921	830.4009
FT	GAAAPGEQAGGAGAE	95.00%	36.00	55.40	3.440	1213.545
FT	GAQFSKTAAKGE	95.00%	42.70	55.30	3.960	1194.6121
FT	GASASSTSSPKAE	95.00%	52.90	55.40	3.800	1179.5493
FT	KAEEPAPGATAGDASSAAGPE	95.00%	00.00	00.00	3.820	1883.8625
FT	KAEEPAPGATAGDASSAAGPEQE	95.00%	00.00	00.00	3.620	2140.9636
FT	LQANGSAPAADKEE	67.40%	00.00	00.00	1.660	1400.6659
FT	LQANGSAPAADKEEPASGSAATPAAAE	93.40%	00.00	00.00	2.820	2482.1697
FT	LQANGSAPAADKEEPASGSAATPAAAEKDE	95.00%	00.00	00.00	3.800	2854.3342
FT	NGHVKVNGDASPAAAE	95.00%	47.80	55.30	5.070	1536.7408
FT	NGHVKVNGDASPAAAEPG	95.00%	00.00	00.00	3.920	1690.8152
FT	NGHVKVNGDASPAAAEPGAKE	95.00%	42.10	54.70	2.960	2018.9899
FT	NGHVKVNGDASPAAAEPGAKEE	95.00%	00.00	00.00	5.920	2148.0325
FT	PAPGATAGDASSAAGPEQE	95.00%	00.00	00.00	3.260	1683.7463
FT	PGAGAADKE	67.40%	00.00	00.00	1.660	815.3901

Table 3-1. Continued 1.

Fraction	Peptide sequence	Best peptide identification probability	Best Mascot Ion score	Best Mascot identity score	Best X! Tandem - log(e) score	Calculated peptide mass (AMU)
FT	QPEQPAAEEPQAE	95.00%	00.00	00.00	3.420	1406.6079
FT	QPEQPAAEEPQAEE	89.20%	00.00	00.00	2.460	1552.677
FT	QPEQPEQPAAEEPQAE	95.00%	00.00	00.00	4.430	1760.7618
FT	QPEQPEQPAAEEPQAEE	95.00%	00.00	00.00	7.080	1906.8309
Wash	AAAATEPGAGAADKE	95.00%	70.90	55.50	6.000	1329.6288
Wash	AAASAAPAASPEPQPE	51.70%	35.10	55.30	- 0.362	1464.6973
Wash	AAGEKAEEPAPGATAGDASSAAGPE	95.00%	00.00	00.00	7.320	2212.0007
Wash	AAGEKAEEPAPGATAGDASSAAGPEQE	95.00%	00.00	00.00	4.440	2469.1018
Wash	AAVASSPSKANGQE	95.00%	46.30	55.70	3.220	1317.6287
Wash	AAVASSPSKANGQENGHVKVNGDASPAAAE	95.00%	00.00	00.00	4.600	2835.3511
Wash	AEPAEPSSPAAEAE	95.00%	55.40	55.20	5.060	1355.5967
Wash	ATAERPGE	95.00%	45.20	56.60	9.300	830.4009
Wash	GAAGGEPREAE	95.00%	45.40	55.60	1.720	1043.476
Wash	GASASSTSSPKAE	95.00%	57.40	55.40	3.920	1179.5493
Wash	KAEEPAPGATAGDASSAAGPE	87.10%	00.00	00.00	2.600	1883.8625
Wash	KAEEPAPGATAGDASSAAGPEQE	95.00%	00.00	00.00	6.420	2140.9636
Wash	LQANGSAPAADKEEPASGSAATPAAAE	95.00%	00.00	00.00	3.520	2482.1697
Wash	LQANGSAPAADKEEPASGSAATPAAAEKDE	95.00%	00.00	00.00	4.390	2854.3342
Wash	NGHVKVNGDASPAAAE	95.00%	45.40	54.90	0.495	1538.7089
Wash	NGHVKVNGDASPAAAEPGAKEE	95.00%	00.00	00.00	4.340	2148.0325
Wash	QPEQPEQPAAEEPQAE	95.00%	00.00	00.00	3.770	1777.7883

Table 3-1. Continued 2.

Fraction	Peptide sequence	Best peptide identification probability	Best Mascot Ion score	Best Mascot identity score	Best X! Tandem - log(e) score	Calculated peptide mass (AMU)
Wash	QPEQPEQPAAEEPQAEE	95.00%	00.00	00.00	4.020	1906.8309
50 mM KCl	AAAATEPGAGAADKE	95.00%	73.40	55.50	6.000	1329.6288
50 mM KCl	AAEAEPAEPSSPAAEAE	95.00%	00.00	00.00	4.320	1626.7136
50 mM KCl	AAGEKAEEPAPGATAGDASSAAGPE	95.00%	00.00	00.00	3.280	2212.0007
50 mM KCl	AAGEKAEEPAPGATAGDASSAAGPEQE	95.00%	00.00	00.00	5.100	2469.1018
50 mM KCl	AAVASSPSKANGQE	95.00%	41.60	55.70	0.854	1317.6287
50 mM KCl	AEPAEPSSPAAE	93.30%	00.00	00.00	2.680	1155.517
50 mM KCl	AEPAEPSSPAAEAE	95.00%	00.00	00.00	4.960	1355.5967
50 mM KCl	GAAAPGEQAGGAGAE	95.00%	00.00	00.00	2.920	1213.545
50 mM KCl	GAAAPGEQAGGAGAEGAAGGEPREAE	95.00%	00.00	00.00	7.960	2238.0022
50 mM KCl	GASASSTSSPKAE	95.00%	42.10	55.40	3.150	1179.5493
50 mM KCl	KAEEPAPGATAGDASSAAGPE	95.00%	00.00	00.00	3.200	1883.8625
50 mM KCl	KAEEPAPGATAGDASSAAGPEQE	95.00%	00.00	00.00	3.410	2140.9636
50 mM KCl	LQANGSAPAADKEEPASGSAATPAAAE	95.00%	00.00	00.00	3.750	2482.1697
50 mM KCl	LQANGSAPAADKEEPASGSAATPAAAEKDE	95.00%	00.00	00.00	9.960	2854.3342
50 mM KCl	NGHVKVNGDASPAAAE	67.10%	23.00	55.30	1.500	1536.7408
50 mM KCl	PAPGATAGDASSAAGPEQE	95.00%	00.00	00.00	4.390	1683.7463
50 mM KCl	QPEQPAAEEPQAEE	85.30%	00.00	00.00	2.170	1552.677
50 mM KCl	QPEQPEQPAAEEPQAE	95.00%	00.00	00.00	4.390	1777.7883
50 mM KCl	QPEQPEQPAAEEPQAEE	95.00%	00.00	00.00	3.770	1906.8309
100 mM KCl	AAAAAGGEGAAAPGEQAGGAGAE	73.40%	00.00	00.00	1.800	1811.8162

Table 3-1. Continued 3.

Fraction	Peptide sequence	Best peptide identification probability	Best Mascot Ion score	Best Mascot identity score	Best X! Tandem - log(e) score	Calculated peptide mass (AMU)
100 mM KCl	AAAAAGGEGAAAPGEQAGGAGAEGAAGGEPREAE	95.00%	00.00	00.00	5.460	2836.2732
100 mM KCl	AAAATEPGAGAADKE	95.00%	77.40	55.50	6.000	1329.6288
100 mM KCl	AAASAAPAASPEPQPE	95.00%	46.60	55.30	2.570	1464.6973
100 mM KCl	AAEAEPAEPSSPAAEAE	95.00%	00.00	00.00	5.750	1626.7136
100 mM KCl	AEPAEPSSPAAEAE	95.00%	44.70	55.20	4.050	1355.5967
100 mM KCl	ATAERPGE	95.00%	60.10	56.60	1.140	830.4009
100 mM KCl	GAAAPGEQAGGAGAEGAAGGEPREAE	95.00%	00.00	00.00	3.700	2238.0022
100 mM KCl	GAAGGEPREAE	95.00%	33.50	55.60	1.820	1043.476
100 mM KCl	LQANGSAPAADKEEPASGSAATPAAAE	94.00%	00.00	00.00	2.770	2482.1697
100 mM KCl	LQANGSAPAADKEEPASGSAATPAAAEKDE	95.00%	00.00	00.00	3.770	2854.3342
150 mM KCl	AAAAAGGEGAAAPGEQAGGAGAE	91.00%	00.00	00.00	2.600	1811.8162
150 mM KCl	AAAAAGGEGAAAPGEQAGGAGAEGAAGGEPREAE	95.00%	00.00	00.00	3.570	2836.2732
150 mM KCl	AAASAAPAASPEPQPE	95.00%	29.40	55.30	2.080	1464.6973
150 mM KCl	AAEAEPAEPSSPAAEAE	95.00%	00.00	00.00	6.620	1626.7136
150 mM KCl	AEPAEPSSPAAEAE	95.00%	39.50	55.30	1.020	1355.5967
150 mM KCl	ATAERPGEAAVASSPSKANGQE	95.00%	00.00	00.00	10.800	2128.0271
150 mM KCl	GAAAPGEQAGGAGAEGAAGGEPREAE	95.00%	00.00	00.00	3.570	2238.0022
150 mM KCl	KANGQENGHVKVNGDASPAAAEPGAKEE	82.40%	00.00	00.00	2.150	2757.3193
150 mM KCl	LQANGSAPAADKEEPASGSAATPAAAE	95.00%	00.00	00.00	5.310	2482.1697
150 mM KCl	LQANGSAPAADKEEPASGSAATPAAAEKDE	95.00%	00.00	00.00	12.800	2854.3342
150 mM KCl	NGHVKVNGDASPAAAEPGAKEE	95.00%	00.00	00.00	4.340	2148.0325

Table 3-1. Continued 4.

Fraction	Peptide sequence	Best peptide identification probability	Best Mascot Ion score	Best Mascot identity score	Best X! Tandem - log(e) score	Calculated peptide mass (AMU)
200 mM KCl	AAAAAGGEGAAAPGEQAGGAGAE	90.40%	00.00	00.00	2.750	1811.8162
200 mM KCl	AAAAAGGEGAAAPGEQAGGAGAEGAAGGEPREAE	95.00%	00.00	00.00	7.770	2836.2732
200 mM KCl	AAASAAPAASPEPQPE	95.00%	28.80	55.30	3.820	1464.6973
200 mM KCl	AAEAEPAEPSSPAAEAE	95.00%	00.00	00.00	6.280	1626.7136
200 mM KCl	AEPAEPSSPAAEAE	95.00%	37.40	55.30	3.220	1355.5967
200 mM KCl	GAAAPGEQAGGAGAEGAAGGEPREAE	95.00%	00.00	00.00	5.430	2238.0022
200 mM KCl	LQANGSAPAADKEEPASGSAATPAAAEKDE	87.00%	00.00	00.00	2.540	2854.3342

A

B

C

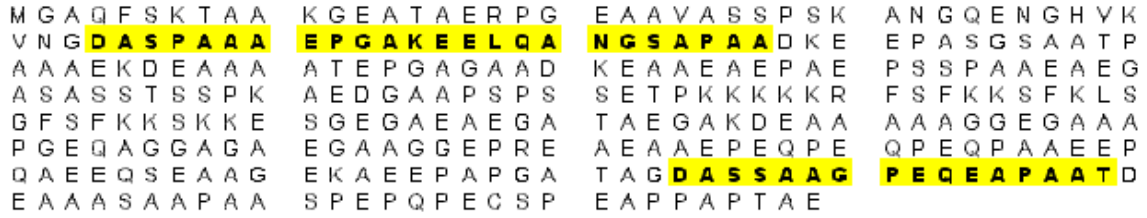

Figure 3-1. Peptide coverage for salt fractions of Asp-N digested MARCKS eluted from biotin-PSD column. A) Wash 1: 6 unique peptides, 6 unique spectra, 7 total spectra, 92/309 amino acids (30% coverage). B) Wash 2: 3 unique peptides, 5 unique spectra, 5 total spectra, 49/309 amino acids (16% coverage). C) Fraction 1: 50 mM KCl: 2 unique peptides, 2 unique spectra, 2 total spectra, 40/309 amino acids (13% coverage).

A

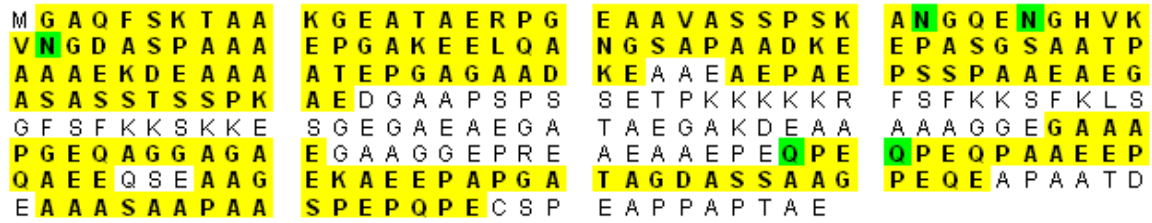

B

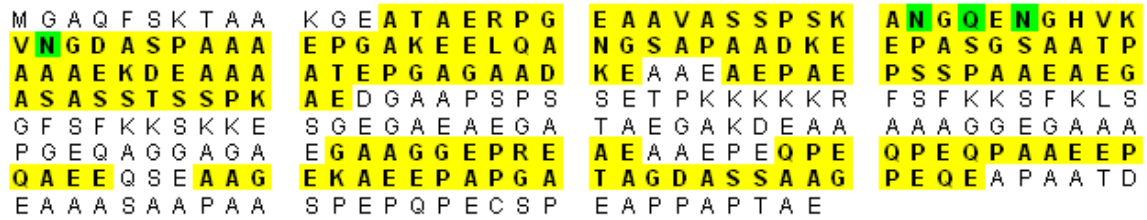

C

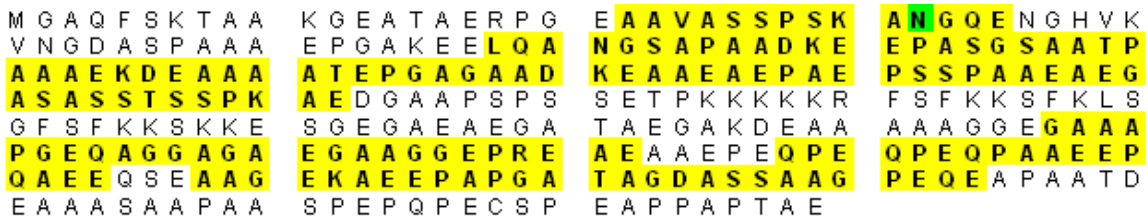

D

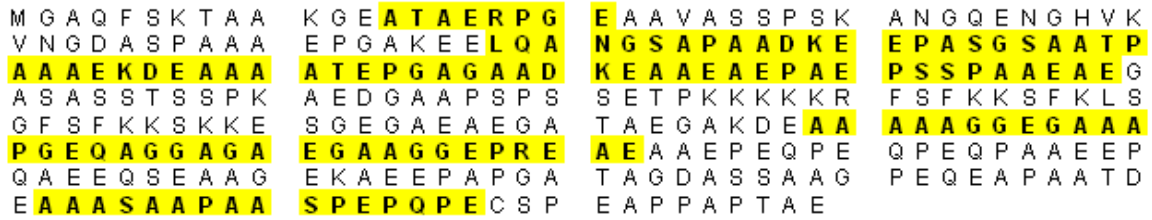

Figure 3-2. Peptide coverage for salt fractions of GluC digested MARCKS eluted from biotin-PSD column. A) Flow through: 22 unique peptides, 23 unique spectra, 27 total spectra, 203/309 amino acids (66% coverage). B) Wash: 16 unique peptides, 17 unique spectra, 20 total spectra, 171/309 amino acids (55% coverage). C) Fraction 1: 50 mM KCl: 17 unique peptides, 19 unique spectra, 20 total spectra, 159/309 amino acids (51% coverage). D) Fraction 2: 100 mM KCl: 10 unique peptides, 10 unique spectra, 10 total spectra, 120/309 amino acids (39% coverage). E) Fraction 3: 150 mM KCl: 10 unique peptides, 10 unique spectra, 10 total spectra, 141/309 amino acids (46% coverage). F) Fraction 4: 200 mM KCl: 6 unique peptides, 6 unique spectra, 6 total spectra, 67/309 amino acids (22% coverage).

E

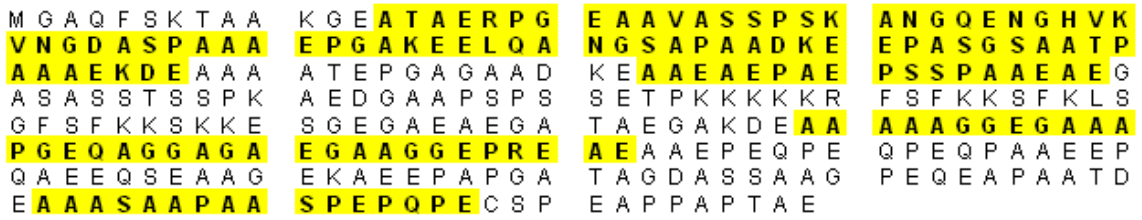

F

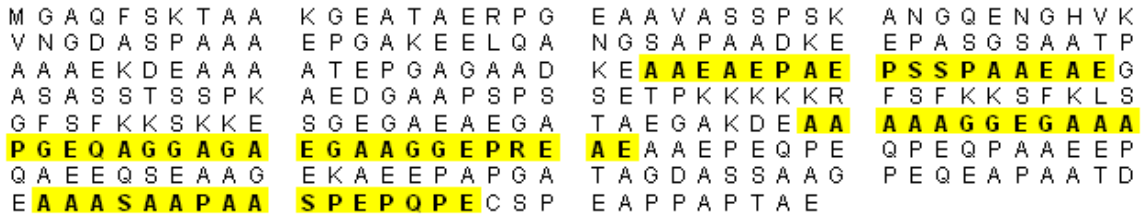

Figure 3-2. Continued.

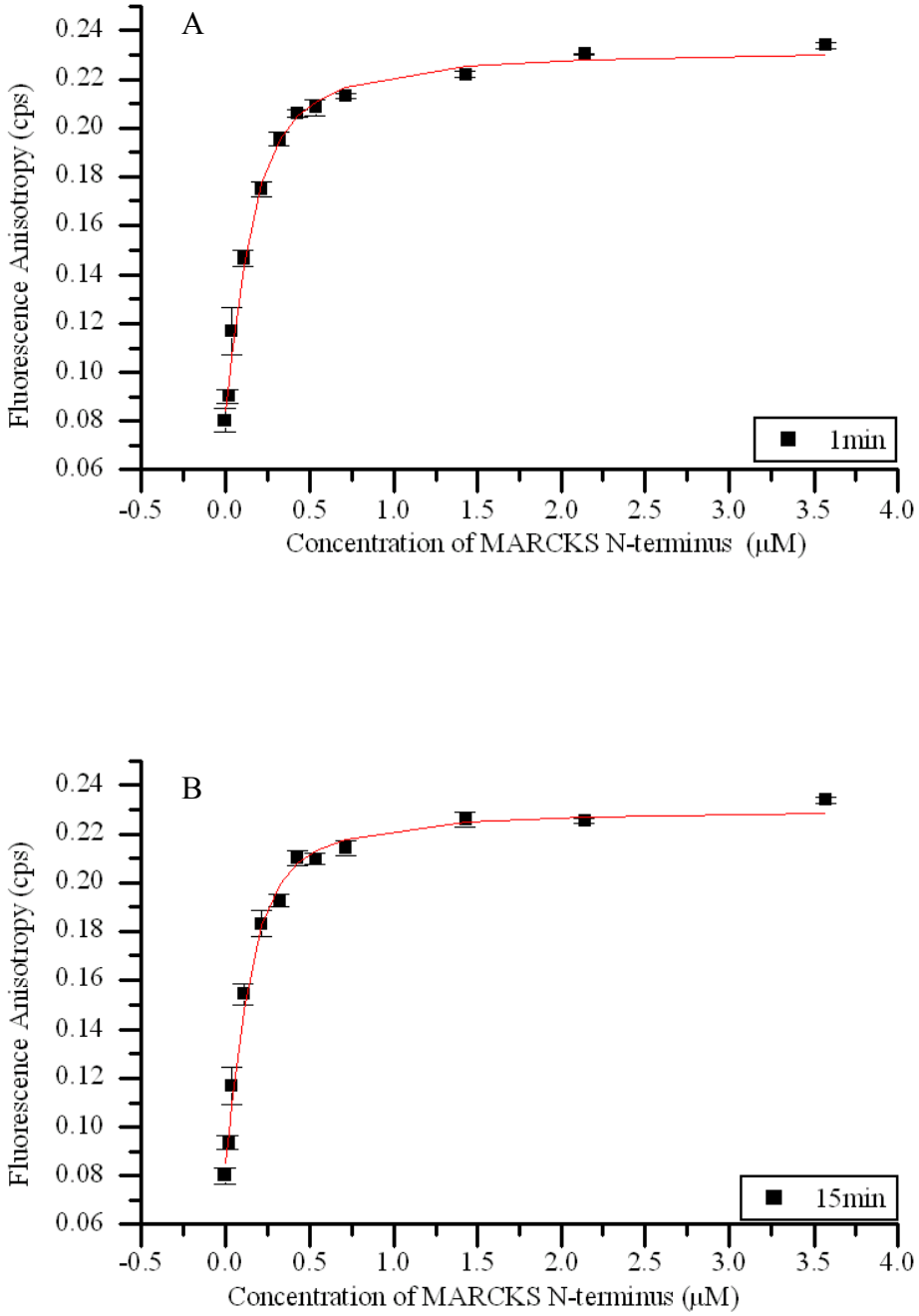

Figure 3-3. Direct binding fluorescence anisotropy of MARCKS N-terminus to Rh-PSD. A) 1 minute after addition of Rh-PSD to sample, where K_d=72nM. B) 15 minutes after addition of Rh-PSD to sample, where K_d=56nM.

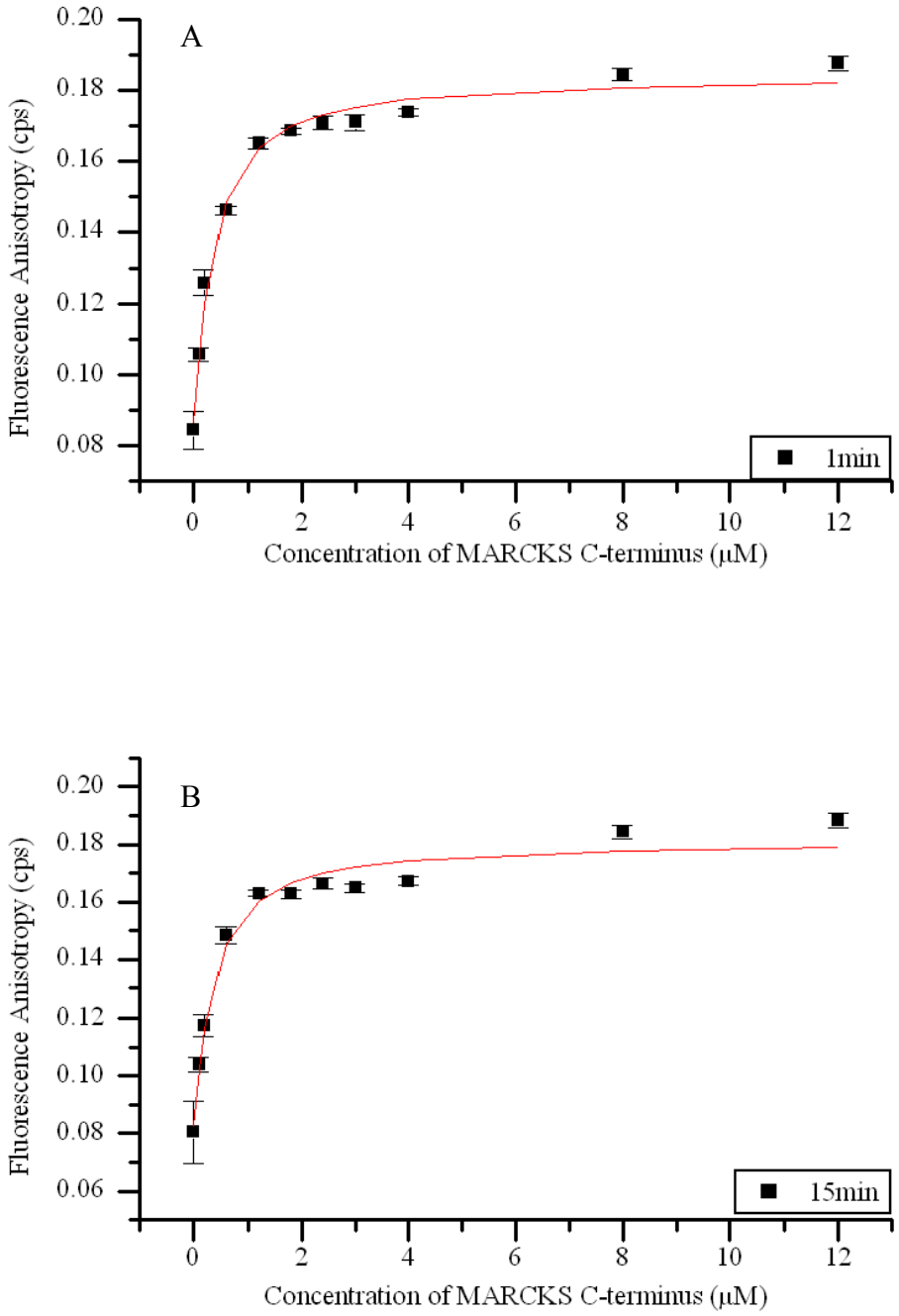

Figure 3-4. Direct binding fluorescence anisotropy of MARCKS C-terminus to Rh-PSD. A) 1 minute after addition of Rh-PSD to sample, where K_d=287nM. B) 15 minutes after addition of Rh-PSD to sample, where K_d=288nM.

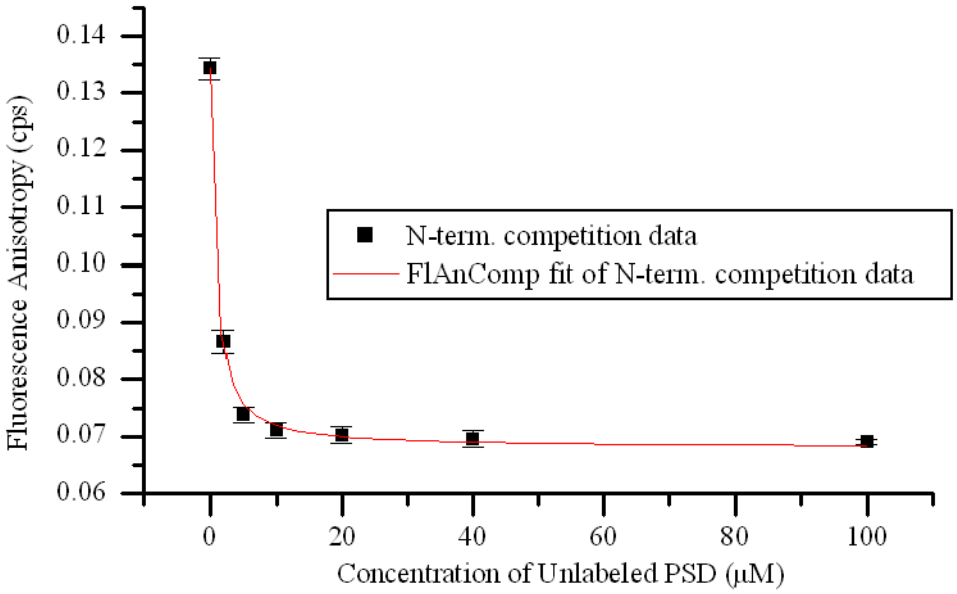

Figure 3-5. Fluorescence anisotropy competition with MARCKS N-terminus, Rh-PSD and unlabeled PSD. 0.5 μM N-terminus, 0.2 μM Rh-PSD and increasing concentrations of unlabeled PSD were used. Kl=0.072, Ku=0.0715, rf=0.068 and rb=0.148.

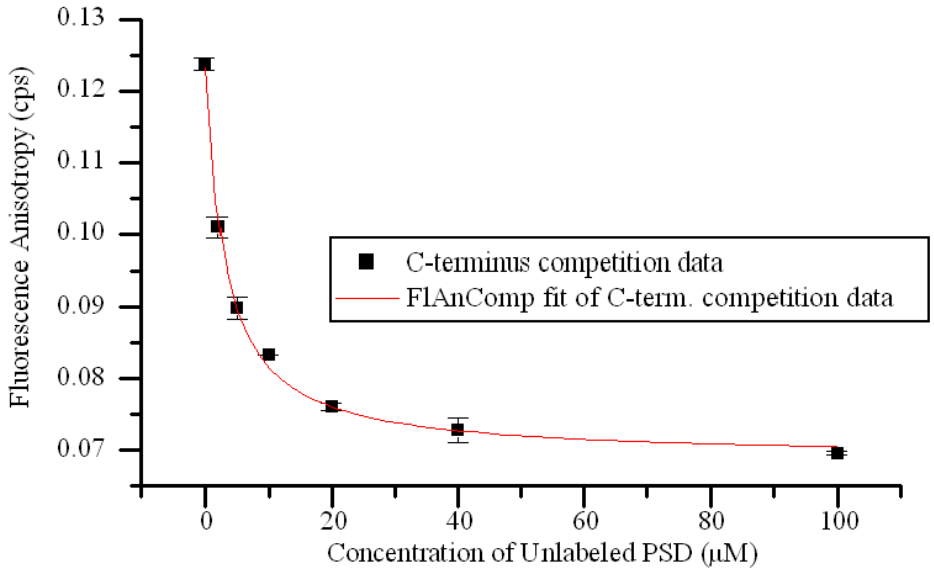

Figure 3-6. Fluorescence anisotropy competition with MARCKS C-terminus, Rh-PSD and unlabeled PSD. 0.5 μM C-terminus, 0.2 μM Rh-PSD and increasing concentrations of unlabeled PSD were used. Kl=0.287, Ku=0.990, rf=0.069 and rb=0.164.

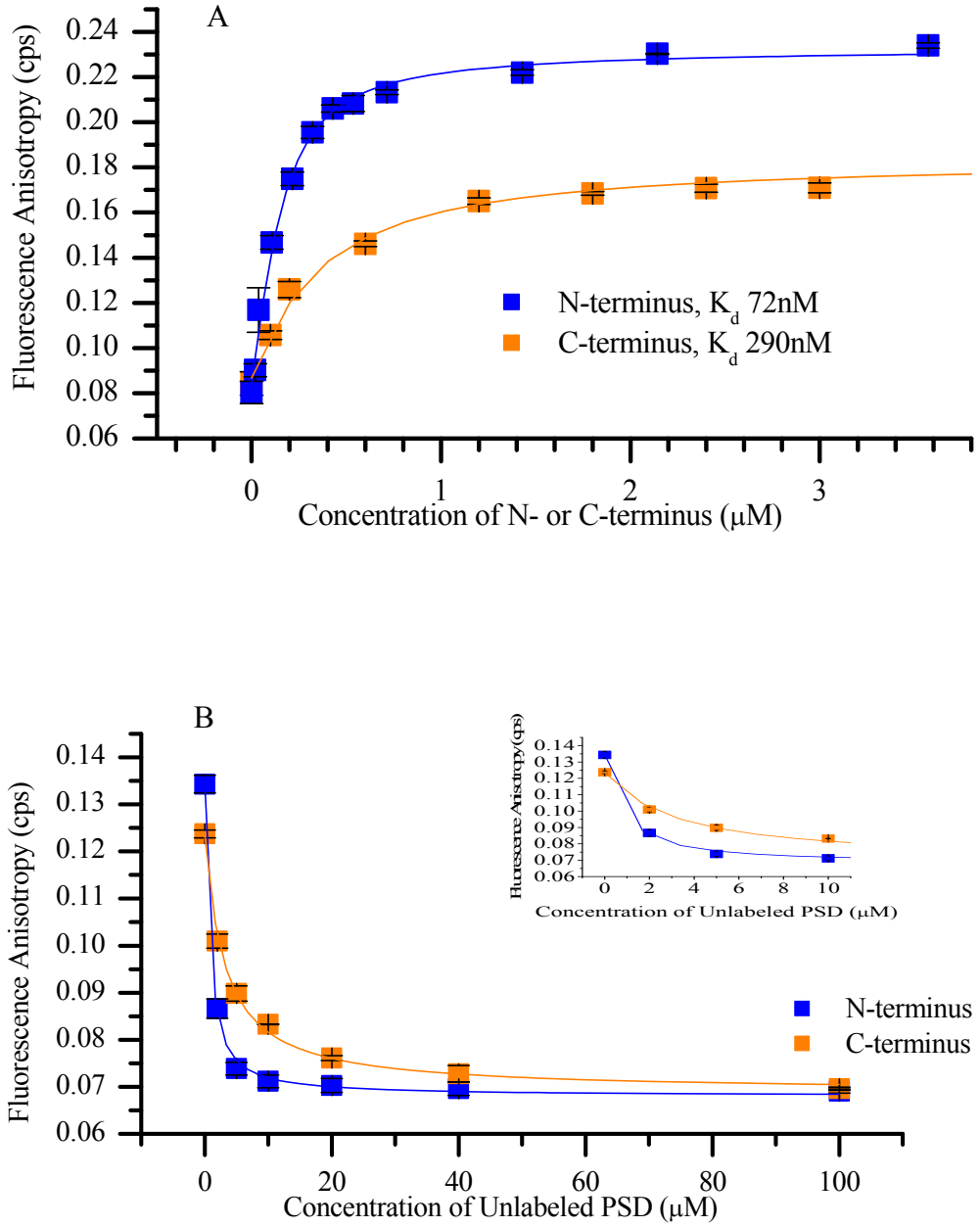

Figure 3-7. Overlay of N-and C-terminus anisotropy and competition data. A) Anisotropy, B) Competition. The inset in B shows the first 4 data points.

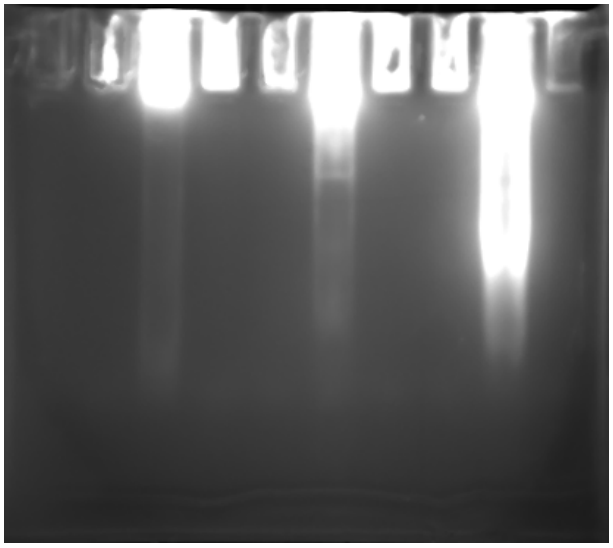

1 2 3 4 5 6 7 8 9 10

Figure 3-8. UV photo of 7% native Tris-tricine polyacrylamide gel of MARCKS proteins with actin and rhodamine-labeled PSD. 1) Actin, 2) MARCKS, 3) MARCKS and Rh-PSD, 4) MARCKS and actin, 5) C-terminus, 6) C-terminus and Rh-PSD, 7) C-terminus and actin, 8) N-terminus, 9) N-terminus and Rh-PSD, 10) N-terminus and actin. Only UV fluorescence from the tetramethylrhodamine labeled PSD appears on this gel.

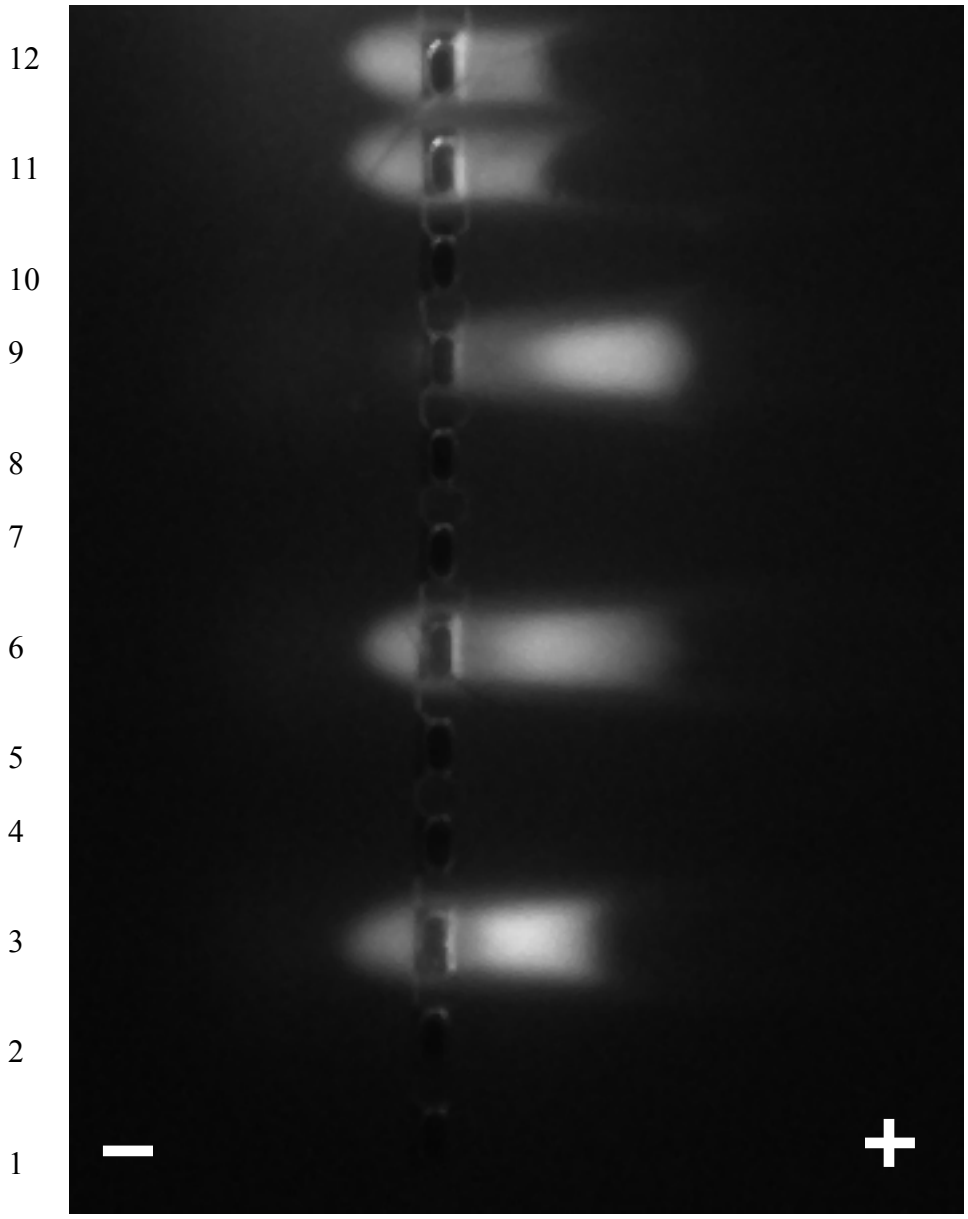

Figure 3-9. UV photo of 1% native Tris-tricine agarose gel of MARCKS proteins with actin and rhodamine-labeled PSD. 1) Actin, 2) MARCKS, 3) MARCKS and Rh-PSD, 4) MARCKS and actin, 5) C-terminus, 6) C-terminus and Rh-PSD, 7) C-terminus and actin, 8) N-terminus, 9) N-terminus and Rh-PSD, 10) N-terminus and actin, 11) Rh-PSD, 12) Rh-PSD. Only UV fluorescence from the tetramethylrhodamine labeled PSD appears on this gel.

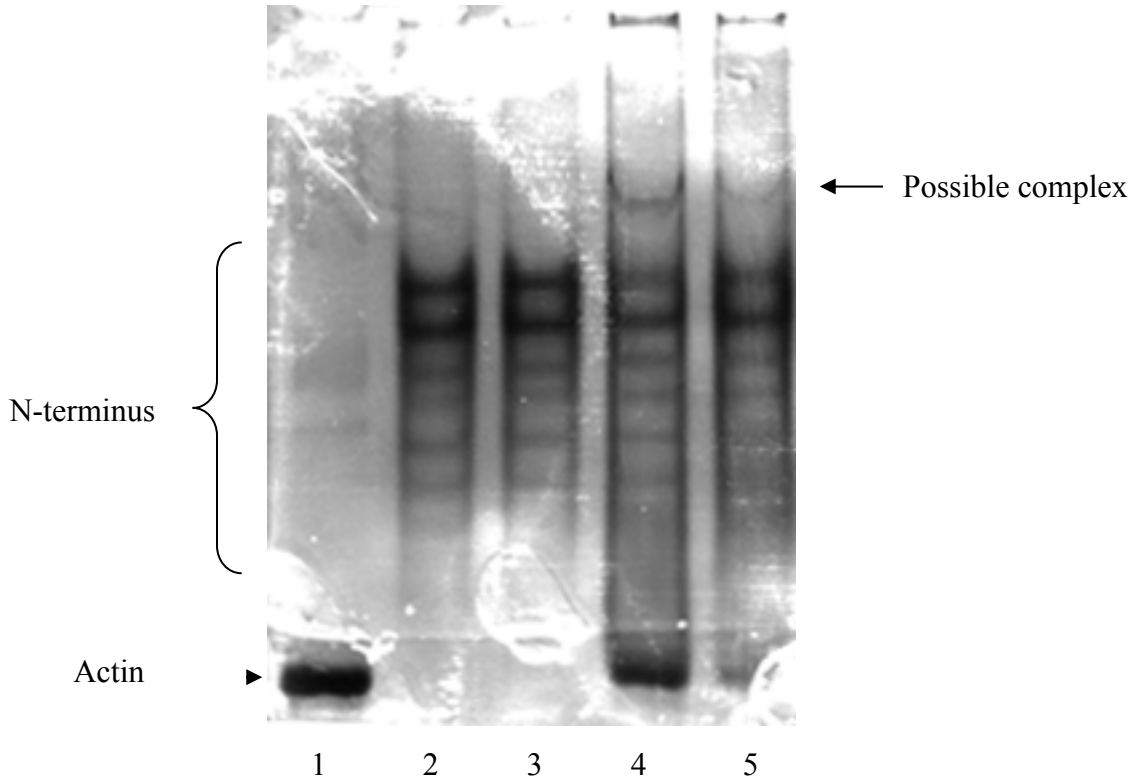

Figure 3-10. MARCKS N-terminus forms oligomers in a native gel. 7% Tris-Tricine native gel with 1) 4 μM G-actin, 2) 15 μM N-terminus, 3) 18.5 μM N-terminus, 4) 15 μM N-terminus + 4 μM G-actin , 5) 18.5 μM N-terminus + 4 μM G-actin. Lanes 4 and 5 contain an extra band that may represent a complex between MARKCS N-terminus and actin.

.

CHAPTER 4
MARCKS AND TNF

Introduction

As previously described, TNF induces reorganization of the actin cytoskeleton in different cell types [75, 111, 112, 118, 121, 122], resulting in filopodia and lamellopodia formation, stress fibers, F-actin polymerization or depolymerization, actin synthesis, membrane ruffles, chemotaxis and migration. In endothelial cells, these effects were found to be mediated by members of the Rho family of small GTPases, Rho, Rac and Cdc42 [111]. In addition, TNF-induced apoptosis was shown to require rearrangement of the actin cytoskeleton, which was mediated by Rho-kinase [119]. In contrast, TNF was found to elicit antiapoptotic effects in opossum kidney cells also via redistribution of the actin cytoskeleton through inhibition of caspase-3; this was governed by the phosphatidylinositol-3 kinase, Cdc42/Rac1, and phospholipase-γ1 [120]. The actin cytoskeleton plays an important role in TNF-induced apoptosis, via multiple mechanisms, including delivering apoptosis proteins to where they need to be and causing morphological changes typical of apoptosis such as membrane blebbing [231, 232].

As mentioned previously, MARCKS was shown to constitute 90% of proteins synthesized de novo in response to stimulation with TNF in neutrophils and macrophages [71, 72]. This induction of MARCKS suggests it plays an important role in the signal transduction pathway of this cytokine. MARCKS may play a role in mediating the effects observed on the actin cytoskeleton in response to TNF. MARCKS phosphorylation by both PKC and Rho-kinase [8, 70], two kinases found downstream of TNF and important for actin reorganization, further supports this hypothesis.

To elucidate the role of MARCKS in the TNF signaling pathway, we used RNA interference to knock down MARCKS in the human promyelocytic leukemia cell line HL-60, followed by treatment with TNF, RNA isolation and use of a PCR microarray of TNF ligands and receptors that profiles the expression of 84 genes whose expression is controlled by or involved in the TNF ligand and TNF receptor signaling pathways. Members of the TNF Superfamily and TNF Receptor Superfamily are represented on this array (Tables 4-1 and 4-2).

Methods

Culture conditions and nucleofection

HL-60 cells were grown in Iscove's Modified DMEM (ATCC Cat. No. 30-2005), 100 μg/ml streptomycin, 100 U/ml penicillin and 20% fetal bovine serum (FBS) in a humidified 37ºC incubator with 6%CO_2. Medium was replaced 2-3 times per week (30 mL per 162 cm^2 flask). Cells were seeded at a density of $1x10^5$ cells/mL and passaged at a density of $7\text{-}8x10^5$ cells/mL. Cells were passaged 3 days before nucleofection, and density for nucleofection was $5\text{-}7x10^5$ cells/mL. Each sample required $2x10^6$ cells. Once cells reached the requied density for nucleofection, $2x10^6$ cells were centrifuged at 90xg for 10 minutes at room temperature. The supernatant was discarded completely and the pellet was resuspended in 100μL room temperature Cell Line Nucleofector Solution V. Cells should not be stored longer than 15 minutes in this solution. Two and a half μg of siRNA (MARCKS or Non-Targeting) were pipetted into the 100μL cell suspension and the nucleofection sample was transfered into an amaxa certified cuvette, making sure the sample covered the bottom and that there were no air bubbles. Cuvettes were placed in Nucloefector II cuvette holder and program T-019 was run. Immediately following nucleofection, cuvettes are taken out and 500μL pre-warmed media were added. Samples were removed from cuvette using an Amaxa certified pipette and placed in a

well with 1.5 mL pre-warmed media in a 12-well plate. The plate was placed in a humidified 37ºC incubator with 6%CO_2.

TNF treatment and qRT-PCR

Twenty four hours after nucleofection, cells were scraped and split into 2 wells of a 12-well plate. One mL fresh culture medium was added to each well. Cells were counted and their viability determined using Trypan blue. Forty eight hours after nucleofection, one well of each sample was treated with 200 U/mL TNF. The other well was an untreated control. This was done for both MARCKS and Non-targeting siRNA treated cells. Four hours after TNF treatment, reactions were inhibited by addition of 1 mM EGTA and placing flasks on ice. Cells were scraped and wells washed with 1 mL PBS + 1 mM EDTA. Cells were pelleted mRNA isolated using QIAGEN's RNeasy RNA purification kit. To verify MARCKS knockdown, qRT-PCR was carried out as described in Chapter 4. Briefly, following DNase I treatment of mRNA, concentrations were determined, 2µg of RNA were reverse transcribed into cDNA and used in qRT-PCR using TaqMan probes for MARCKS and GAPDH. After verification of knockdown as determined by qRT-PCR, the Human Tumor Necrosis Factor (TNF) Ligand and Receptor Signaling Pathways RT² Profiler™ PCR Array was used (SuperArray, Cat. No. APHS-063) by following the kit's instructions.

Results

Nucleofection of MARCKS (Dharmacon, human MARCKS smart pool reagent Cat. No. M-00477200-0050) and non-targeting siRNAs (Dharmacon, Non-Targeting siRNA Pool #2 Cat. No. NC9554221) into HL-60 cells using Amaxa's Nucleofector II machine and the HL-60 Cell Line Nucleofector Kit V (Amaxa, Cat. No. VCA-1003) successfully silenced MARCKS message in HL-60 cells 48 hours after nucleofection. Cells had a viability of 75-78% as determined by a Trypan blue exclusion test of cell viability test. To determine whether MARCKS was

successfully silenced, we used qRT-PCR with TaqMan probes for MARCKS and GAPDH as described in Chapter 4. As determined by qRT-PCR using the ΔΔCt method and GAPDH as a housekeeping control gene, MARCKS was found to be knocked down to about 18% of control non-targeting siRNA-transfected HL-60 cells (Table 4-4).

Four TNF SuperArrays were run: non-targeting siRNA transfected HL-60 cells with and without TNF treatment and MARCKS siRNA transfected HL-60 cells with and without TNF treatment. For each RNAi sample, the non-TNF treated sample was used as a control for quantifying fold change in each gene in response to TNF treatment using the delta delta Ct method. Fold changes thus obtained were then compared to determine the effect of silencing MARCKS on genes involved in TNF signaling (Table 4-5).

Listed below are TNF SuperArray genes grouped functionally; genes that are up-regulated more than 1 fold in HL-60 cells where MARCKS was silenced by RNA interference following treatment with TNF are shown in red, those that were down-regulated more than 1 fold following TNF treatment are shown in blue. Of 71 genes assayed, 31 had less than a 1 fold difference between TNF-treated MARCKS silenced or unsilenced cells, 33 were more than 1 fold upregulated in MARCKS knock down cells following TNF treatment, and only 7 were more than 1 fold downregulated compared to TNF-treated non silenced HL-60 cells. Knocking down MARCKS expression seems to affect expression of genes from all pathways of TNF, including those that are important to the inflammatory response and apoptosis.

TNF Superfamily Members:

- Induction of Apoptosis: FASLG, LTA, TNFSF10, TNFSF14, TNFSF8.
- Caspase Activation: TNFSF15.
- Caspase Inhibition: TNFSF14.
- Anti-apoptosis Genes: CD40LG, TNF, TNFSF18.
- Other Apoptosis-Related Genes: CD70 (TNFSF7), TNFSF9.
- Inflammatory Response: CD40LG, TNF.

- NFκB Signaling Pathway: FASLG, TNF, TNFSF10, TNFSF14, TNFSF15.
- Other TNF Superfamily Members: LTB, PGLYRP1, TNFSF11, TNFSF12, TNFSF13, TNFSF13B, TNFSF4, TNFSF5IP1.

TNF Receptor Superfamily Members:

- Induction of Apoptosis: FAS, TNFRSF10A, TNFRSF10B, TNFRSF19, TNFRSF25, CD27 (TNFRSF7), TNFRSF9, TRADD.
- Caspase Activation: TNFRSF10A, TNFRSF10B.
- Caspase Inhibition: CD27 (TNFRSF7).
- Anti-apoptosis Genes: FAS, TNFRSF10D, TNFRSF18, TNFRSF6B, CD27 (TNFRSF7).
- Other Apoptosis Genes: CD40, LTBR, NGFR, TNFRSF10C, TNFRSF11B, TNFRSF12A, TNFRSF14, TNFRSF1A, TNFRSF1B, TNFRSF21.
- Inflammatory Response: CD40, TNFRSF1A.
- NFκB Signaling Pathway: CD40, EDA2R, LTBR, TNFRSF10A, TNFRSF10B, TNFRSF1A, CD27 (TNFRSF7), TRADD.
- JNK Signaling Pathway: EDA2R, TNFRSF19, CD27 (TNFRSF7).
- Other TNF Receptor Superfamily Members: TNFRSF11A, TNFRSF13B, TNFRSF13C, TNFRSF17, TNFRSF19L, TNFRSF4, TNFRSF8.

TNFR1 Signaling Pathway:

- Induction of Apoptosis: CASP3, CRADD, FADD, TRADD.
- Caspases: CASP2, CASP3, CASP8.
- Anti-apoptosis Genes: BAG4, CASP2, TNF.
- Other Apoptosis Genes: DFFA, PAK1, TNFRSF1A, TRAF2.
- Inflammatory Response: TNF, TNFRSF1A.
- NFκB Signaling Pathway: CASP8, FADD, TNF, TNFRSF1A, TRADD.
- JNK Signaling Pathway: MAP2K4, MAPK8, PAK1.
- Transcription Regulators: JUN, PARP1, RB1, TNF, TNFRSF1A.
- TNFR1 Signaling Pathway: ARHGDIB, CAD, HRB, LMNA, LMNB1, LMNB2, MADD, MAP3K1, MAP3K7, PAK2, PRKDC, SPTAN1.

TNFR2 Signaling Pathway:

- Induction of Apoptosis: IKBKG, LTA, TRAF3.
- Anti-apoptosis Genes: NFKB1, TNFAIP3.
- Other Apoptosis Genes: NFKBIA, TNFRSF1B, TRAF1, TRAF2.
- Inflammatory Response: NFKB1.
- NFκB Signaling Pathway: CHUK, IKBKB, IKBKG, NFKBIA, TNFAIP3.
- Transcription Regulators: IKBKB, IKBKG, NFKB1, NFKBIA.
  TNFR2 Signaling Pathway: DUSP1, HRB, IKBKAP, MAP3K1, MAP3K14, TANK

Interestingly, there seemed to be an upregulation of anti-apoptotic genes (5: BAG-4/SODD, CD154/CD40L, DIF/TNF-alpha, AITR/GITR, DCR3/M68) and a down-regulation of pro-apoptotic genes (2: CPP32/CPP32B, APO2L/Apo-2L); of course, there were exceptions: 3 up-regulated pro-apoptotic genes (APT1LG1/CD178,LT/TNFB,TAJ/TAJ-alpha) and 1 down-regulated anti-apoptotic gene (CD264/DCR2; Table 4-6). In genes marked as "no change" between MARCKS RNAi and non-targeting RNAi, TNF-treated samples, there was also up-regulation of 3 anti-apoptotic genes, down-regulation of 5 pro-apoptotic genes and upregulation of 2 pro-apoptotic genes (Table 4-6).

In addition, knocking down MARCKS seemed to cause a general down-regulation of the expression of genes involved in TNF signaling (Tables 4-7 to 4-9, last column). This was measured by using results for non-targeting siRNA treated HL-60 cells without TNF treatment as a control and comparing it to MARCKS siRNA treated HL-60 cells also wihoout TNF treatment using the $\Delta\Delta$Ct method. When MARCKS was knocked down, 58 genes were downregulated and 22 were up-regulated. Following TNF treatment, genes that were up-regulated due to MARCKS RNAi, end up being less up-regulated and sometimes down-regulated compared to non-targeting RNAi treated samples. Similarly, genes that were downregulated due to MARCKS RNAi are up-regulated in response to TNF treatment.

Curiously, MARCKS RNAi treated HL-60 cells behaved similarly to non-targeting siRNA treated HL-60 cells that have been treated with TNF. Of 73 genes, 27 behaved the same way in non-TNF treated MARCKS silenced HL-60 cells and TNF-treated non-targeting siRNA cells, 23 genes were unchanged due to any treatment or RNA interference, and 23 were the same in TNF-treated MARCKS silenced and un-silenced HL-60 cells. In all, 50 out of 73 genes acted the same way in MARCKS RNAi treated HL-60 cells and non-targeting siRNA treated HL-60

cells that have been treated with TNF. Although many more experiments would have to be done to test this hypothesis, these preliminary data suggest that MARCKS may play a role in a negative feedback loop initiated by TNF in HL-60 cells to silence itself.

Conclusion

MARCKS has many reported functions, many of which appear to be related to its interactions with actin. It binds and cross-links actin filaments, resulting in the remodeling of the actin cytoskeleton and cytoskeletal processes, i.e. phagocytosis, endocytosis, cell morphology, motility, and adhesion to the extracellular matrix. Many of these processes are also important for apoptosis. For example, the actin cytoskeleton is required for delivering all the proteins required to the death receptors to activate caspases and transduce the apoptotic signal from the receptor. For instance, the cytoskeletal protein ezrin which provides a link between the plasma membrane and the actin cytoskeleton, was shown to be required for mediating Fas-induced apoptosis [233]. As previously described, the binding of TNF to its receptors causes an immediate polymerization and/or depolymerization of the actin cytoskeleton, depending on cell type. Ruffles, filopodia, lamelopodia and stress fibers have all been described to occur following TNF treatment (see Chapter 1). As the phosphorylation site domain of MARCKS has been shown to influence actin polymerization and depolymerization, it can potentially play a role in these observed phenomena.

During apoptosis, other cytoskeletal processes such as endocytosis and phagocytosis also take place. Coincidentally, these two important cellular processes were reported to require MARCKS activity [29-33]. One to a few hours after the TNF receptor is bound by TNF molecules, the TNFR is internalized by endocytosis, a process that is essential for the rest of the apoptotic pathway to successfully resume as well as to down-regulate the TNF signal [234, 235]. Interestingly, if cells are pre-treated with PMA, an activator of PKC, this endocytosis is inhibited, and TNF is not down-regulated. As the major substrate for PKC and having such an

important role in endocytosis, MARCKS is certainly a likely player in the process of TNF receptor internalization.

Finally, phagocytosis is an essential step in apoptosis which ensures that dying cells do not spill their content, causing inflammation and autoimmunity. Debris from dying cells is packaged and phagocytosed by neighboring cells. Phagocytosis has also been shown to require MARCKS to take place.

Table 4-1. TNF Superarray array layout. Cat. No. APHS-063.

1	2	3	4	5	6	7	8	9	10	11	12
ARHGDIB	BAG4	CAD	CASP2	CASP3	CASP8	CD40	CD40LG	CHUK	CRADD	DFFA	DUSP1
EDA2R	FADD	FAS	FASLG	HRB	IKBKAP	IKBKB	IKBKG	JUN	LMNA	LMNB1	LMNB2
LTA	LTB	LTBR	MADD	MAP2K4	MAP3K1	MAP3K7	MAPK8	NFKB1	NFKBIA	NGFR	PAK1
PAK2	PARP1	PGLYRP1	PRKDC	RB1	SPTAN1	TNF	TNFAIP3	TNFRSF10A	TNFRSF10B	TNFRSF10C	TNFRSF10D
TNFRSF11A	TNFRSF11B	TNFRSF12A	TNFRSF13B	TNFRSF13C	TNFRSF14	TNFRSF17	TNFRSF18	TNFRSF19	RELT	TNFRSF1A	TNFRSF1B
TNFRSF 21	TNFRSF25	TNFRSF4	TNFRSF6B	CD27	TNFRSF8	TNFRSF9	TNFSF10	TNFSF11	TNFSF12	TNFSF13	TNFSF13B
TNFSF14	TNFSF15	TNFSF18	TNFSF4	PSMG2	CD70	TNFSF8	TNFSF9	TRADD	TRAF1	TRAF2	TRAF3
B2M	HPRT1	RPL13A	GAPDH	ACTB	HGDC	RTC	RTC	RTC	PPC	PPC	PPC

Table 4-2. TNF SuperArray gene table. Cat. No. APHS-063.

Well	UniGene	RefSeq	Symbol	Description	Gene Name
A01	Hs.504877	NM_001175	ARHGDIB	Rho GDP dissociation inhibitor (GDI) beta	D4/GDIA2
A02	Hs.194726	NM_004874	BAG4	BCL2-associated athanogene 4	BAG-4/SODD
A03	Hs.377010	NM_004341	CAD	Carbamoyl-phosphate synthetase 2, aspartate transcarbamylase, and dihydroorotase	CAD
A04	Hs.368982	NM_032982	CASP2	Caspase 2, apoptosis-related cysteine peptidase (neural precursor cell expressed, developmentally down-regulated 2)	CASP-2/ICH-1L
A05	Hs.141125	NM_004346	CASP3	Caspase 3, apoptosis-related cysteine peptidase	CPP32/CPP32B
A06	Hs.591630	NM_001228	CASP8	Caspase 8, apoptosis-related cysteine peptidase	CAP4/FLICE
A07	Hs.472860	NM_001250	CD40	CD40 molecule, TNF receptor superfamily member 5	Bp50/CDW40
A08	Hs.592244	NM_000074	CD40LG	CD40 ligand (TNF superfamily, member 5, hyper-IgM syndrome)	CD154/CD40L
A09	Hs.198998	NM_001278	CHUK	Conserved helix-loop-helix ubiquitous kinase	IKBKA/IKK-alpha
A10	Hs.38533	NM_003805	CRADD	CASP2 and RIPK1 domain containing adaptor with death domain	RAIDD
A11	Hs.484782	NM_004401	DFFA	DNA fragmentation factor, 45kDa, alpha polypeptide	DFF-45/DFF1
A12	Hs.171695	NM_004417	DUSP1	Dual specificity phosphatase 1	CL100/HVH1
B01	Hs.302017	NM_021783	EDA2R	Ectodysplasin A2 receptor	EDA-A2R/EDAA2R
B02	Hs.86131	NM_003824	FADD	Fas (TNFRSF6)-associated via death domain	GIG3/MORT1
B03	Hs.244139	NM_000043	FAS	Fas (TNF receptor superfamily, member 6)	ALPS1A/APO-1
B04	Hs.2007	NM_000639	FASLG	Fas ligand (TNF superfamily, member 6)	APT1LG1/CD178
B05	Hs.591619	NM_004504	HRB	HIV-1 Rev binding protein	RAB/RIP

Table 4-2. Continued 1.

Well	UniGene	RefSeq	Symbol	Description	Gene Name
B06	Hs.494738	NM_003640	IKBKAP	Inhibitor of kappa light polypeptide gene enhancer in B-cells, kinase complex-associated protein	DKFZp781H1425/ DYS
B07	Hs.413513	NM_001556	IKBKB	Inhibitor of kappa light polypeptide gene enhancer in B-cells, kinase beta	IKK-beta/IKK2
B08	Hs.43505	NM_003639	IKBKG	Inhibitor of kappa light polypeptide gene enhancer in B-cells, kinase gamma	FIP-3/FIP3
B09	Hs.525704	NM_002228	JUN	Jun oncogene	AP1/c-Jun
B10	Hs.594444	NM_005572	LMNA	Lamin A/C	CDCD1/CDDC
B11	Hs.89497	NM_005573	LMNB1	Lamin B1	LMN/LMN2
B12	Hs.538286	NM_032737	LMNB2	Lamin B2	LAMB2/LMN2
C01	Hs.36	NM_000595	LTA	Lymphotoxin alpha (TNF superfamily, member 1)	LT/TNFB
C02	Hs.376208	NM_002341	LTB	Lymphotoxin beta (TNF superfamily, member 3)	TNFC/TNFSF3
C03	Hs.1116	NM_002342	LTBR	Lymphotoxin beta receptor (TNFR superfamily, member 3)	CD18/D12S370
C04	Hs.82548	NM_003682	MADD	MAP-kinase activating death domain	DENN/IG20
C05	Hs.514681	NM_003010	MAP2K4	Mitogen-activated protein kinase kinase 4	JNKK/JNKK1
C06	Hs.634810	XM_042066	MAP3K1	Mitogen-activated protein kinase kinase kinase 1	MAPKKK1/ MEKK
C07	Hs.652105	NM_003188	MAP3K7	Mitogen-activated protein kinase kinase kinase 7	TAK1/TGF1a
C08	Hs.138211	NM_002750	MAPK8	Mitogen-activated protein kinase 8	JNK/JNK1
C09	Hs.431926	NM_003998	NFKB1	Nuclear factor of kappa light polypeptide gene enhancer in B-cells 1 (p105)	DKFZp686C01211/ EBP-1
C10	Hs.81328	NM_020529	NFKBIA	Nuclear factor of kappa light polypeptide gene enhancer in B-cells inhibitor, alpha	IKBA/MAD-3

Table 4-2. Continued 2.

Well	UniGene	RefSeq	Symbol	Description	Gene Name
C11	Hs.415768	NM_002507	NGFR	Nerve growth factor receptor (TNFR superfamily, member 16)	CD271/ TNFRSF16
C12	Hs.435714	NM_002576	PAK1	P21/Cdc42/Rac1-activated kinase 1 (STE20 homolog, yeast)	PAKalpha
D01	Hs.518530	NM_002577	PAK2	P21 (CDKN1A)-activated kinase 2	PAK65/ PAKgamma
D02	Hs.177766	NM_001618	PARP1	Poly (ADP-ribose) polymerase family, member 1	ADPRT/ ADPRT1
D03	Hs.137583	NM_005091	PGLYRP1	Peptidoglycan recognition protein 1	PGLYRP/PGRP
D04	Hs.491682	NM_006904	PRKDC	Protein kinase, DNA-activated, catalytic polypeptide	DNAPK/DNPK1
D05	Hs.408528	NM_000321	RB1	Retinoblastoma 1 (including osteosarcoma)	OSRC/RB
D06	Hs.372331	NM_003127	SPTAN1	Spectrin, alpha, non-erythrocytic 1 (alpha-fodrin)	αII-SPECTRIN
D07	Hs.241570	NM_000594	TNF	Tumor necrosis factor (TNF superfamily, member 2)	DIF/TNF-alpha
D08	Hs.211600	NM_006290	TNFAIP3	Tumor necrosis factor, alpha-induced protein 3	A20/OTUD7C
D09	Hs.591834	NM_003844	TNFRSF10A	Tumor necrosis factor receptor superfamily, member 10a	APO2/CD261
D10	Hs.521456	NM_003842	TNFRSF10B	Tumor necrosis factor receptor superfamily, member 10b	CD262/DR5
D11	Hs.655801	NM_003841	TNFRSF10C	Tumor necrosis factor receptor superfamily, member 10c, decoy without an intracellular domain	CD263/DCR1
D12	Hs.213467	NM_003840	TNFRSF10D	Tumor necrosis factor receptor superfamily, member 10d, decoy with truncated death domain	CD264/DCR2
E01	Hs.204044	NM_003839	TNFRSF11A	Tumor necrosis factor receptor superfamily, member 11a, NFKB activator	CD265/ODFR
E02	Hs.81791	NM_002546	TNFRSF11B	Tumor necrosis factor receptor superfamily, member 11b (osteoprotegerin)	OCIF/OPG
E03	Hs.355899	NM_016639	TNFRSF12A	Tumor necrosis factor receptor superfamily, member 12A	CD266/FN14

Table 4-2. Continued 3.

Well	UniGene	RefSeq	Symbol	Description	Gene Name
E04	Hs.158341	NM_012452	TNFRSF13B	Tumor necrosis factor receptor superfamily, member 13B	CD267/CVID
E05	Hs.344088	NM_052945	TNFRSF13C	Tumor necrosis factor receptor superfamily, member 13C	BAFF-R/BAFFR
E06	Hs.512898	NM_003820	TNFRSF14	Tumor necrosis factor receptor superfamily, member 14 (herpesvirus entry mediator)	ATAR/HVEA
E07	Hs.2556	NM_001192	TNFRSF17	Tumor necrosis factor receptor superfamily, member 17	BCM/BCMA
E08	Hs.212680	NM_004195	TNFRSF18	Tumor necrosis factor receptor superfamily, member 18	AITR/GITR
E09	Hs.149168	NM_018647	TNFRSF19	Tumor necrosis factor receptor superfamily, member 19	TAJ/TAJ-alpha
E10	Hs.533720	NM_032871	TNFRSF19L	Tumor necrosis factor receptor superfamily, member 19-like	RELT
E11	Hs.279594	NM_001065	TNFRSF1A	Tumor necrosis factor receptor superfamily, member 1A	CD120a/FPF
E12	Hs.256278	NM_001066	TNFRSF1B	Tumor necrosis factor receptor superfamily, member 1B	CD120b/TBPII
F01	Hs.443577	NM_014452	TNFRSF21	Tumor necrosis factor receptor superfamily, member 21	BM-018/DR6
F02	Hs.462529	NM_003790	TNFRSF25	Tumor necrosis factor receptor superfamily, member 25	APO-3/DDR3
F03	Hs.129780	NM_003327	TNFRSF4	Tumor necrosis factor receptor superfamily, member 4	ACT35/CD134
F04	Hs.554786	NM_003823	TNFRSF6B	Tumor necrosis factor receptor superfamily, member 6b, decoy	DCR3/M68
F05	Hs.355307	NM_001242	CD27	CD27 molecule	S152/T14
F06	Hs.1314	NM_001243	TNFRSF8	Tumor necrosis factor receptor superfamily, member 8	CD30/D1S166E
F07	Hs.193418	NM_001561	TNFRSF9	Tumor necrosis factor receptor superfamily, member 9	4-1BB/CD137
F08	Hs.478275	NM_003810	TNFSF10	Tumor necrosis factor (ligand) superfamily, member 10	APO2L/Apo-2L
F09	Hs.333791	NM_003701	TNFSF11	Tumor necrosis factor (ligand) superfamily, member 11	CD254/ODF

Table 4-2. Continued 4.

Well	UniGene	RefSeq	Symbol	Description	Gene Name
F10	Hs.415839	NM_003809	TNFSF12	Tumor necrosis factor (ligand) superfamily, member 12	APO3L/DR3LG
F11	Hs.54673	NM_003808	TNFSF13	Tumor necrosis factor (ligand) superfamily, member 13	APRIL/CD256
F12	Hs.525157	NM_006573	TNFSF13B	Tumor necrosis factor (ligand) superfamily, member 13b	BAFF/BLYS
G01	Hs.129708	NM_003807	TNFSF14	Tumor necrosis factor (ligand) superfamily, member 14	CD258/HVEML
G02	Hs.241382	NM_005118	TNFSF15	Tumor necrosis factor (ligand) superfamily, member 15	TL1/TL1A
G03	Hs.248197	NM_005092	TNFSF18	Tumor necrosis factor (ligand) superfamily, member 18	AITRL/GITRL
G04	Hs.181097	NM_003326	TNFSF4	Tumor necrosis factor (ligand) superfamily, member 4 (tax-transcriptionally activated glycoprotein 1, 34kDa)	CD134L/CD252
G05	Hs.464652	NM_020232	TNFSF5IP1	Tumor necrosis factor superfamily, member 5-induced protein 1	CLAST3/HCCA3
G06	Hs.501497	NM_001252	CD70	CD70 molecule	CD27L/CD27LG
G07	Hs.494901	NM_001244	TNFSF8	Tumor necrosis factor (ligand) superfamily, member 8	CD153/CD30L
G08	Hs.1524	NM_003811	TNFSF9	Tumor necrosis factor (ligand) superfamily, member 9	4-1BB-L
G09	Hs.460996	NM_003789	TRADD	TNFRSF1A-associated via death domain	Hs.89862
G10	Hs.531251	NM_005658	TRAF1	TNF receptor-associated factor 1	EBI6/MGC:10353
G11	Hs.522506	NM_021138	TRAF2	TNF receptor-associated factor 2	MGC:45012/ TRAP
G12	Hs.510528	NM_003300	TRAF3	TNF receptor-associated factor 3	CAP-1/CD40bp
H01	Hs.534255	NM_004048	B2M	Beta-2-microglobulin	B2M
H02	Hs.412707	NM_000194	HPRT1	Hypoxanthine phosphoribosyltransferase 1 (Lesch-Nyhan syndrome)	HGPRT/HPRT
H03	Hs.546356	NM_012423	RPL13A	Ribosomal protein L13a	RPL13A

Table 4-2. Continued 5.

Well	UniGene	RefSeq	Symbol	Description	Gene Name
H04	Hs.544577	NM_002046	GAPDH	Glyceraldehyde-3-phosphate dehydrogenase	G3PD/GAPD
H05	Hs.520640	NM_001101	ACTB	Actin, beta	PS1TP5BP1
H06	N/A	X66290	HGDC	Human Genomic DNA Contamination	HGDC
H07	N/A	SA_00104	RTC	Reverse Transcription Control	RTC
H08	N/A	SA_00104	RTC	Reverse Transcription Control	RTC
H09	N/A	SA_00104	RTC	Reverse Transcription Control	RTC
H10	N/A	SA_00103	PPC	Positive PCR Control	PPC
H11	N/A	SA_00103	PPC	Positive PCR Control	PPC
H12	N/A	SA_00103	PPC	Positive PCR Control	PPC

Table 4-3. Cell viability 48 hours after nucleofection.

	MARCKS siRNA		Non-Targeting siRNA	
	Total	# dead	Total	# dead
count 1	18	5	36	8
count 2	26	5	34	13
count 3	36	10	24	5
count 4	23	3	24	4
Total	103	23	118	30
% Viability	77.7		74.6	

Table 4-4. Results of qRT-PCR to measure MARCKS knockdown by RNA interference. Delta delta Ct method was used to calculate MARCKS knockdown, using sample nucleofected with non-targeting siRNA as control.

Sample	Ct GAPDH	Ct TNF	Ct MARCKS	Ct MARCKS-Ct GAPDH	% of Control
HL-60, 48hr MARCKS siRNA, no TNF-α	20.116	24.686	24.642	4.5	17.8
HL-60, 48hr Non-Targeting siRNA, no TNF-α	24.55	27.323	26.589	2.0	100.0

Table 4-5. TNF SuperArray results following RNA interference in response to TNF treatment.

Well	Symbol	Gene Name	Non-Targeting RNAi fold change	MARCKS RNAi fold change	Absolute Difference
A01	ARHGDIB	D4/GDIA2	1.25	1.40	0.14
A02	BAG4	BAG-4/SODD	- 1.24	1.13	2.37
A03	CAD	CAD	- 5.51	-1.07	4.44
A04	CASP2	CASP-2/ICH-1L	N/A	1.04	N/A
A05	CASP3	CPP32/CPP32B	1.71	-1.14	2.85
A06	CASP8	CAP4/FLICE	- 1.24	-1.82	0.58
A07	CD40	Bp50/CDW40	11.61	5.95	5.66
A08	CD40LG	CD154/CD40L	- 1.43	1.02	2.45
A09	CHUK	IKBKA/IKK-alpha	- 2.07	1.10	3.18
A10	CRADD	RAIDD	- 1.45	-1.41	0.03
A11	DFFA	DFF-45/DFF1	- 1.16	-1.20	0.05
A12	DUSP1	CL100/HVH1	- 3.17	-2.02	1.14
B01	EDA2R	EDA-A2R/EDAA2R	- 1.43	1.02	2.45
B02	FADD	GIG3/MORT1	- 1.21	-1.01	0.20
B03	FAS	ALPS1A/APO-1	2.17	2.87	0.70
B04	FASLG	APT1LG1/CD178	- 1.43	1.02	2.45
B05	HRB	RAB/RIP	- 1.31	-1.24	0.08
B06	IKBKAP	DKFZp781H1425/DYS	1.08	1.10	0.03
B07	IKBKB	IKK-beta/IKK2	- 1.11	1.24	2.35
B08	IKBKG	FIP-3/FIP3	- 1.55	-1.02	0.53
B09	JUN	AP1/c-Jun	- 2.15	-1.43	0.72
B10	LMNA	CDCD1/CDDC	- 1.37	1.17	2.54
B11	LMNB1	LMN/LMN2	- 1.48	-1.30	0.18
B12	LMNB2	LAMB2/LMN2	- 1.72	-1.08	0.64
C01	LTA	LT/TNFB	- 2.33	1.99	4.32
C02	LTB	TNFC/TNFSF3	1.6	2.68	1.08
C03	LTBR	CD18/D12S370	- 1.06	-1.06	0.00
C04	MADD	DENN/IG20	- 1.18	1.03	2.21
C05	MAP2K4	JNKK/JNKK1	1.32	1.13	0.19
C06	MAP3K1	MAPKKK1/MEKK	- 1.04	1.26	2.30
C07	MAP3K7	TAK1/TGF1a	- 1.48	-1.59	0.11
C08	MAPK8	JNK/JNK1	3.01	1.04	1.97
C09	NFKB1	DKFZp686C01211/EBP-1	2.07	2.52	0.45
C10	NFKBIA	IKBA/MAD-3	4.85	9.60	4.75
C11	NGFR	CD271/TNFRSF16	- 2.02	-1.15	0.86
C12	PAK1	PAKalpha	- 1.51	-1.34	0.16

Table 4-5. Continued 1.

Well	Symbol	Gene Name	Non-Targeting RNAi fold change	MARCKS RNAi fold change	Absolute Difference
D01	PAK2	PAK65/PAKgamma	- 1.04	-1.01	0.03
D02	PARP1	ADPRT/ADPRT1	- 1.17	-1.13	0.04
D03	PGLYRP1	PGLYRP/PGRP	- 1.14	1.09	2.23
D04	PRKDC	DNAPK/DNPK1	1.67	1.59	0.07
D05	RB1	OSRC/RB	2.62	2.38	0.23
D06	SPTAN1	(ALPHA)II-SPECTRIN	- 1.43	1.02	2.45
D07	TNF	DIF/TNF-alpha	- 1.07	1.37	2.44
D08	TNFAIP3	A20/OTUD7C	8.68	7.12	1.56
D09	TNFRSF10A	APO2/CD261	- 2.48	-1.45	1.03
D10	TNFRSF10B	CD262/DR5	1.38	1.50	0.11
D11	TNFRSF10C	CD263/DCR1	- 1.6	-1.17	0.43
D12	TNFRSF10D	CD264/DCR2	2.54	1.02	1.52
E01	TNFRSF11A	CD265/ODFR	1.04	2.85	1.81
E02	TNFRSF11B	OCIF/OPG	1.08	-3.38	4.47
E03	TNFRSF12A	CD266/FN14	- 1.99	-1.30	0.69
E04	TNFRSF13B	CD267/CVID	- 1.43	1.02	2.45
E05	TNFRSF13C	BAFF-R/BAFFR	- 5.29	1.16	6.45
E06	TNFRSF14	ATAR/HVEA	- 1.26	1.44	2.70
E07	TNFRSF17	BCM/BCMA	1.74	9.66	7.93
E08	TNFRSF18	AITR/GITR	- 1.62	1.21	2.82
E09	TNFRSF19	TAJ/TAJ-alpha	- 1.43	1.48	2.90
E10	TNFRSF19L	RELT	- 1.42	1.87	3.29
E11	TNFRSF1A	CD120a/FPF	- 2.87	1.24	4.11
E12	TNFRSF1B	CD120b/TBPII	1.02	1.03	0.01
F01	TNFRSF21	BM-018/DR6	- 1.18	-1.73	0.54
F02	TNFRSF25	APO-3/DDR3	- 1.43	-1.90	0.48
F03	TNFRSF4	ACT35/CD134	1.51	8.53	7.02
F04	TNFRSF6B	DCR3/M68	- 1.86	2.70	4.56
F05	CD27	S152/T14	1.23	2.02	0.79
F06	TNFRSF8	CD30/D1S166E	- 1.19	-1.94	0.75
F07	TNFRSF9	4-1BB/CD137	6.18	5.29	0.89
F08	TNFSF10	APO2L/Apo-2L	4.22	1.86	2.36
F09	TNFSF11	CD254/ODF	- 1.43	1.02	2.45
F10	TNFSF12	APO3L/DR3LG	1.06	2.74	1.68
F11	TNFSF13	APRIL/CD256	- 1.99	1.00	2.99
F12	TNFSF13B	BAFF/BLYS	91.61	234.35	142.73

Table 4-5. Continued 2.

Well	Symbol	Gene Name	Non-Targeting RNAi fold change	MARCKS RNAi fold change	Absolute Difference
G01	TNFSF14	CD258/HVEML	N/A	N/A	N/A
G02	TNFSF15	TL1/TL1A	N/A	N/A	N/A
G03	TNFSF18	AITRL/GITRL	N/A	N/A	N/A
G04	TNFSF4	CD134L/CD252	N/A	N/A	N/A
G05	TNFSF5IP1	CLAST3/HCCA3	N/A	N/A	N/A
G06	CD70	CD27L/CD27LG	N/A	N/A	N/A
G07	TNFSF8	CD153/CD30L	N/A	N/A	N/A
G08	TNFSF9	4-1BB-L	N/A	N/A	N/A
G09	TRADD	Hs.89862	N/A	N/A	N/A
G10	TRAF1	EBI6/MGC:10353	N/A	N/A	N/A
G11	TRAF2	MGC:45012/TRAP	N/A	N/A	N/A
G12	TRAF3	CAP-1/CD40bp	N/A	N/A	N/A
H01	B2M	B2M	1.06	1.19	0.13
H02	HPRT1	HGPRT/HPRT	8.04	1.09	6.95
H03	RPL13A	RPL13A	1.19	-1.04	2.23
H04	GAPDH	G3PD/GAPD	- 1.34	-1.24	0.10
H05	ACTB	PS1TP5BP1	1.06	1.08	0.02

Genes with <1 fold change between MARCKS and non-targeting RNAi samples following TNF treatment shown in green; >1 fold higher in MARCKS RNAi samples shown in red and >1 fold lower than non-targeting in blue. N/A, not available.

Table 4-6. Differential expression of apoptosis genes in TNF-treated HL-60 cells following MARCKS and non-targeting RNAi.

Gene Name	Apoptosis	Non-targeting RNAi fold change	MARCKS RNAi fold change	Effect
BAG-4/SODD	anti	-1.24	1.13	up-regulated
CPP32/CPP32B	pro	1.71	-1.14	down-regulated
CD154/CD40L	anti	-1.43	1.02	up-regulated
RAIDD	pro	-1.45	-1.41	no change
GIG3/MORT1	pro	-1.21	-1.01	no change
ALPS1A/APO-1	pro? anti?	2.17	2.87	no change
APT1LG1/CD178	pro	-1.43	1.02	up-regulated
FIP-3/FIP3	pro	-1.55	-1.02	no change
LT/TNFB	pro	-2.33	1.99	up-regulated
DKFZp686C01211/EBP-1	anti	2.07	2.52	no change
DIF/TNF-alpha	anti	-1.07	1.37	up-regulated
A20/OTUD7C	anti	8.68	7.12	no change
APO2/CD261	pro	-2.48	-1.45	no change
CD262/DR5	pro	1.38	1.50	no change
CD264/DCR2	anti	2.54	1.02	down-regulated
AITR/GITR	anti	-1.62	1.21	up-regulated
TAJ/TAJ-alpha	pro	-1.43	1.48	up-regulated
APO-3/DDR3	pro	-1.43	-1.90	no change
DCR3/M68	anti	-1.86	2.70	up-regulated
S152/T14	pro? anti?	1.23	2.02	no change
4-1BB/CD137	pro	6.18	5.29	no change
APO2L/Apo-2L	pro	4.22	1.86	down-regulated
CD258/HVEML	pro? anti?	N/A	N/A	N/A
TL1/TL1A	pro	N/A	N/A	N/A
AITRL/GITRL	anti	N/A	N/A	N/A
CD153/CD30L	pro	N/A	N/A	N/A
Hs.89862	pro	N/A	N/A	N/A
CAP-1/CD40bp	pro	N/A	N/A	N/A

Table 4-7. Genes in TNF SuperArray whose expression was similar in TNF-treated non-targeting siRNA transfected cells and non-TNF-treated MARCKS siRNA transfected cells.

Well	Symbol	Gene Name	Non-Targeting RNAi fold change--with TNF	MARCKS RNAi fold change--with TNF	MARCKS RNAi fold change--No TNF
A02	BAG4	BAG-4/SODD	-1.24	1.13	-1.24
A03	CAD	CAD	-5.51	-1.07	-7.94
A05	CASP3	CPP32/CPP32B	1.71	-1.14	1.31
A08	CD40LG	CD154/CD40L	-1.43	1.02	-1.88
A09	CHUK	IKBKA/IKK-alpha	-2.07	1.10	-1.31
B01	EDA2R	EDA-A2R/EDAA2R	-1.43	1.02	-1.88
B04	FASLG	APT1LG1/CD178	-1.43	1.02	-1.88
B07	IKBKB	IKK-beta/IKK2	-1.11	1.24	-1.36
B10	LMNA	CDCD1/CDDC	-1.37	1.17	-1.59
C01	LTA	LT/TNFB	-2.33	1.99	-7.73
C04	MADD	DENN/IG20	-1.18	1.03	-1.74
D03	PGLYRP1	PGLYRP/PGRP	-1.14	1.09	-2.03
D06	SPTAN1	(ALPHA)II-SPECTRIN	-1.43	1.02	-1.88
D07	TNF	DIF/TNF-alpha	-1.07	1.37	-1.88
E02	TNFRSF11B	OCIF/OPG	1.08	-3.38	1.84
E04	TNFRSF13B	CD267/CVID	-1.43	1.02	-1.88
E05	TNFRSF13C	BAFF-R/BAFFR	-5.29	1.16	-6.77
E06	TNFRSF14	ATAR/HVEA	-1.26	1.44	-1.61
E08	TNFRSF18	AITR/GITR	-1.62	1.21	-4.11
E09	TNFRSF19	TAJ/TAJ-alpha	-1.43	1.48	-1.55
E10	TNFRSF19L	RELT	-1.42	1.87	-2.13
E11	TNFRSF1A	CD120a/FPF	-2.87	1.24	-2.77
F04	TNFRSF6B	DCR3/M68	-1.86	2.70	-4.11
F09	TNFSF11	CD254/ODF	-1.43	1.02	-1.88
F11	TNFSF13	APRIL/CD256	-1.99	1.00	-2.55

Table 4-7. Continued.

Well	Symbol	Gene Name	Non-Targeting RNAi fold change--with TNF	MARCKS RNAi fold change--with TNF	MARCKS RNAi fold change--No TNF
H02	HPRT1	HGPRT/HPRT	8.04	1.09	8.69
H03	RPL13A	RPL13A	1.19	-1.04	1.43

Table 4-8. Genes in TNF SuperArray whose expression was unchanged in RNAi and TNF treated HL-60 cells.

Well	Symbol	Gene Name	Non-Targeting RNAi fold change--with TNF	MARCKS RNAi fold change--with TNF	MARCKS RNAi fold change--No TNF
B05	HRB	RAB/RIP	-1.31	-1.24	-1.37
B08	IKBKG	FIP-3/FIP3	-1.55	-1.02	-1.78
B09	JUN	AP1/c-Jun	-2.15	-1.43	-1.55
B11	LMNB1	LMN/LMN2	-1.48	-1.30	-1.30
B12	LMNB2	LAMB2/LMN2	-1.72	-1.08	-1.47
C03	LTBR	CD18/D12S370	-1.06	-1.06	-1.16
C05	MAP2K4	JNKK/JNKK1	1.32	1.13	1.21
C07	MAP3K7	TAK1/TGF1a	-1.48	-1.59	-1.45
C08	MAPK8	JNK/JNK1	3.01	1.04	2.89
C09	NFKB1	DKFZp686C01211/EBP-1	2.07	2.52	1.12
C11	NGFR	CD271/TNFRSF16	-2.02	-1.15	-2.25
C12	PAK1	PAKalpha	-1.51	-1.34	-1.59
D01	PAK2	PAK65/PAKgamma	-1.04	-1.01	-1.01
D05	RB1	OSRC/RB	2.62	2.38	1.79
D08	TNFAIP3	A20/OTUD7C	8.68	7.12	1.32
D09	TNFRSF10A	APO2/CD261	-2.48	-1.45	-1.74
D11	TNFRSF10C	CD263/DCR1	-1.60	-1.17	-1.96
D12	TNFRSF10D	CD264/DCR2	2.54	1.02	3.25
E03	TNFRSF12A	CD266/FN14	-1.99	-1.30	-1.97
F06	TNFRSF8	CD30/D1S166E	-1.19	-1.94	-1.27
F07	TNFRSF9	4-1BB/CD137	6.18	5.29	1.23
F08	TNFSF10	APO2L/Apo-2L	4.22	1.86	1.85
H04	GAPDH	G3PD/GAPD	-1.34	-1.24	-1.15

Table 4-9. Genes in TNF SuperArray whose expression was unchanged following TNF treatment of both MARCKS and non-targeting siRNA transfected HL-60 cells.

Well	Symbol	Gene Name	Non-Targeting RNAi fold change--with TNF	MARCKS RNAi fold change--with TNF	MARCKS RNAi fold change--No TNF
A01	ARHGDIB	D4/GDIA2	1.25	1.40	-1.38
A06	CASP8	CAP4/FLICE	-1.24	-1.82	2.85
A10	CRADD	RAIDD	-1.45	-1.41	1.07
A11	DFFA	DFF-45/DFF1	-1.16	-1.20	1.11
B02	FADD	GIG3/MORT1	-1.21	-1.01	1.02
B03	FAS	ALPS1A/APO-1	2.17	2.87	-1.28
B06	IKBKAP	DKFZp781H1425/DYS	1.08	1.10	-1.11
C10	NFKBIA	IKBA/MAD-3	4.85	9.60	-2.04
C02	LTB	TNFC/TNFSF3	1.60	2.68	-1.93
D02	PARP1	ADPRT/ADPRT1	-1.17	-1.13	1.08
D04	PRKDC	DNAPK/DNPK1	1.67	1.59	-1.16
D10	TNFRSF10B	CD262/DR5	1.38	1.50	-1.15
E01	TNFRSF11A	CD265/ODFR	1.04	2.85	-2.08
E07	TNFRSF17	BCM/BCMA	1.74	9.66	-7.62
E12	TNFRSF1B	CD120b/TBPII	1.02	1.03	-1.53
F01	TNFRSF21	BM-018/DR6	-1.18	-1.73	1.18
F02	TNFRSF25	APO-3/DDR3	-1.43	-1.90	1.04
F03	TNFRSF4	ACT35/CD134	1.51	8.53	-1.68
F05	CD27	S152/T14	1.23	2.02	-1.72
F10	TNFSF12	APO3L/DR3LG	1.06	2.74	-1.58
F12	TNFSF13B	BAFF/BLYS	91.61	234.35	-2.39
H01	B2M	B2M	1.06	1.19	-1.14
H05	ACTB	PS1TP5BP1	1.06	1.08	-1.09

CHAPTER 5
MARCKS IN RHEUMATOID ARTHRITIS

Introduction

Recent reports highlight the early onset of structural damage in patients with rheumatoid arthritis (RA) [236, 237]. There is a lack of a distinct clinical, laboratory or radiological marker to support an early diagnosis of RA: diagnosis is defined by the 1987 criteria of the American College of Rheumatology, which have low sensitivity in early RA. Therefore, a more specific and sensitive marker for progressive RA is needed which ideally should be present at an early stage of the disease.

Standard immunosuppressive treatment regimens have multiple potential complications, limiting their use in the absence of a definite diagnosis. Recently, TNF-α blockade therapy has emerged as a successful therapy for the treatment of this disease. However, these drugs are used only after the failure of standard drug regimens because of cost and lack of data for long-term safety [238]. Overall, this leads to under-treatment of RA, resulting in deformity and disability that may have been avoided with early use of TNF-α blockade. Although a very strong tool, TNF-α blockade is not always successful. Due to its high cost and potentially harmful side effects, it would be useful to have a test that allows differentiation between cases where this therapy will be successful, versus those where it will not [239, 240].

An increase in the protein MARCKS accounts for 90% or more of the cellular response to treatment with TNF-α in macrophages and monocytes [71, 72]. Based on its known function as a regulator of the actin cytoskeleton, [17, 241] we hypothesize that MARCKS has a major functional role in the cellular response to TNF-α in RA and therefore MARCKS levels may have specificity for the diagnosis of RA [242]. We reason that MARCKS levels may be indicative of not only the extent of cumulative stimulation by TNF-α in patients with RA, thus indicating

prognosis, but also that MARCKS levels may correlate with the capacity of these patients to respond to TNF-α blockade, thus predicting whether TNF-α blockade will be successful. Higher MARCKS mRNA or protein level in patients' blood may predict a better response to TNF-α blockade, and if MARCKS levels are comparable to normal constitutive levels, then therapy may be less effective. Even if MARCKS does not have a major functional role in TNF-α signaling, the striking increase in this protein observed after chronic stimulation by TNF-α makes MARCKS an attractive candidate as a marker for RA disease, for prognosis, and for response to TNF-α blockade.

One percent of the population has RA, with a female predominance. Disability and mortality are common in this disease. Recently, the most common cause of death in RA was shown to be due to cardiovascular disease [243]. Effective treatments begun early in the course of disease are the only known way to prevent disability [237]. Factors associated with a bad outcome include delays in diagnosis and treatment. Therapy with TNF-α blockade has been shown to decrease both the occurrence of disability and death [238]. Presumably these therapies decrease the inflammation that is responsible for an increase in cardiovascular events in RA. Yet the cost of TNF-α blockade is high and in the range of $20,000 per year when all associated costs are included. Our work has the potential to alter several factors related to disability and death, including improvements in early diagnosis and the potential to identify RA patients most likely to benefit from treatment with TNF-α blockade.

If an individual's TNF-α is causally related to disease it may be the cellular responses to TNF-α rather than the time-dependent average level of TNF-α secretion that is responsible for disease severity or activity. MARCKS or maybe levels of MARCKS metabolites (e.g., phosphorylated MARCKS, proteolyzed MARCKS, etc…) may best reflect the level of

"activated" cellular response and therefore may be better predictive of disease. Specific findings related to MARCKS could tell us that a patient has severe RA or that the disease, in this particular patient, is caused by the cellular response to TNF-α and therefore this patient is a good candidate to respond to TNF-α inhibition.

Study Subjects

Patients and controls were recruited for this study following IRB approval. We were aiming to collect blood samples from the four following subject groups:

- Group 1: patients presenting with early synovitis;
- Group 2: RA patients at different disease stages: untreated, treated with classical RA drugs, treated with TNF-inhibitors;
- Group 3: patients with other inflammatory polyarthritides (e.g. SLE, gout); this is a control group;
- Group 4: healthy controls with similar age, sex and race characteristics as study subjects; this is another control group.

Initially, we were hoping to collect at least 10-15 blood samples from each of the four subject groups described above; however, we were unable to reach our goal in the time period of the study. In addition, some of our subjects did not return for follow up, making it impossible to track their progress and changes in MARCKS.

Levels of MARCKS parameters were compared for early synovitis patients who later developed RA versus those who did not to assess the usefulness of MARCKS as a specific marker for diagnosis. We also compared MARCKS parameters in RA patients who responded to TNF blockade therapy versus those who failed therapy to test the usefulness of MARCKS as predictor of response to TNF blockade therapy. We looked for a correlation between a MARCKS-related parameter or a change in a MARCKS-related parameter, pre- and post-TNF blockade therapy, which would measure activated MARCKS and thus indicate long-term

outcome, i.e. prognosis: pre-treatment levels may help determine whether a patient should be treated more or less aggressively, whereas post-treatment levels may help determine whether therapy has changed prognosis.

Cell Isolation from Whole Blood

Both mononuclear cells and granulocytes were isolated from whole blood of study subjects. Leukocytes were separated using Histopaque-1119 (polysucrose, 6.0g/dl and sodium diatrizoate, 16.7g/dl, density=1.119) and Histopaque-1077 (polysucrose, 5.7g/dl and sodium diatrizoate, 9.0g/dl, density=1.077) (Sigma-Aldrich, St. Louis, MO). According to the Sigma-Aldrich procedure, a double gradient is formed by layering an equal volume of Histopaque-1077 and Histopaque-1119. Whole blood is carefully layered onto the upper Histopaque-1077 medium. The tubes are then centrifuged at 700xg for 30 minutes. Cells of the granulocytic series are found at the 1077/1119 interphase whereas lymphocytes, other mononuclear cells and platelets are found at the plasma/1077 interphase (Figure 5-1).

Detailed Cell Isolation Protocol

Whole blood was diluted 1:2 in room temperature 1xPBS. To 17 mL blood isolated in Heparin vaccutainers, 34 mL of 1xPBS were added. Two Histopaque-1077/Histopaque-1119 double gradients were made by layering 12.5 mL of Histopaque-1077 over 12.5 mL Histopaque-1119 in a 50 mL conical tube. Twenty five mL of diluted blood was then carefully layered onto the upper gradient of the tube and centrifuged at 700xg for 30 minutes at room temperature. Two distinct opaque layers were formed following centrifugation, corresponding to leukocytes (A and B in Figure 5-1). Plasma was aspirated to within 0.5 cm of layer A and frozen. Cells from layer A were transfered to a tube marked “mononuclear.” Remaining fluid was aspirated to within 0.5cm of layer B and discarded. Cells from this layer were transferred to a tube labeled “granulocytes.” Cells were washed three times with cold 10 mL of isotonic PBS, centrifuged for

10 minutes at 200xg and the supernatant discarded. Cells were counted using a hemacytometer. At the final wash, after resuspension, cells were divided into two 5 mL aliquots. RNA was immediately isolated RNA from the first aliquot using QIAGEN's RNeasy Kit for RT-PCR analysis and pellets of second aliquot were frozen for future protein isolation for use in ELISA.

Quantitative Real Time RT-PCR for Determination of mRNA Concentration

Quantitative real time RT-PCR using TaqMan probes (Applied Biosystems Gene Expression Assays) was performed on mRNA isolated from patient blood cells. MARCKS, TNF-α, IL-1β, MCP-1 and IL-17 mRNA levels were measured to compare healthy and patient samples.

Detailed qRT-PCR Protocol

DNAse I treatment. Frozen RNA was thawed and samples spun to bring all to the bottom. Volume in all tubes was brought up to 100 µL with 40 µL RNAse-free sterile water. Ten µL 10X DNase I reaction buffer (10 mM Tris-HCl, 2.5 mM $MgCl_2$, 0.5 mM $CaCl_2$, pH 7.6 @ 25ºC) were added to each sample. Five Kunits (5 µL) of DNase I (bovine pancreas Dnase I, USB, Amersham Cat # 14345, lyophilized powder dissolved in storage buffer, 50% glycerol+10 mM Tris-HCl+2 mM $CaCl_2$, pH 7.6 @ 25ºC, powder was 2,974 Kunits/mg, I made a 1,000 Kunits/mL stock and froze at -20ºC) were added to each sample, mixed by pipetting and incubated at 37ºC for 15 minutes. Two µL of 0.27 M EDTA (protects RNA from being degraded during heat inactivation) were added to a final concentration of ~ 5 mM and samples mixed. DNase I was heat inactivated at 75-80ºC for 10 minutes. To quantify the RNA, 10 µL of each RNA sample were added to 90 µL RNase-free water (10X dilution) and OD 260 and 280 measured to determine RNA concentration and purity following DNase I digestion.

Reverse transcribing RNA into cDNA for RT-PCR. Two micrograms of RNA were brought to a final volume of 60 µL with nuclease-free water. Sixty microliters of a 2X reverse transcription master mix (High Capacity cDNA Archive kit (Cat. # 4322171, Applied Biosystems), 12 µL 10X reverse transcription buffer, 4.8 µL 25X dNTPs, 12 µL 10X random primers, 6 µL 50 U/µL MultiScribe™ Reverse Transciptase, 25.2 µL nuclease-free water) were added. Samples were incubated at 25°C for 10 minutes, then at 37°C for 2 hours in a water bath. cDNA was then frozen until used.

Real-time PCR of cDNA samples. Real time PCR was carried out in 96-well plates in an Applied Biosystems 7500 Standard 96-well block thermal cycler. Samples were prepared by mixing 1.25 µL 20X TaqMan Gene Expression Assay (catalog number varies with each gene, for MARCKS (Hs00158992_m1), TNF-α (Hs00174128_m1), GAPDH (Hs99999905_m1), 18S (Hs99999901_s1), IL-1β (Hs00174097), MCP-1 (Hs002344140_m1) and IL-17 (Hs00174383_m1)), 11.25 µL cDNA template and 12.5 µL 2X TaqMan Universal PCR Master Mix (Applied Biosystems Cat. # 4304437). The PCR parameters used were as follows:

- Stage 1: 1 rep at 50°C for 2 minutes;
- Stage 2: 1 rep at 95°C for 10 minutes;
- Stage 3: 50 reps of:
    a. 95°C for 15 seconds;
    b. 60°C for 1 minute.

Quantitative real time RT-PCR data were analyzed using the comparative C_t method (also called the $2^{\Delta\Delta Ct}$ method). This involves comparing the C_t values (cycle at which the fluorescence of our sample crosses the threshold, the cycle number at which the increase in fluorescence (and therefore cDNA) is exponential) of the samples of interest with a control or calibrator such as a non-treated sample or RNA from normal tissue or a healthy control. The C_t values of both the calibrator and the samples of interest are normalized to an appropriate endogenous housekeeping

gene (GAPDH was our choice). So, $\Delta\Delta C_t = \Delta C_{t,sample} - \Delta C_{t,reference}$, where $\Delta C_{t,sample}$ is the C_t value for any sample (e.g., cDNA from patient samples) normalized to the endogenous housekeeping gene (GAPDH) and $\Delta C_{t,reference}$ is the C_t value for the calibrator (e.g., cDNA from healthy controls) also normalized to the endogenous housekeeping gene (GAPDH).

Results

RT-PCR data (Tables 5-1 to 5-6) from mRNA isolated from white blood cells of patients with inflammatory diseases, mainly RA, show a strong correlation between the levels of TNF mRNA and MARCKS mRNA (Figures 5-2 and 5-3). This correlation is similar to that observed for other cytokines known to be important for TNF signaling such as IL-1β and MCP-1 (Figure 5-2 and 5-3). The highest correlation with TNF was for IL-1β in mononuclear cells (F-statistic 216), followed by MARCKS in mononuclear cells (F-statistic 179), MCP-1 in mononuclear cells (F-statistic 135), MCP-1 in granulocytes (F-statistic = 52), IL-1β in granulocytes (F-statistic = 36) and finally MARCKS in granulocytes (F-statistic = 29). IL-17 had no correlation with TNF in mononuclear cells, with an F-statistic of 0.1; to be significant a correlation, the F-statistic should be much larger than 1. We noticed that there were a few outliers in each graph that seemed to skew the data and weigh heavily into the analysis. To overcome this problem, we threw out the most obvious outlier in each case and re-calculated F-values. In mononuclear cells, the values became 31 for IL-1β, 18 for MARCKS and 9 for MCP-1, but the order was retained. However, in granulocytes, the order was changed and became similar to that observed in mononuclear cells, where IL-1β had the highest correlation with TNF with an F-value of 35, followed by MARCKS whose F-value was 29 and finally MCP-1 whose F-value was 17. IL-17 could not be detected in healthy controls' granulocytes and so a fold change could not be calculated using the ΔΔCt method, which requires a control sample.

Quantitative Sandwich ELISA of MARCKS and TNF-α

Enzyme-linked immunosorbent assays (ELISAs) allow the detection and quantification of substances such as peptides, proteins, antibodies and hormones [244, 245]. In a standard ELISA, the antigen is first immobilized to a solid surface. It is then complexed with an antibody that is linked to an enzyme. Detection is accomplished by incubating this enzyme-complex with a substrate that produces a detectable product. The most crucial element of the detection is a highly specific antibody-antigen interaction.

A more common type of ELISA is the sandwich assay. This is a more sensitive and robust type of ELISA which allows better quantification of the antigen of interest [246]. It is called a sandwich ELISA because the antigen is bound between two antibodies, the capture antibody and detection antibody. The capture and detection antibody ideally recognize different non-overlapping epitopes. Binding by the capture antibody should in no way alter or obscure the epitope recognized by the detection antibody, and both antibodies should be able to bind simultaneously to the analyte to be measured. Either monoclonal or polyclonal antibodies can be used as an ELISA pair. A detection enzyme (most commonly horseradish peroxidase or alkaline phosphatase) may be linked directly to the detection antibody or introduced through a secondary antibody that recognizes the detection antibody.

We were interested in measuring the amounts of TNF-α and MARCKS in our patient samples. TNF-α can be assayed in plasma, whereas MARCKS can be measured in leukocytes. Commercially available sandwich ELISA kits are widespread for commonly measured cytokines such as TNF-α. We used the Human TNF OptEIA™ ELISA Set (BD Biosciences, Cat. # 555212) to measure TNF-α in the plasma of our patient and control samples.

To measure MARCKS concentrations in our samples, we had to develop and test a sandwich ELISA, as neither a commercially available kit exists, nor has one been described in the literature. This was done by testing different commercially available MARCKS antibodies for coating and detection, as well as testing different coating buffers and blocking buffers until a useful assay was reached, as determined by use of purified recombinant MARCKS as an antigen.

Quantification of Plasma TNF-α Using a Commercial Sandwich ELISA

Plasma was collected during the Histopaque-1077/Histopaque-1119 double gradient leukocyte isolation described previously. Following centrifugation, plasma was kept on ice and then frozen at -80°C. Plasma was thawed quickly under running water and used as is in our ELISA. In most cases, this plasma had been diluted 1:2 with 1X PBS for the leukocyte isolation protocol. A TNF-α standard ranging from 5000 pg/mL to 2.5 pg/mL was loaded on the plates for construction of a standard curve. The recommended assay procedure from the kit was followed exactly.

Microwells were coated with 100µL per well of capture antibody diluted in coating buffer. Seal plate and incubate overnight at 4° C. Wells were aspirated and washed 3 times with ≥ 300µL/well Wash Buffer. After the last wash, plates were inverted and blotted on absorbent paper to remove any residual buffer. Wells were blocked with ≥ 200µL/well assay diluent and incubated at RT for 1 hour. Wells were aspirated and washed 3 times. Standards and sample dilutions were prepared in assay diluent. One hundred µL of each standard, sample, and control were pipetted into appropriate wells, plate sealed and incubated for 2 hours at RT. Wells were aspirated and washed 5 times. One hundred µL of working detector (detection Antibody + SAv-HRP reagent) were added to each well, plate sealed and incubated for 1 hour at RT. Wells were aspirated and washed 7 times. NOTE: In this final wash step, wells were soaked in wash buffer for 30 seconds to 1 minute for each wash. One hundred µL of substrate solution were added to

each well and the plate was incubated (without plate sealer) for 30 minutes at room temperature in the dark. Fifty µL of stop solution were added to each well. Absorbance was read at 450 nm within 30 minutes of stopping reaction.

Quantification of Cellular MARCKS Using Optimized Sandwich ELISA

MARCKS Serotec antibody (Goat anti-human MARCKS polyclonal antibody, raised against synthetic peptide ECSPEAPPAEAAE derived from C-terminus of MARCKS protein, immunoaffinity purified against the MARCKS synthetic peptide, Cat. # AHP695) was diluted to 2 µg/mL in coating buffer (40 µL of 0.5 mg/mL antibody into 10 mL coating buffer=0.1 M sodium carbonate, pH 9.5). Microwells were coated with 100 µL per well of diluted coating (=capture) antibody, the plate was sealed and incubated at 4°C overnight. Wells were aspirated and washed 3X with 300 µL/well of wash buffer=TBS with 0.05%Tween-20. After washing, the plate was inverted and blotted on paper towels. Wells were blocked with 200 µL blocking buffer (0.5%BSA, 150 mM NacCl, 2 mM EDTA, 50 mM Tris, pH7.5, 0.3% Nonidet P-40) for 1.5 hours at RT. Standard and samples were prepared in lysis buffer (0.5 M NaCl, 50 mM Tris, 2 mM EDTA, 1% NP-40, pH 7.5). Wells were aspirated and washed 2X with 300 µL/well of wash buffer=TBS with 0.05%Tween-20. After washing, the plate was inverted and blotted on paper towels. One hundred µL of each standard or sample were pipetted into appropriate wells, plate sealed and incubated overnight at 4°C. Wells were aspirated and washed 3X with 300 µL/well of wash buffer=TBS with 0.05%Tween-20. After washing, the plate was inverted and blotted on paper towels. Calbiochem antibody (=detection antibody, Rabbit anti-mouse MARCKS antibody, purified against native MARCKS from mouse brain, polyclonal antibody, total IgG immunoaffinity purification, Cat. # 442707) was diluted to 2.7 µg/mL (40 µL in 10 mL of blocking buffer) and 100 µL added per well. The plate was sealed and incubated for 2 hours at RT. Wells were aspirated and washed 3X with 300 µL/well of wash buffer=TBS with

0.05%Tween-20. After washing, the plate was inverted and blotted on paper towels. One hundred µL of AP-conjugated monoclonal mouse anti-rabbit IgG were pipetted into each well (secondary detection antibody, diluted 1:1000 in blocking buffer, Sigma, Cat. No. A2556) and the plate was incubated at RT for 1 hour. . Wells were aspirated and washed 5 times. NOTE: In this final wash step, wells were soaked in wash buffer for 30 seconds for each wash. One hundred µL of substrate solution (two 5 mg tablets of p-nitrophenyl phosphate (AP substrate, Sigma-Aldrich, Cat. No. N 9389), 5 µL 1 M $MgCl_2$, 10 µL diethanolamine and 10 mL ddH_2O) were added to each well and the plate was incubated (without plate sealer) for 30 minutes at room temperature in the dark. Absorbance was read at 450 nm at 30 minutes and read again every 30 minutes until we got good development in all wells without overdeveloping the highest standard concentration.

Standard Preparation:

Recombinant murine MARCKS was purified from *E. coli* as described previously. The concentration of MARCKS was determined by amino acid analysis to be 4.65 µM. To make a serial dilution of stock MARCKS to make ELISA standards, 20 ELISA dilution tubes were placed on a used ELISA plate. Five hundred µL of diluted MARCKS stock (250 µL into 3.75 mL lysis buffer) were pipetted into the first tube and 250 µL of lysis buffer into tubes 2-20. Two hundred and fifty µL were transfered from tube 1 to tube 2 and mixed well by pipetting. Two hundred and fifty µL were transfered from tube 2 to tube 3 and mixed well by pipetting. This was repeated until tube 20.

Sample Preparation:

Frozen cell pellets of leukocytes isolated from human blood were resuspended in 500 µL lysis buffer containing 5 mM DFP, 0.25 mM leupeptin, 1 mM PMSF, and 0.125 mg trypsin

inhibitor. Samples were vortexed briefly to resuspend cells and kept on ice for 1 hour. Samples were sonicated for 30 seconds to break the cells and placed back on ice. Samples were centrifuged for 15 minutes at 4°C at 4,000 rpm. Supernatants were taken and used for ELISA. The remaining samples were frozen.

Results

The serum levels of TNF measured by quantitative sandwich ELISA in patient samples were within the range of what is expected (Table 5-10). There appeared to be no statistically significant difference between healthy controls and RA patients, either untreated or on any of the treatments shown (Figure 5-4). The only statistical significance in terms of TNF serum levels was found between healthy controls and the MCTD group ($p=0.03$). However, this group only had two subjects and therefore no conclusions could be drawn.

MARCKS levels appeared to be reduced overall in RA patients (Table 5-10). With the small number of samples we had in each group, it was difficult to determine whether the observed differences were meaningful. In a few cases, it appeared that MARCKS levels were much lower in patients with active RA versus those with inactive RA (Figure 5-5). For example, patients 19 and 38 both have RA and are taking Humira. At the particular visit where blood was drawn for this analysis, patient 19 had active RA, whereas 38 had inactive RA. MARCKS levels for patient 19 were very low (0.03ng/100,000 cells) whereas patient 38 had higher MARCKS levels (0.51ng/100,000 cells). However, as tested by a Mann-Whitney 2-tailed U test, only statistically significant differences were found between healthy controls and patients with juvenile rheumatoid arthritis (JRA, $p=0.02$). There was also a nearly statistical significant ($p=0.08$) that patients whom had untreated early synovitis that later developed into RA had lower levels of MARCKS. Again, in both these goups (JRA and untreated early synovitis) we only had 3 samples and therefore it was hard to determine at this point whether it is meaningful.

Conclusions

The RT-PCR correlation data were interesting in further establishing MARCKS as an important signaling molecule downstream of TNF in the TNF signal transduction pathway.

Due to the limited number of samples obtained in each category, it was not possible to draw meaningful conclusions from this study. However, we can come up with a few hypotheses and our data can be used in a power analysis to determine the number of patients that would be needed to yield statistically significant results in a future followup study.

As previously described, TNF serum levels in our analysis did not appear to be sensitive or specific for diagnosis or prognosis of early synovitis, RA or response to treatment. They were also highly variable, and this has been previously reported presumably because they can be affected by a simple bacterial infection or a common cold.

MARCKS data appeared a little more promising than TNF for diagnosis and/or prognosis of RA. Opposite to what we had expected based on the finding that TNF induces a large increase in MARCKS protein levels in macrophages and neutrophils, it appeared that MARCKS levels are reduced in RA patients. This may point to an aberrant TNF signaling transduction in those patients or that their cells are somehow no longer responsive to TNF. An analysis of parameters related to disease activity (as measured for example by CRP or an activity score) may be more revealing.

Increasing evidence suggests that the chronic persistence of the inflamed condition of joint tissue in RA can be attributed to mechanisms that inhibit programmed cell death of activated cells within the joint tissues in RA [247]. Because the cells that drive the pathology of RA are resistant to pathways that would otherwise enable their natural clearance, the inflamed condition is maintained indefinitely. Numerous histologic studies of joint tissues recovered from RA paitents suggest that the occurrence of apoptosis in the synovium of the RA joint is particularly

rare, and that proteins that block apoptosis are prevalent in cells and tissues of the afflicted joints [248-252]. Thus, it has been suggested that therapies that can amplify apoptotic signals or block inhibitors of apoptosis may be successful in down-regulating the chronic inflammation and work in synergy with existing therapies to cure RA [247, 253, 254]. If MARCKS is important for normal signaling by TNF, specifically for TNF-induced apoptosis as our preliminary data in Chapter 4 point to, having lower levels of MARCKS may cause this resistance to apoptosis found in those cells and finding strategies to activate MARCKS or increase its levels in synovial joint tissues may aid in the treatment of RA.

In addition, it has been reported that RA synovial fibroblasts acquire many characteristics of transformed cells, becoming more invasive [242]. This is also quiet interesting in terms of MARCKS involvement because reduced levels of MARCKS are found to cause cell proliferation and tumor progression in many cell types, and again may play a role in the "transformed" phenotype of RASFs [53-56].

As previously described (Chapters 1-3), MARCKS is strictly regulated by various mechanisms including at least a dozen post-translational modifications and proteolysis which may activate or inactivate the protein depending on their location, as well as change its distribution from membrane-bound to cytosolic and vice versa. MARCKS is also regulated at the transcription level by different promoters; and the MARCKS transcript contains CU-rich elements making it unstable unless bound by RNA binding proteins whose presence is cell specific and variable. All these regulatory requirements make it such that if any of them should go wrong (for example, by a mutation in a phosphorylation site, cleavage site or site of intramolecular interaction), it could have a detrimental effect on MARCKS function. Given MARCKS's important roles this can potentially cause disease.

Table 5-1. Ct values obtained by quantitative real time RT-PCR for mononuclear cells from patient samples.

Sample #	MCP-1	IL-17A	GAPDH	IL-1β	MARCKS	TNF-α	GAPDH
1A	27.66	31.73	19.07	18.69	21.35	21.89	19.24
2A	26.52	32.48	20.14	16.79	21.00	20.22	20.69
3A	28.05	30.69	19.77	17.07	21.89	20.39	20.25
4A	30.34	40.52	19.41	20.42	23.13	20.87	19.69
5A	27.90	32.38	18.90	22.67	22.97	23.59	19.31
7A	31.09	40.23	20.16	21.47	24.13	23.44	20.44
8A	25.04	34.54	21.13	21.18	23.39	22.60	21.44
9A	29.80	34.00	20.10	20.06	22.51	21.16	20.37
10A	29.31	40.49	19.17	19.85	23.22	21.13	19.58
11A	29.24	30.20	18.34	20.67	21.69	22.64	18.95
12A	31.71	34.18	21.85	22.72	24.11	24.38	22.23
13A	29.00	36.10	19.22	23.75	23.54	25.08	19.69
14A	28.84	36.29	20.33	25.28	23.98	25.64	20.70
15A	29.10	37.38	19.84	24.69	23.12	24.39	20.17
16A	28.35	und	21.69	26.13	23.92	25.00	20.49
17A	28.96	34.92	21.88	19.12	22.68	22.23	20.59
18A	24.47	31.73	20.75	18.48	21.31	19.82	19.25
19A	28.42	33.33	21.10	18.52	21.44	20.60	20.48
20A	30.11	33.31	22.86	18.69	22.23	21.13	21.32
21A	32.72	37.31	22.65	20.34	23.55	23.10	21.96
22A	26.87	34.38	22.51	16.37	20.61	20.27	21.19
24A	25.79	33.90	22.43	17.68	21.39	20.55	21.55
25A	27.56	34.84	22.07	17.48	21.33	20.54	21.15
26A	28.52	34.84	22.00	18.22	21.59	20.97	20.99
27A	29.53	34.34	23.44	18.03	21.88	21.00	22.00
28A	25.21	37.49	22.12	18.85	22.90	21.50	21.63
29A	29.13	34.29	21.47	21.65	22.59	23.02	20.86
30A	27.78	34.06	22.00	20.65	22.34	21.04	21.31
31A	34.00	35.49	26.29	22.45	23.00	23.06	22.80
32A	33.29	36.81	22.80	21.30	22.72	23.96	21.56
33A	34.65	36.07	26.45	22.30	23.46	23.21	23.91
34A	29.26	34.29	23.65	19.13	21.76	21.10	22.01
35A	25.73	35.00	23.29	19.23	21.44	22.14	21.50
36A	28.44	und	22.23	20.95	23.10	21.43	21.00
37A	27.23	36.09	23.41	21.64	22.55	22.54	20.48
38A	30.70	31.03	23.70	26.36	22.85	24.35	21.05
39A	31.98	und	25.68	29.00	24.18	28.96	25.68

Table 5-1. Continued.

Sample #	MCP-1	IL-17A	GAPDH	IL-1β	MARCKS	TNF-α	GAPDH
40A	30.60	und	23.33	19.54	22.82	23.64	23.33
41A	27.29	und	24.25	23.35	24.08	25.03	24.25
42A	25.41	42.74	27.61	20.08	23.55	24.46	27.61
43A	28.38	und	23.29	20.59	23.70	22.06	23.29
44A	26.05	und	22.98	20.51	23.27	21.57	22.98
45A	26.95	und	23.49	20.52	22.29	22.00	23.49
46A	30.92	und	24.47	27.49	23.51	26.00	24.47
47A	29.84	und	23.60	23.14	24.00	25.89	23.60
48A	26.36	und	19.43	24.41	22.23	24.79	19.43
49A	28.73	37.94	20.16	25.28	23.40	24.66	20.16
50A	29.29	und	20.57	24.83	23.27	24.33	20.57
51A	28.83	und	20.63	23.43	23.11	23.07	20.63
52A	27.03	und	20.32	24.10	23.43	23.44	20.32
53A	27.40	41.70	20.26	21.00	21.59	21.30	20.26
54A	27.38	und	20.92	23.33	23.82	23.24	20.92
55A	28.52	40.56	20.23	25.93	23.00	25.00	20.23
56A	27.91	und	26.11	23.86	24.44	25.81	26.11
57A	28.13	und	19.99	24.89	22.32	24.31	19.99

und=undetermined

Table 5-2. Ct values obtained by quantitative real time RT-PCR for granulocytes from patient samples.

Sample #	MCP-1	IL-17A	GAPDH	IL-1β	MARCKS	TNF-α	GAPDH
1B	33.78	39.73	21.82	23.82	21.16	27.00	22.00
2B	31.59	33.28	22.04	18.12	20.23	22.65	22.30
3B	33.07	33.88	23.68	21.00	22.76	25.27	24.28
4B	33.15	und	21.20	21.58	21.12	24.74	22.02
5B	32.46	und	24.58	23.27	23.66	26.24	24.91
9B	34.72	40.48	21.50	24.23	22.70	26.02	22.06
10B	31.01	und	21.08	22.24	22.55	24.32	21.47
11B	34.48	und	20.58	21.23	21.36	25.38	21.04
14B	33.24	und	23.42	23.95	23.15	26.65	23.89
15B	34.00	und	26.00	25.41	24.19	27.77	26.59
16B	32.47	und	26.09	24.01	22.95	25.62	24.09
18B	31.78	und	25.46	24.29	24.28	26.21	24.29
19B	36.05	36.00	26.49	25.52	24.35	26.78	25.42
21B	35.95	35.76	25.37	24.26	22.97	26.86	23.47
22B	32.67	35.90	24.86	22.59	22.46	25.35	22.95
25B	32.13	38.76	27.58	24.95	24.57	27.12	26.27
26B	34.81	39.21	25.17	24.18	23.00	26.14	24.13
27B	37.14	und	26.02	24.66	23.33	27.43	26.02
29B	36.00	43.08	24.17	24.79	22.51	26.91	23.54
30B	32.62	und	24.73	24.00	22.07	25.56	24.17
32B	39.89	und	26.45	26.21	22.13	27.89	23.92
34B	34.93	36.21	26.14	23.41	21.22	25.85	24.17
35B	35.36	und	29.00	24.84	24.30	27.26	26.83
37B	35.66	37.78	29.42	27.00	25.21	28.00	24.66
40B	35.28	und	26.50	26.51	24.23	29.51	26.50
41B	34.21	und	28.13	25.69	25.05	29.30	28.13
42B	30.30	und	28.18	24.09	24.38	27.28	28.18
43B	36.00	und	29.30	27.46	26.00	31.87	29.30
44B	30.66	und	27.00	24.75	24.39	26.76	27.00
48B	34.27	und	23.53	25.78	23.83	28.63	23.53
49B	37.00	und	24.48	27.11	23.28	29.15	24.48
54B	36.20	und	28.00	26.04	23.40	27.82	28.00
55B	39.43	und	29.41	31.34	27.77	32.18	29.41
57B	36.14	und	25.54	27.59	24.03	29.54	25.54

Table 5-3. $\Delta\Delta C_t$ and fold change calculations for monocytic cells qRT-PCR from patient samples. Results shown in this table are for MCP-1, IL-1β and IL-17A.

Sample #	Ct MCP-1-Ct GAPDH	% of control	MCP-1 fold change	Ct IL-1β-Ct GAPDH	% of control	IL-1β fold change	Ct IL-17A-Ct GAPDH	% of control	IL-17A fold change
1A	8.60	135.50	1.36	- 0.38	1508.63	15.09	12.66	241.59	2.42
2A	6.38	627.38	6.27	- 3.35	11845.27	118.45	12.34	300.96	3.01
3A	8.28	168.69	1.69	- 2.69	7507.01	75.07	10.92	806.44	8.06
4A	10.94	26.76	0.27	1.02	574.05	5.74	21.11	0.69	0.01
5A	9.01	101.98	1.02	3.78	84.63	0.85	13.49	136.00	1.36
7A	10.93	26.82	0.27	1.31	467.24	4.67	20.07	1.41	0.01
8A	3.91	3478.36	34.78	0.06	1115.92	11.16	13.41	142.96	1.43
9A	9.70	62.87	0.63	- 0.04	1195.19	11.95	13.90	102.07	1.02
10A	10.14	46.50	0.47	0.68	721.58	7.22	21.32	0.60	0.01
11A	10.90	27.50	0.27	2.33	230.24	2.30	11.86	418.60	4.19
12A	9.86	56.30	0.56	0.87	635.18	6.35	12.33	303.47	3.03
13A	9.78	59.68	0.60	4.53	50.39	0.50	16.88	12.97	0.13
14A	8.51	143.33	1.43	4.95	37.61	0.38	15.96	24.43	0.24
15A	9.26	85.58	0.86	4.85	40.25	0.40	17.54	8.19	0.08
16A	6.67	516.34	5.16	4.44	53.37	0.53	und	und	und
17A	7.07	388.88	3.89	- 2.77	7896.64	78.97	13.04	185.26	1.85
18A	3.72	3970.73	39.71	- 2.27	5583.77	55.84	10.98	770.91	7.71
19A	7.32	327.46	3.27	- 2.58	6927.04	69.27	12.23	324.80	3.25
20A	7.24	345.89	3.46	- 4.18	20998.85	209.99	10.45	1115.46	11.15
21A	10.07	48.61	0.49	- 2.31	5744.73	57.45	14.66	60.27	0.60
22A	4.36	2553.37	25.53	- 6.14	81811.89	818.12	11.87	415.42	4.15
24A	3.36	5099.67	51.00	- 4.75	31238.18	312.38	11.46	552.34	5.52
25A	5.49	1163.45	11.63	- 4.58	27823.63	278.24	12.77	223.08	2.23
26A	6.51	573.32	5.73	- 3.79	15991.56	159.92	12.83	213.70	2.14

Table 5-3. Continued 1.

Sample #	Ct MCP-1-Ct GAPDH	% of control	MCP-1 fold change	Ct IL-1β-Ct GAPDH	% of control	IL-1β fold change	Ct IL-17A-Ct GAPDH	% of control	IL-17A fold change
27A	6.09	769.72	7.70	- 5.42	49495.95	494.96	10.90	816.56	8.17
28A	3.09	6162.03	61.62	- 3.27	11183.02	111.83	15.37	36.72	0.37
29A	7.66	259.43	2.59	0.18	1022.60	10.23	12.82	216.38	2.16
30A	5.78	950.93	9.51	- 1.35	2959.26	29.59	12.06	366.44	3.66
31A	7.71	250.76	2.51	- 3.85	16670.65	166.71	9.20	2654.87	26.55
32A	10.49	36.46	0.36	- 1.51	3301.77	33.02	14.01	94.58	0.95
33A	8.20	178.43	1.78	- 4.16	20695.40	206.95	9.61	1991.20	19.91
34A	5.62	1066.15	10.66	- 4.51	26469.12	264.69	10.64	977.14	9.77
35A	2.44	9682.67	96.83	- 4.06	19376.53	193.77	11.71	466.72	4.67
36A	6.22	704.86	7.05	- 1.27	2805.46	28.05	und	und	und
37A	3.82	3709.96	37.10	- 1.76	3937.39	39.37	12.69	236.29	2.36
38A	7.00	409.07	4.09	2.66	183.80	1.84	7.33	9697.67	96.98
39A	6.30	663.61	6.64	3.32	116.16	1.16	und	und	und
40A	7.27	340.42	3.40	- 3.79	16058.20	160.58	und	und	und
41A	3.04	6374.91	63.75	- 0.90	2158.81	21.59	und	und	und
42A	- 2.20	240919.15	2409.19	- 7.53	214411.51	2144.12	15.13	43.36	0.43
43A	5.09	1538.37	15.38	- 2.70	7553.99	75.54	und	und	und
44A	3.08	6217.80	62.18	- 2.47	6427.41	64.27	und	und	und
45A	3.46	4761.46	47.61	- 2.97	9102.35	91.02	und	und	und
46A	6.46	597.25	5.97	3.02	142.62	1.43	und	und	und
47A	6.24	692.27	6.92	- 0.46	1600.18	16.00	und	und	und
48A	6.92	432.39	4.32	4.98	36.81	0.37	und	und	und
49A	8.58	137.01	1.37	5.12	33.31	0.33	17.78	6.91	0.07
50A	8.72	124.00	1.24	4.26	60.51	0.61	und	und	und

Table 5-3. Continued 2.

Sample #	Ct MCP-1-Ct GAPDH	% of control	MCP-1 fold change	Ct IL-1β-Ct GAPDH	% of control	IL-1β fold change	Ct IL-17A-Ct GAPDH	% of control	IL-17A fold change
51A	8.21	177.19	1.77	2.80	166.57	1.67	und	und	und
52A	6.71	500.14	5.00	3.79	84.16	0.84	und	und	und
53A	7.14	371.75	3.72	0.74	694.59	6.95	21.44	0.55	0.01
54A	6.47	592.30	5.92	2.42	217.22	2.17	und	und	und
55A	8.29	167.29	1.67	5.71	22.24	0.22	20.33	1.18	0.01
56A	1.80	15088.79	150.89	- 2.26	5545.20	55.45	und	und	und
57A	8.14	185.23	1.85	4.90	38.77	0.39	und	und	und

Table 5-4. $\Delta\Delta C_t$ and fold change calculations for monocytic cells qRT-PCR from patient samples. Results shown in this table are for MARCKS and TNF-α.

Sample #	Ct MARCKS-Ct GAPDH	% of control	MARCKS fold change	Ct TNF-α-Ct GAPDH	% of control	TNF-α-fold change
1A	2.11	184.59	1.85	2.65	248.08	2.48
2A	0.31	640.56	6.41	- 0.47	2161.31	21.61
3A	1.65	254.09	2.54	0.15	1412.16	14.12
4A	3.43	73.73	0.74	1.17	692.99	6.93
5A	3.67	62.65	0.63	4.28	80.32	0.80
7A	3.69	61.57	0.62	3.00	195.05	1.95
8A	1.94	206.96	2.07	1.16	700.72	7.01
9A	2.14	180.04	1.80	0.79	901.19	9.01
10A	3.64	63.83	0.64	1.55	532.52	5.33
11A	2.74	119.28	1.19	3.68	121.57	1.22
12A	1.88	215.75	2.16	2.15	352.55	3.53
13A	3.85	55.30	0.55	5.39	37.34	0.37
14A	3.29	81.53	0.82	4.95	50.69	0.51
15A	2.95	103.12	1.03	4.23	83.44	0.83
16A	3.43	73.78	0.74	4.51	68.67	0.69
17A	2.09	186.91	1.87	1.64	499.97	5.00
18A	2.07	190.04	1.90	0.57	1051.10	10.51
19A	0.96	408.78	4.09	0.12	1436.85	14.37
20A	0.91	422.32	4.22	- 0.19	1784.98	17.85
21A	1.59	263.96	2.64	1.14	708.53	7.09
22A	- 0.58	1192.02	11.92	- 0.92	2960.63	29.61
24A	- 0.16	892.18	8.92	- 1.00	3129.44	31.29
25A	0.18	703.88	7.04	- 0.61	2384.86	23.85
26A	0.60	525.01	5.25	- 0.02	1583.27	15.83

Table 5-4. Continued 1.

Sample #	Ct MARCKS-Ct GAPDH	% of control	MARCKS fold change	Ct TNF-α-Ct GAPDH	% of control	TNF-α-fold change
27A	- 0.12	862.98	8.63	- 1.00	3131.61	31.32
28A	1.28	328.83	3.29	- 0.12	1701.62	17.02
29A	1.73	239.39	2.39	2.16	348.90	3.49
30A	1.03	389.96	3.90	- 0.27	1884.14	18.84
31A	0.20	690.83	6.91	0.27	1297.65	12.98
32A	1.16	356.85	3.57	2.39	297.49	2.97
33A	- 0.46	1090.81	10.91	- 0.70	2531.35	25.31
34A	- 0.25	945.67	9.46	- 0.91	2925.95	29.26
35A	- 0.06	828.98	8.29	0.64	1003.41	10.03
36A	2.10	185.62	1.86	0.43	1163.04	11.63
37A	2.06	190.44	1.90	2.06	375.77	3.76
38A	1.80	228.52	2.29	3.29	159.20	1.59
39A	- 1.50	2255.43	22.55	3.28	160.97	1.61
40A	- 0.51	1137.14	11.37	0.31	1259.55	12.60
41A	- 0.17	892.80	8.93	0.78	910.61	9.11
42A	- 4.06	13282.04	132.82	- 3.15	13850.88	138.51
43A	0.41	597.25	5.97	- 1.23	3657.62	36.58
44A	0.29	650.85	6.51	- 1.40	4132.19	41.32
45A	- 1.20	1833.25	18.33	- 1.49	4398.18	43.98
46A	- 0.96	1550.15	15.50	1.53	540.33	5.40
47A	0.40	603.49	6.03	2.28	320.61	3.21
48A	2.79	114.82	1.15	5.36	38.10	0.38
49A	3.25	83.93	0.84	4.51	68.67	0.69
50A	2.71	121.95	1.22	3.76	114.94	1.15

Table 5-4. Continued 2.

Sample #	Ct MARCKS-Ct GAPDH	% of control	MARCKS fold change	Ct TNF-α-Ct GAPDH	% of control	TNF-α-fold change
51A	2.48	142.34	1.42	2.45	286.16	2.86
52A	3.11	92.23	0.92	3.12	179.98	1.80
53A	1.33	316.75	3.17	1.04	760.44	7.60
54A	2.91	106.24	1.06	2.33	311.20	3.11
55A	2.77	116.34	1.16	4.77	57.07	0.57
56A	- 1.67	2539.25	25.39	- 0.31	1930.41	19.30
57A	2.34	157.61	1.58	4.33	77.80	0.78

Table 5-5. $\Delta\Delta C_t$ and fold change calculations for granulocyte qRT-PCR from patient samples. Results shown in this table are for MCP-1, IL-1β and IL-17A.

Sample #	Ct MCP-1-Ct GAPDH	% of control	MCP-1 fold change	Ct IL-1β- Ct GAPDH	% of control	IL-1β fold change	Ct IL-17A-Ct GAPDH	% of control	IL-17A fold change
1B	11.96	14.69	0.15	2.00	16.86	0.17	17.91	und	und
2B	9.55	78.18	0.78	- 3.91	1018.09	10.18	11.24	und	und
3B	9.39	87.53	0.88	- 2.68	432.83	4.33	10.20	und	und
4B	11.95	14.79	0.15	0.37	52.19	0.52	und	und	und
5B	7.88	249.29	2.49	- 1.31	167.81	1.68	und	und	und
9B	13.23	6.11	0.06	2.74	10.16	0.10	18.98	und	und
10B	9.93	59.99	0.60	1.16	30.35	0.30	und	und	und
11B	13.90	3.84	0.04	0.64	43.31	0.43	und	und	und
14B	9.82	65.01	0.65	0.52	47.07	0.47	und	und	und
15B	8.00	228.91	2.29	- 0.59	102.16	1.02	und	und	und
16B	6.38	702.65	7.03	- 2.08	286.16	2.86	und	und	und
18B	6.32	733.50	7.34	- 1.18	152.71	1.53	und	und	und
19B	9.56	77.64	0.78	- 0.97	132.39	1.32	9.51	und	und
21B	10.57	38.50	0.38	- 1.11	146.19	1.46	10.39	und	und
22B	7.81	260.77	2.61	- 2.27	325.31	3.25	11.04	und	und
25B	4.55	2508.58	25.09	- 2.64	420.99	4.21	11.18	und	und
26B	9.63	73.75	0.74	- 0.99	134.24	1.34	14.04	und	und
27B	11.12	26.28	0.26	- 1.36	173.97	1.74	und	und	und
29B	11.83	16.09	0.16	0.62	43.98	0.44	18.91	und	und
30B	7.89	247.74	2.48	- 0.73	112.49	1.12	und	und	und
32B	13.44	5.27	0.05	- 0.24	80.04	0.80	und	und	und
34B	8.78	133.03	1.33	- 2.74	450.27	4.50	10.07	und	und
35B	6.36	713.94	7.14	- 4.16	1209.89	12.10	und	und	und
37B	6.25	771.04	7.71	- 2.42	360.70	3.61	8.36	und	und

Table 5-5. Continued.

Sample #	Ct MCP-1-Ct GAPDH	% of control	MCP-1 fold change	Ct IL-1β- Ct GAPDH	% of control	IL-1β fold change	Ct IL-17A-Ct GAPDH	% of control	IL-17A fold change
40B	8.78	132.94	1.33	0.01	67.12	0.67	und	und	und
41B	6.08	868.06	8.68	- 2.45	368.79	3.69	und	und	und
42B	2.12	13509.21	135.09	- 4.10	1157.39	11.57	und	und	und
43B	6.70	565.22	5.65	- 1.84	242.30	2.42	und	und	und
44B	3.66	4623.14	46.23	- 2.25	321.94	3.22	und	und	und
48B	10.74	34.31	0.34	2.25	14.20	0.14	und	und	und
49B	12.52	9.98	0.10	2.63	10.92	0.11	und	und	und
54B	8.20	199.42	1.99	- 1.96	262.95	2.63	und	und	und
55B	10.02	56.64	0.57	1.92	17.84	0.18	und	und	und
57B	10.60	37.81	0.38	2.05	16.29	0.16	und	und	und

Table 5-6. $\Delta\Delta C_t$ and fold change calculations for granulocyte qRT-PCR from patient samples. Results shown in this table are for MARCKS and TNF-α.

Sample #	Ct MARCKS-Ct GAPDH	% of control	MARCKS fold change	Ct TNF-α-Ct GAPDH	% of control	TNF-α- fold change
1B	- 0.84	87.03	0.87	5.00	14.64	0.15
2B	- 2.07	204.29	2.04	0.35	367.62	3.68
3B	- 1.53	140.11	1.40	0.98	236.89	2.37
4B	- 0.90	90.60	0.91	2.73	70.82	0.71
5B	- 1.25	115.64	1.16	1.33	186.24	1.86
9B	0.64	31.11	0.31	3.96	30.13	0.30
10B	1.08	23.03	0.23	2.85	65.08	0.65
11B	0.32	38.95	0.39	4.34	23.10	0.23
14B	- 0.74	81.43	0.81	2.75	69.51	0.70
15B	- 2.39	255.19	2.55	1.18	206.37	2.06
16B	- 1.14	106.85	1.07	1.53	162.02	1.62
18B	- 0.01	48.86	0.49	1.92	123.56	1.24
19B	- 1.07	101.93	1.02	1.36	182.54	1.83
21B	- 0.50	68.95	0.69	3.38	44.88	0.45
22B	- 0.49	68.09	0.68	2.40	88.65	0.89
25B	- 1.71	158.95	1.59	0.84	261.57	2.62
26B	- 1.13	106.41	1.06	2.01	116.73	1.17
27B	- 2.69	313.53	3.14	1.41	176.32	1.76
29B	- 1.03	99.28	0.99	3.37	45.35	0.45
30B	- 2.10	208.15	2.08	1.39	179.03	1.79
32B	- 1.78	167.09	1.67	3.97	29.82	0.30
34B	- 2.96	378.06	3.78	1.68	146.73	1.47
35B	- 2.54	282.18	2.82	0.43	348.51	3.49
37B	0.55	33.21	0.33	3.34	46.40	0.46

Table 5-6. Continued.

Sample #	Ct MARCKS-Ct GAPDH	% of control	MARCKS fold change	Ct TNF-α-Ct GAPDH	% of control	TNF-α- fold change
40B	- 2.26	233.21	2.33	3.02	57.96	0.58
41B	- 3.09	413.13	4.13	1.16	209.39	2.09
42B	- 3.80	677.21	6.77	- 0.90	876.16	8.76
43B	- 3.30	480.19	4.80	2.57	79.02	0.79
44B	- 2.61	296.82	2.97	- 0.24	554.12	5.54
48B	0.30	39.41	0.39	5.10	13.71	0.14
49B	- 1.20	111.62	1.12	4.67	18.43	0.18
54B	- 4.60	1176.64	11.77	- 0.18	532.29	5.32
55B	- 1.64	151.85	1.52	2.76	68.98	0.69
57B	- 1.51	138.86	1.39	4.00	29.24	0.29

Table 5-7. Linear regression for correlations between RA patient RT-PCR data for various parameters and TNF. Y=A+B*X

Cell type	Sample	Parameter	Value	Error	t-Value	Prob>|t|
Monocytic Cells	IL-17A	A	6.80520	3.11253	2.18639	0.03537
		B	- 0.03533	0.11688	- 0.30227	0.76419
	IL-1β	A	- 61.14649	22.49072	- 2.71874	0.00884
		B	13.54019	0.92178	14.68922	<0.0001
	MARCKS	A	- 2.92789	1.40129	- 2.08942	0.04149
		B	0.76921	0.05743	13.39353	<0.0001
	MCP-1	A	-117.58328	27.89971	- 4.21450	<0.0001
		B	13.29173	1.14346	11.62409	<0.0001
Granulocytic Cells	IL-1β	A	0.45705	0.50370	0.90739	0.37098
		B	1.21444	0.20365	5.96327	<0.0001
	MARCKS	A	0.65038	0.38486	1.68990	0.10077
		B	0.83305	0.15560	5.35363	<0.0001
	MCP-1	A	- 9.0570	3.50184	- 2.58635	0.01445
		B	10.23483	1.41585	7.22876	<0.0001

Table 5-8. R, R-square, adj. R-square and standard deviation for correlations between RA patient RT-PCR data for various parameters and TNF.

Cell type	Sample	R	R-Square (COD)	Adj. R-Square	Root-MSE (SD)	N
Monocytic Cells	IL-17A	-0.0503	0.00253	-0.02518	16.28726	38
	IL-1β	0.896	0.80281	0.79909	139.92565	55
	MARCKS	0.8786	0.77193	0.76763	8.71813	55
	MCP-1	0.8475	0.71826	0.71295	173.57764	55
Granulocytic Cells	IL-1β	0.7255	0.52635	0.51155	2.17161	34
	MARCKS	0.68737	0.47248	0.456	1.65926	34
	MCP-1	0.78753	0.6202	0.60833	15.09761	34

Table 5-9. ANOVA table for correlations between RA patient RT-PCR data for various parameters and TNF.

Cell type	Sample	Item	Degrees of Freedom	Sum of Squares	Mean Square	F Statistic	Prob>F
Monocytic Cells	IL-17A	Model	1	2.42E+01	2.42E+01	0.09136	0.76419
		Error	36	9.55E+03	2.65E+02		
		Total	37	9.57E+03			
	IL-1β	Model	1	4.22E+06	4.22E+06	215.77324	<0.0001
		Error	53	1.04E+06	1.96E+04		
		Total	54	5.26E+06			
	MARCKS	Model	1	1.36E+04	1.36E+04	179.38671	<0.0001
		Error	53	4.03E+03	7.60E+01		
		Total	54	1.77E+04			
	MCP-1	Model	1	4.07E+06	4.07E+06	135.11952	<0.0001
		Error	53	1.60E+06	3.01E+04		
		Total	54	5.67E+06			
Granulocytic Cells	IL-1β	Model	1	1.68E+02	1.68E+02	35.56062	<0.0001
		Error	32	1.51E+02	4.72E+00		
		Total	33	3.19E+02			
	MARCKS	Model	1	7.89E+01	7.89E+01	28.66131	<0.0001
		Error	32	8.81E+01	2.75E+00		
		Total	33	1.67E+02			
	MCP-1	Model	1	1.19E+04	1.19E+04	52.25498	<0.0001
		Error	32	7.29E+03	2.28E+02		
		Total	33	1.92E+04			

Table 5-10. MARCKS and TNF protein levels in patient samples as determined by ELISA.

Group	Sample #	MARCKS (ng/100,000 cells)	TNF (pg/mL)	Diagnosis	Prognosis	Therapy
Group 1: Healthy controls						
5	5	0.11	2.81	Healthy		
11	11	0.10	587.35	Healthy		
12	12	0.21	21.42	Healthy		
13	13	0.70	3.76	Healthy		
14	14	0.24	3.76	Healthy		
15	15	0.23	3.87	Healthy		
16	16	0.32	1.77	Healthy		
50	50	0.09	4.05	Healthy		
51	51	0.03	23.28	Healthy		
52	52	0.29	40.65	Healthy		
53	53	0.27	2.01	Healthy		
Group 2: RA+MTX						
4	4	0.18		RA		on Methotrexate
7	7	0.13	2.73	RA		on Methotrexate
22	22	0.15	0.19	RA		on Methotrexate
27	27	0.02	2.94	RA		on Methotrexate
29	29	0.14	3.60	RA		on Methotrexate
39	39	0.27	15.35	RA		on Methotrexate
40	40	0.41	1.57	RA		on Methotrexate
48	48	0.32		RA		on prednisone and MTX
Group 3: RA+TNF inhibitor						
19	19	0.03	4.99	RA		on Humira--has active RA
20	20	0.12	0.62	RA		on Humira--5 months
21	21	0.06		RA		on Humira--4 months
36	36	0.06	0.07	RA		on Humira
38	38	0.51	0.77	RA		on Humira--RA not active
46	46	0.25		RA		on Humira
47	47	0.47	28.62	RA		on Enbrel
54	54	0.50	23.80	RA		on MTX and Enbrel

Table 5-10. Continued

Group	Sample #	MARCKS (ng/100,000 cells)	TNF (pg/mL)	Diagnosis	Prognosis	Therapy
Group 4: RA--no therapy						
10	10	0.47		RA		start Methotrexate
17	17	0.02	3.15	RA		no therapy
30	30	0.15	1.83	RA		starting Humira
31	31	0.15	5.74	RA		Starting Humira
33	33	0.03	1.85	RA		Starting Methotrexate AND Humira
Group 5: Untreated early synovitis						
18	18	0.12	24.27	polyarthritis, early synovitis	developed RA	no therapy
43	43	0.06	5.53	early synovitis	developed RA	no therapy
57	57	0.03	6.80	early synovitis, breast cancer	developed RA	no therapy
Group 6: Early synovitis on MTX or prednisone						
1	1	0.46	5.56	early synovitis	MCTD+RA	on prednisone
26	26	0.18	1.32	early synovitis		on Methotrexate
34	34	0.11		early synovitis	developed RA	on prednisone
45	45	0.20	11.62	unknown	developed RA	on Methotrexate
Group 7: JRA						
9	9	0.07	0.74	JRA		starting TNF inhibitor
49	49	0.04	6.61	JRA		no therapy
55	55	0.02	7.60	JRA		on Enbrel
Group 8: MCTD						
6	6	0.33	0.54	MCTD		no therapy
8	8	0.27	0.05	MCTD, polymyocitis		no therapy
24	24	0.05		MCTD		
Group 9: Other						
25	25	0.14	3.21	Psoriatic arthritis		Starting Methotrexate
28	28	0.90	1.32	SLE+RA		on prednisone and MTX
32	32	0.22		Wegner's		
37	37	0.10	5.88	Blau's syndrome		on Humira
44	44	0.04	0.62	Psoriatic arthritis		on Methotrexate

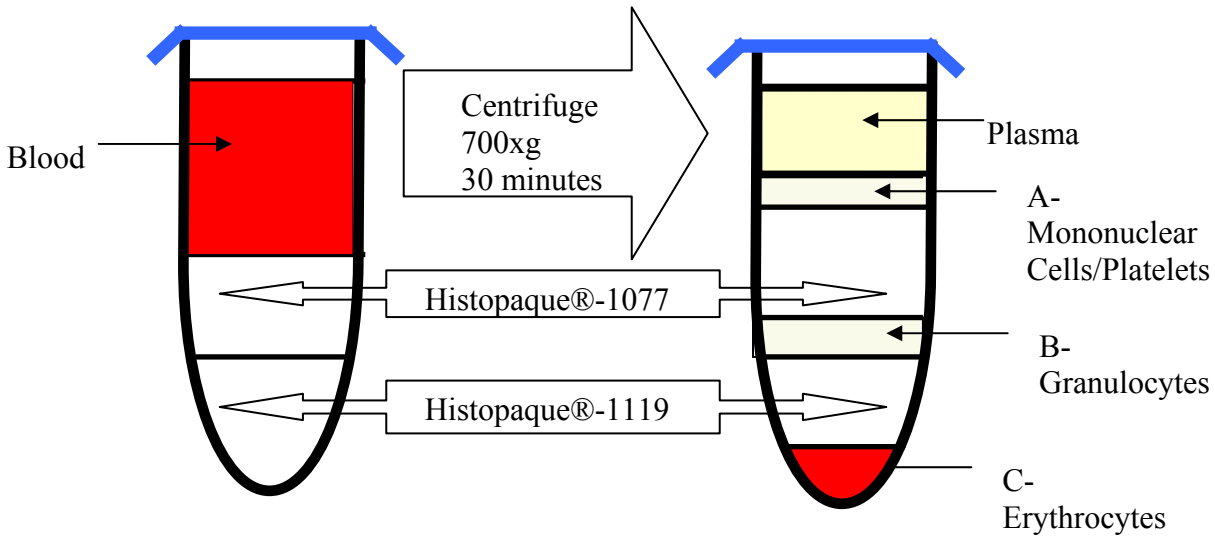

Figure 5-1. Histopaque double-gradient for leukocyte isolation from whole blood.

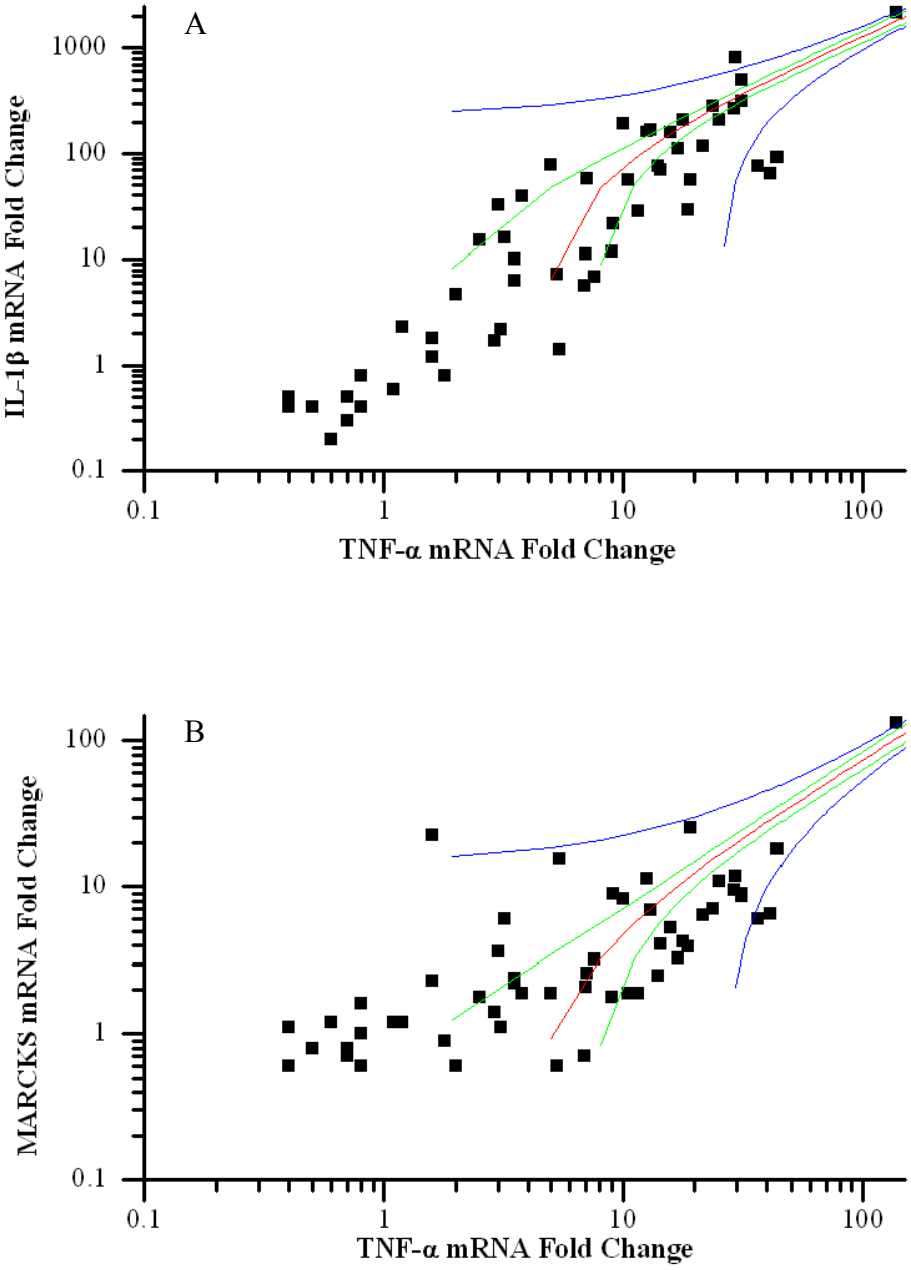

Figure 5-2. Correlation between mRNA levels of TNF-α and other proteins in mononuclear cells. A) IL-1β, B) MARCKS, C) MCP-1, and D) IL-17A. The red line represents the best fit to the data; blue lines, upper and lower prediction limits; and green lines, upper and lower 95% correlation limits.

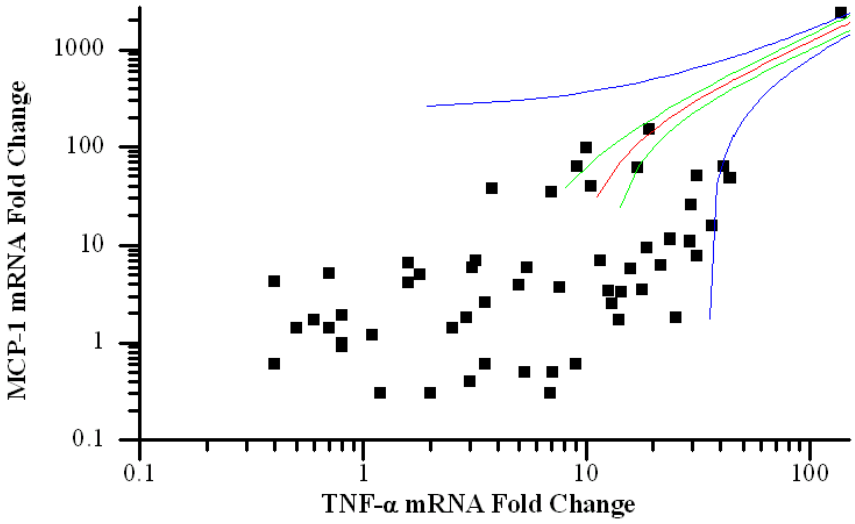

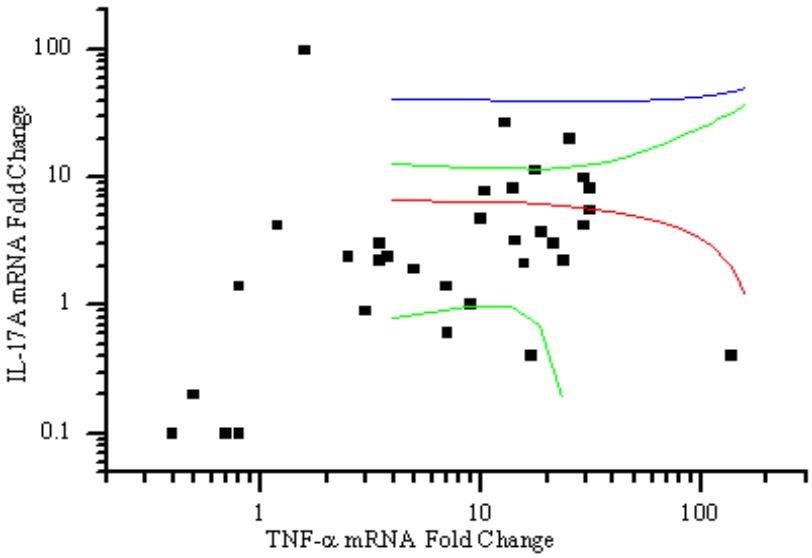

Figure 5-2. Continued.

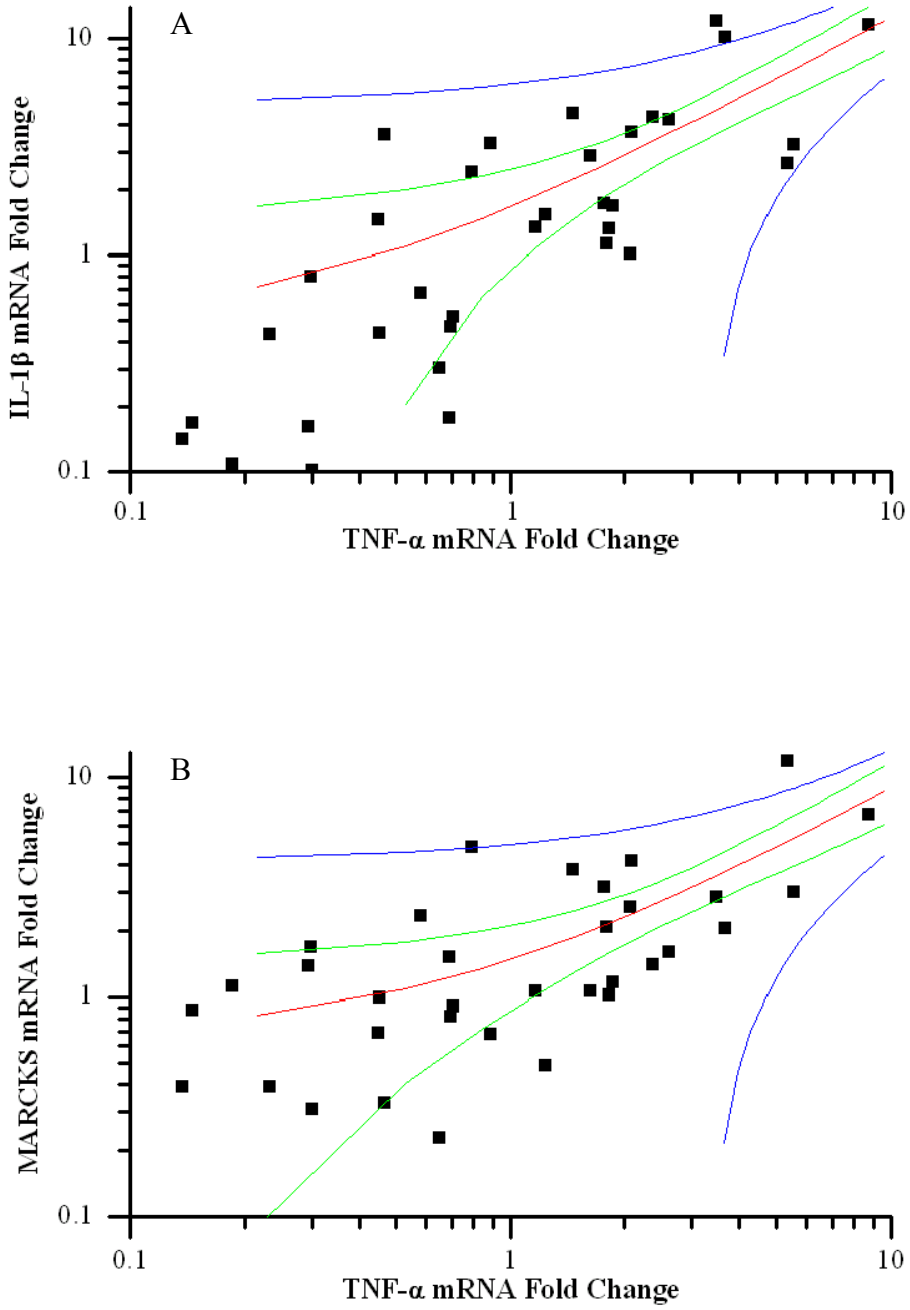

Figure 5-3. Correlation between mRNA levels of TNF-α and other proteins in granulocytes. A) IL-1β, B) MARCKS and C) MCP-1. The red line represents the best fit to the data; blue lines, upper and lower prediction limits; and green lines, upper and lower 95% correlation limits.

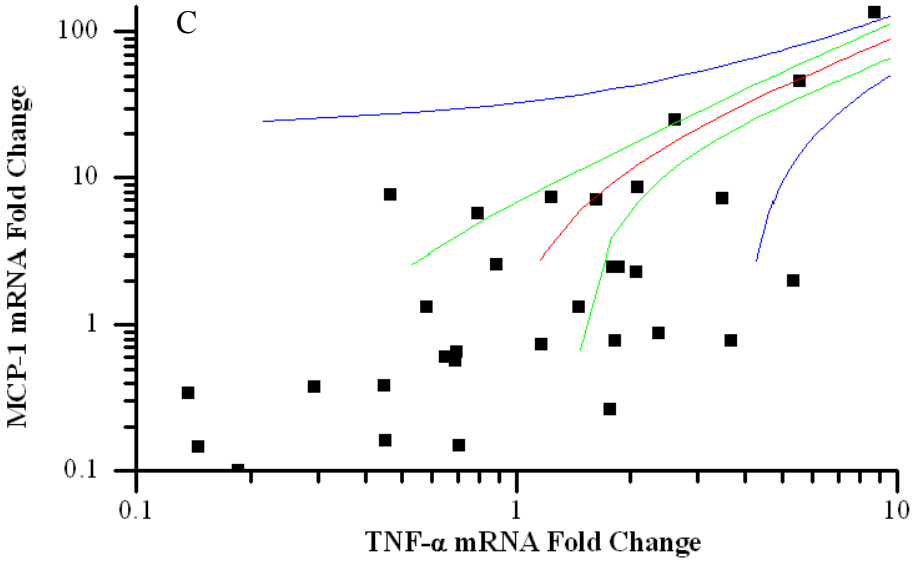

Figure 5-3. Continued.

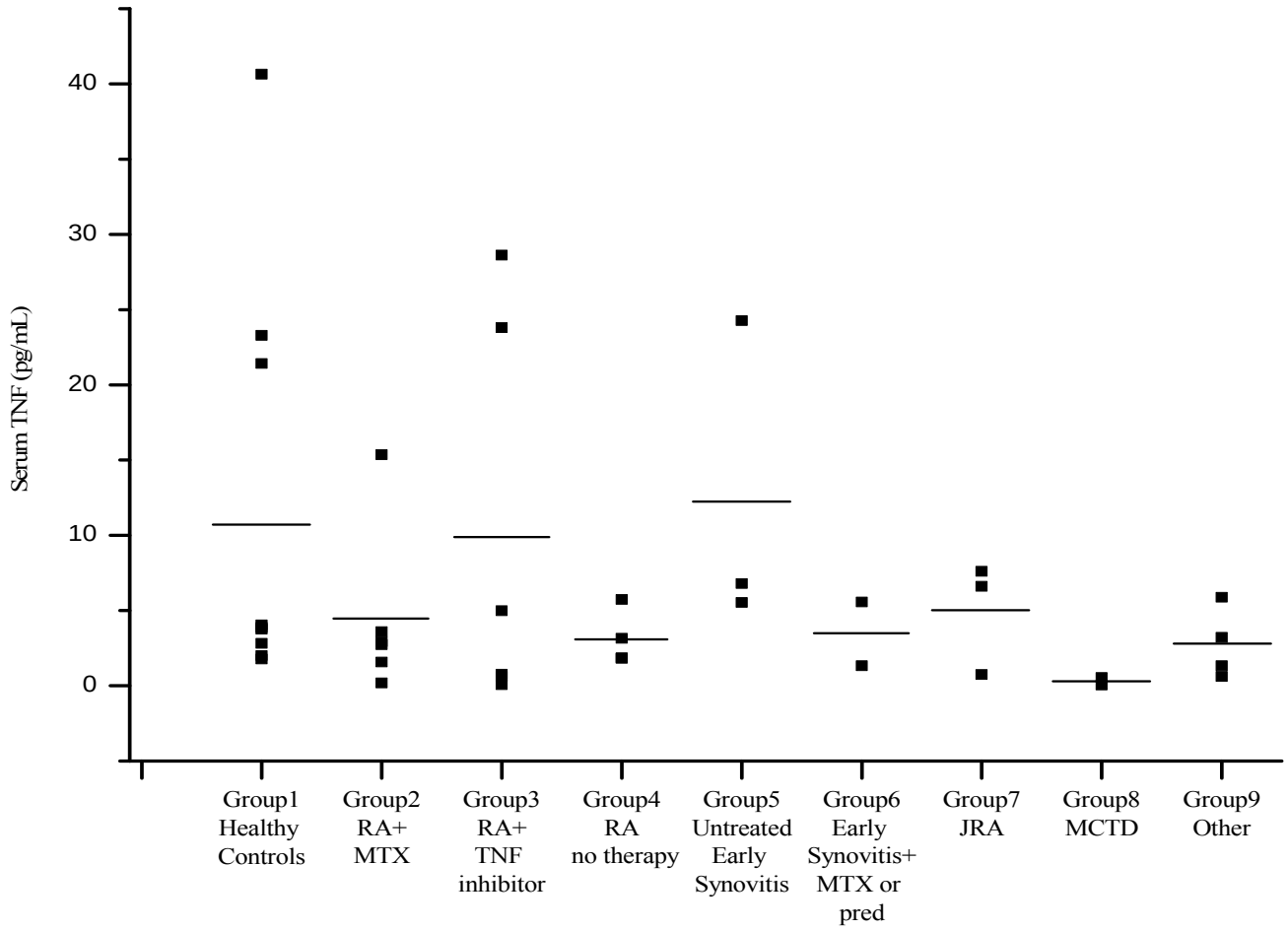

Figure 5-4. TNF serum protein levels of different patient groups as determined by quantitative sandwich ELISA. Horizontal lines indicate the mean protein levels in each group

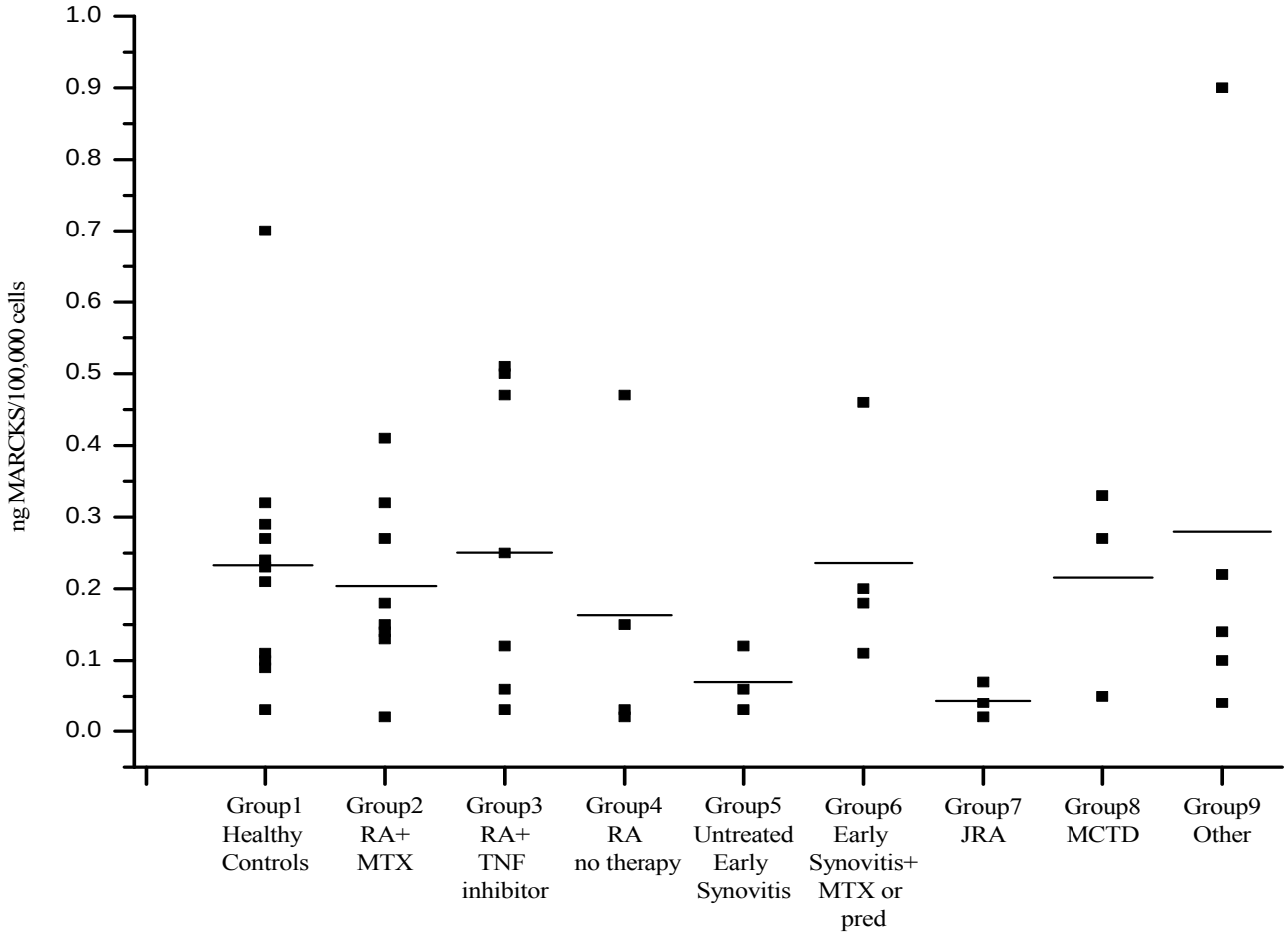

Figure 5-5. MARCKS cellular protein levels of different patient groups as determined by quantitative sandwich ELISA. Horizontal lines indicate the mean protein levels in each group

CHAPTER 6
CONCLUSIONS AND FUTURE DIRECTIONS

It had been widely accepted that using the phosphorylation site domain of MARCKS, an unstructured protein, in biochemical assays can act as a surrogate for using the entire molecule. The rationale was that in an unfolded protein, all parts of the protein should be easily accessible all the time. Whereas this may be true for some proteins, it certainly isn't for MARCKS. The unusual charge distribution on the protein makes ionic interactions between the acidic ends of the protein and its central basic effector domain very plausible, and that is what we have shown in this study. A question then arises as to how these proteins can be activated inside the cell, and there are a few possibilities, which are worth investigating. Cells commonly use post-translational modifications for altering function and interactions of molecules: our EDC neutralization assays, where only a few charges were modified yet caused an increase in activity of MARCKS, suggest that addition of a phosphate group here or there could greatly activate the protein. Specific proteolysis of inhibiting domains or binding by other proteins may also free the effector domain and activate the protein in question. In addition, local changes in ionic strength may disrupt ionic interactions; this may be achieved by changes in calcium or other ions whose concentrations are constantly changing in our cells. Many of these mechanisms can be used simultaneously to regulate these natively unfolded proteins.

Identifying more intrinsically disordered proteins that are inactivated by intramolecular interactions would be an important next step in validating our observations with MARCKS. We will first start by looking at other proteins that contain the MARCKS phosphorylation site domain (e.g., adducin, diacylglycerol kinase ζ) to see whether they demonstrate similar properties as those observed for MARCKS.

Mapping the sites of intramolecular interactions for the PSD on MARCKS and other proteins may prove to be useful in the development of biological therapies. The binding sites identified by mass spectrometry will first need to be tested and validated by biochemical assays. The actin cytoskeleton is believed to play an important role in the pathogenesis of RA [242]. If an inhibitor of MARCKS can be thus identified, it may be used in the treatment of autoimmune diseases such as RA in place of tumor necrosis factor inhibitors, because MARCKS is a downstream effector of TNF in immune cells. This may be helpful because inhibiting MARCKS may potentially have fewer side effects than inhibiting TNF, which plays many important roles in immunity. Inhibiting MARCKS using a competitive inhibitor corresponding to the N-terminal domain of the protein has already been shown to block mucus hypersecretion in a mouse model of asthma, [62] with potential uses in cystic fibrosis and chronic bronchitis.

LIST OF REFERENCES

[1] Wu WC, Walaas SI, Nairn AC, Greengard P. Calcium/phospholipid regulates phosphorylation of a Mr "87k" substrate protein in brain synaptosomes. Proc Natl Acad Sci U S A 1982;79:5249-5253.

[2] Rozengurt E, Rodriguez-Pena M, Smith KA. Phorbol esters, phospholipase C, and growth factors rapidly stimulate the phosphorylation of a Mr 80,000 protein in intact quiescent 3T3 cells. Proc Natl Acad Sci U S A 1983;80:7244-7248.

[3] Albert KA, Walaas SI, Wang JK, Greengard P. Widespread occurrence of "87 kDa," a major specific substrate for protein kinase C. Proc Natl Acad Sci U S A 1986;83:2822-2826.

[4] Yarmola EG, Edison AS, Lenox RH, Bubb MR. Actin filament cross-linking by MARCKS: characterization of two actin-binding sites within the phosphorylation site domain. J Biol Chem 2001;276:22351-22358.

[5] Graff JM, Young TN, Johnson JD, Blackshear PJ. Phosphorylation-regulated calmodulin binding to a prominent cellular substrate for protein kinase C. J Biol Chem 1989;264:21818-21823.

[6] McIlroy BK, Walters JD, Blackshear PJ, Johnson JD. Phosphorylation-dependent binding of a synthetic MARCKS peptide to calmodulin. J Biol Chem 1991;266:4959-4964.

[7] Palmer RH, Schonwasser DC, Rahman D, Pappin DJ, Herget T, Parker PJ. PRK1 phosphorylates MARCKS at the PKC sites: serine 152, serine 156 and serine 163. FEBS Lett 1996;378:281-285.

[8] Nagumo H, Ikenoya M, Sakurada K, Furuya K, Ikuhara T, Hiraoka H*, et al.* Rho-associated kinase phosphorylates MARCKS in human neuronal cells. Biochem Biophys Res Commun 2001;280:605-609.

[9] Taniguchi H, Manenti S. Interaction of myristoylated alanine-rich protein kinase C substrate (MARCKS) with membrane phospholipids. J Biol Chem 1993;268:9960-9963.

[10] Chao D, Severson DL, Zwiers H, Hollenberg MD. Radiolabelling of bovine myristoylated alanine-rich protein kinase C substrate (MARCKS) in an ADP-ribosylation reaction. Biochem Cell Biol 1994;72:391-396.

[11] Althaus FR, Kleczkowska HE, Malanga M, Muntener CR, Pleschke JM, Ebner M*, et al.* Poly ADP-ribosylation: a DNA break signal mechanism. Mol Cell Biochem 1999;193:5-11.

[12] Arbuzova A, Schmitz AA, Vergeres G. Cross-talk unfolded: MARCKS proteins. Biochem J 2002;362:1-12.

[13] Uversky VN. What does it mean to be natively unfolded? Eur J Biochem 2002;269:2-12.

[14] Gast K, Damaschun H, Eckert K, Schulze-Forster K, Maurer HR, Muller-Frohne M*, et al.* Prothymosin alpha: a biologically active protein with random coil conformation. Biochemistry 1995;34:13211-13218.

[15] Weinreb PH, Zhen W, Poon AW, Conway KA, Lansbury PT, Jr. NACP, a protein implicated in Alzheimer's disease and learning, is natively unfolded. Biochemistry 1996;35:13709-13715.

[16] Dunker AK, Lawson JD, Brown CJ, Williams RM, Romero P, Oh JS*, et al.* Intrinsically disordered protein. J Mol Graph Model 2001;19:26-59.

[17] Hartwig JH, Thelen M, Rosen A, Janmey PA, Nairn AC, Aderem A. MARCKS is an actin filament crosslinking protein regulated by protein kinase C and calcium-calmodulin. Nature 1992;356:618-622.

[18] Matsubara M, Yamauchi E, Hayashi N, Taniguchi H. MARCKS, a major protein kinase C substrate, assumes non-helical conformations both in solution and in complex with Ca2+-calmodulin. FEBS Lett 1998;421:203-207.

[19] Yamauchi E, Nakatsu T, Matsubara M, Kato H, Taniguchi H. Crystal structure of a MARCKS peptide containing the calmodulin-binding domain in complex with Ca2+-calmodulin. Nat Struct Biol 2003;10:226-231.

[20] Manenti S, Sorokine O, Van Dorsselaer A, Taniguchi H. Affinity purification and characterization of myristoylated alanine-rich protein kinase C substrate (MARCKS) from bovine brain. Comparison of the cytoplasmic and the membrane-bound forms. J Biol Chem 1992;267:22310-22315.

[21] Qin Z, Wertz SL, Jacob J, Savino Y, Cafiso DS. Defining protein-protein interactions using site-directed spin-labeling: the binding of protein kinase C substrates to calmodulin. Biochemistry 1996;35:13272-13276.

[22] Bubb MR, Lenox RH, Edison AS. Phosphorylation-dependent conformational changes induce a switch in the actin-binding function of MARCKS. J Biol Chem 1999;274:36472-36478.

[23] Kim J, Blackshear PJ, Johnson JD, McLaughlin S. Phosphorylation reverses the membrane association of peptides that correspond to the basic domains of MARCKS and neuromodulin. Biophys J 1994;67:227-237.

[24] Arbuzova A, Wang L, Wang J, Hangyas-Mihalyne G, Murray D, Honig B*, et al.* Membrane binding of peptides containing both basic and aromatic residues. Experimental studies with peptides corresponding to the scaffolding region of caveolin and the effector region of MARCKS. Biochemistry 2000;39:10330-10339.

[25] Wang J, Arbuzova A, Hangyas-Mihalyne G, McLaughlin S. The effector domain of myristoylated alanine-rich C kinase substrate binds strongly to phosphatidylinositol 4,5-bisphosphate. J Biol Chem 2001;276:5012-5019.

[26] Zhang W, Crocker E, McLaughlin S, Smith SO. Binding of peptides with basic and aromatic residues to bilayer membranes: phenylalanine in the myristoylated alanine-rich C kinase substrate effector domain penetrates into the hydrophobic core of the bilayer. J Biol Chem 2003;278:21459-21466.

[27] Thelen M, Rosen A, Nairn AC, Aderem A. Regulation by phosphorylation of reversible association of a myristoylated protein kinase C substrate with the plasma membrane. Nature 1991;351:320-322.

[28] Song JC, Hrnjez BJ, Farokhzad OC, Matthews JB. PKC-epsilon regulates basolateral endocytosis in human T84 intestinal epithelia: role of F-actin and MARCKS. Am J Physiol 1999;277:C1239-1249.

[29] Larsson C. Protein kinase C and the regulation of the actin cytoskeleton. Cell Signal 2006;18:276-284.

[30] Salli U, Supancic S, Stormshak F. Phosphorylation of myristoylated alanine-rich C kinase substrate (MARCKS) protein is associated with bovine luteal oxytocin exocytosis. Biol Reprod 2000;63:12-20.

[31] Trifaro J, Rose SD, Lejen T, Elzagallaai A. Two pathways control chromaffin cell cortical F-actin dynamics during exocytosis. Biochimie 2000;82:339-352.

[32] Carballo E, Pitterle DM, Stumpo DJ, Sperling RT, Blackshear PJ. Phagocytic and macropinocytic activity in MARCKS-deficient macrophages and fibroblasts. Am J Physiol 1999;277:C163-173.

[33] Allen LH, Aderem A. A role for MARCKS, the alpha isozyme of protein kinase C and myosin I in zymosan phagocytosis by macrophages. J Exp Med 1995;182:829-840.

[34] Iioka H, Ueno N, Kinoshita N. Essential role of MARCKS in cortical actin dynamics during gastrulation movements. J Cell Biol 2004;164:169-174.

[35] Rose SD, Lejen T, Zhang L, Trifaro JM. Chromaffin cell F-actin disassembly and potentiation of catecholamine release in response to protein kinase C activation by phorbol esters is mediated through myristoylated alanine-rich C kinase substrate phosphorylation. J Biol Chem 2001;276:36757-36763.

[36] Spizz G, Blackshear PJ. Overexpression of the myristoylated alanine-rich C-kinase substrate inhibits cell adhesion to extracellular matrix components. J Biol Chem 2001;276:32264-32273.

[37] Disatnik MH, Boutet SC, Lee CH, Mochly-Rosen D, Rando TA. Sequential activation of individual PKC isozymes in integrin-mediated muscle cell spreading: a role for MARCKS in an integrin signaling pathway. J Cell Sci 2002;115:2151-2163.

[38] Disatnik MH, Boutet SC, Pacio W, Chan AY, Ross LB, Lee CH*, et al.* The bi-directional translocation of MARCKS between membrane and cytosol regulates integrin-mediated muscle cell spreading. J Cell Sci 2004;117:4469-4479.

[39] Dedieu S, Mazeres G, Poussard S, Brustis JJ, Cottin P. Myoblast migration is prevented by a calpain-dependent accumulation of MARCKS. Biol Cell 2003;95:615-623.

[40] Dedieu S, Poussard S, Mazeres G, Grise F, Dargelos E, Cottin P*, et al.* Myoblast migration is regulated by calpain through its involvement in cell attachment and cytoskeletal organization. Exp Cell Res 2004;292:187-200.

[41] Kim SS, Kim JH, Kim HS, Park DE, Chung CH. Involvement of the theta-type protein kinase C in translocation of myristoylated alanine-rich C kinase substrate (MARCKS) during myogenesis of chick embryonic myoblasts. Biochem J 2000;347 Pt 1:139-146.

[42] Blackshear PJ. The MARCKS family of cellular protein kinase C substrates. J Biol Chem 1993;268:1501-1504.

[43] Rauch ME, Ferguson CG, Prestwich GD, Cafiso DS. Myristoylated alanine-rich C kinase substrate (MARCKS) sequesters spin-labeled phosphatidylinositol 4,5-bisphosphate in lipid bilayers. J Biol Chem 2002;277:14068-14076.

[44] Glaser M, Wanaski S, Buser CA, Boguslavsky V, Rashidzada W, Morris A*, et al.* Myristoylated alanine-rich C kinase substrate (MARCKS) produces reversible inhibition of phospholipase C by sequestering phosphatidylinositol 4,5-bisphosphate in lateral domains. J Biol Chem 1996;271:26187-26193.

[45] Gambhir A, Hangyas-Mihalyne G, Zaitseva I, Cafiso DS, Wang J, Murray D*, et al.* Electrostatic sequestration of PIP2 on phospholipid membranes by basic/aromatic regions of proteins. Biophys J 2004;86:2188-2207.

[46] Wang J, Gambhir A, McLaughlin S, Murray D. A computational model for the electrostatic sequestration of PI(4,5)P2 by membrane-adsorbed basic peptides. Biophys J 2004;86:1969-1986.

[47] McLaughlin S, Wang J, Gambhir A, Murray D. PIP(2) and proteins: interactions, organization, and information flow. Annu Rev Biophys Biomol Struct 2002;31:151-175.

[48] Wang J, Gambhir A, Hangyas-Mihalyne G, Murray D, Golebiewska U, McLaughlin S. Lateral sequestration of phosphatidylinositol 4,5-bisphosphate by the basic effector domain of myristoylated alanine-rich C kinase substrate is due to nonspecific electrostatic interactions. J Biol Chem 2002;277:34401-34412.

[49] Morash SC, Rose SD, Byers DM, Ridgway ND, Cook HW. Overexpression of myristoylated alanine-rich C-kinase substrate enhances activation of phospholipase D by protein kinase C in SK-N-MC human neuroblastoma cells. Biochem J 1998;332 (Pt 2):321-327.

[50] Morash SC, Byers DM, Cook HW. Activation of phospholipase D by PKC and GTPgammaS in human neuroblastoma cells overexpressing MARCKS. Biochim Biophys Acta 2000;1487:177-189.

[51] Sundaram M, Cook HW, Byers DM. The MARCKS family of phospholipid binding proteins: regulation of phospholipase D and other cellular components. Biochem Cell Biol 2004;82:191-200.

[52] Brooks G. The role of 80K/MARCKS, a specific substrate of protein kinase C, in cell growth and tumour progression. Pigment Cell Res 1994;7:451-457.

[53] Brooks G, Brooks SF, Goss MW. MARCKS functions as a novel growth suppressor in cells of melanocyte origin. Carcinogenesis 1996;17:683-689.

[54] Manenti S, Malecaze F, Chap H, Darbon JM. Overexpression of the myristoylated alanine-rich C kinase substrate in human choroidal melanoma cells affects cell proliferation. Cancer Res 1998;58:1429-1434.

[55] Joseph CK, Qureshi SA, Wallace DJ, Foster DA. MARCKS protein is transcriptionally down-regulated in v-Src-transformed BALB/c 3T3 cells. J Biol Chem 1992;267:1327-1330.

[56] Reed JC, Rapp U, Cuddy MP. Transformed 3T3 cells have reduced levels and altered subcellular distribution of the major PKC substrate protein MARCKS. Cell Signal 1991;3:569-576.

[57] Sheu FS, McCabe BJ, Horn G, Routtenberg A. Learning selectively increases protein kinase C substrate phosphorylation in specific regions of the chick brain. Proc Natl Acad Sci U S A 1993;90:2705-2709.

[58] Trifaro JM, Lejen T, Rose SD, Pene TD, Barkar ND, Seward EP. Pathways that control cortical F-actin dynamics during secretion. Neurochem Res 2002;27:1371-1385.

[59] Gatlin JC, Estrada-Bernal A, Sanford SD, Pfenninger KH. Myristoylated, alanine-rich C-kinase substrate phosphorylation regulates growth cone adhesion and pathfinding. Mol Biol Cell 2006;17:5115-5130.

[60] Agrawal A, Rengarajan S, Adler KB, Ram A, Ghosh B, Fahim M*, et al.* Inhibition of mucin secretion with MARCKS-related peptide improves airway obstruction in a mouse model of asthma. J Appl Physiol 2007;102:399-405.

[61] Li Y, Martin LD, Spizz G, Adler KB. MARCKS protein is a key molecule regulating mucin secretion by human airway epithelial cells in vitro. J Biol Chem 2001;276:40982-40990.

[62] Singer M, Martin LD, Vargaftig BB, Park J, Gruber AD, Li Y*, et al.* A MARCKS-related peptide blocks mucus hypersecretion in a mouse model of asthma. Nat Med 2004;10:193-196.

[63] Park J, Fang S, Adler KB. Regulation of airway mucin secretion by MARCKS protein involves the chaperones heat shock protein 70 and cysteine string protein. Proc Am Thorac Soc 2006;3:493.

[64] Calabrese B, Halpain S. Essential role for the PKC target MARCKS in maintaining dendritic spine morphology. Neuron 2005;48:77-90.

[65] Matus A. MARCKS for maintenance in dendritic spines. Neuron 2005;48:4-5.

[66] Mosevitsky MI. Nerve ending "signal" proteins GAP-43, MARCKS, and BASP1. Int Rev Cytol 2005;245:245-325.

[67] Shiraishi M, Tanabe A, Saito N, Sasaki Y. Unphosphorylated MARCKS is involved in neurite initiation induced by insulin-like growth factor-I in SH-SY5Y cells. J Cell Physiol 2006;209:1029-1038.

[68] Stumpo DJ, Bock CB, Tuttle JS, Blackshear PJ. MARCKS deficiency in mice leads to abnormal brain development and perinatal death. Proc Natl Acad Sci U S A 1995;92:944-948.

[69] Manji HK, Lenox RH. Ziskind-Somerfeld Research Award. Protein kinase C signaling in the brain: molecular transduction of mood stabilization in the treatment of manic-depressive illness. Biol Psychiatry 1999;46:1328-1351.

[70] Tatsumi S, Mabuchi T, Katano T, Matsumura S, Abe T, Hidaka H*, et al.* Involvement of Rho-kinase in inflammatory and neuropathic pain through phosphorylation of myristoylated alanine-rich C-kinase substrate (MARCKS). Neuroscience 2005;131:491-498.

[71] Thelen M, Rosen A, Nairn AC, Aderem A. Tumor necrosis factor alpha modifies agonist-dependent responses in human neutrophils by inducing the synthesis and myristoylation of a specific protein kinase C substrate. Proc Natl Acad Sci U S A 1990;87:5603-5607.

[72] Harlan DM, Graff JM, Stumpo DJ, Eddy RL, Jr., Shows TB, Boyle JM*, et al.* The human myristoylated alanine-rich C kinase substrate (MARCKS) gene (MACS). Analysis of its gene product, promoter, and chromosomal localization. J Biol Chem 1991;266:14399-14405.

[73] Siebenlist U, Franzoso G, Brown K. Structure, regulation and function of NF-kappa B. Annu Rev Cell Biol 1994;10:405-455.

[74] Verma IM, Stevenson JK, Schwarz EM, Van Antwerp D, Miyamoto S. Rel/NF-kappa B/I kappa B family: intimate tales of association and dissociation. Genes Dev 1995;9:2723-2735.

[75] Peppelenbosch M, Boone E, Jones GE, van Deventer SJ, Haegeman G, Fiers W*, et al.* Multiple signal transduction pathways regulate TNF-induced actin reorganization in

macrophages: inhibition of Cdc42-mediated filopodium formation by TNF. J Immunol 1999;162:837-845.

[76] Kutsuna H, Suzuki K, Kamata N, Kato T, Hato F, Mizuno K*, et al.* Actin reorganization and morphological changes in human neutrophils stimulated by TNF, GM-CSF, and G-CSF: the role of MAP kinases. Am J Physiol Cell Physiol 2004;286:C55-64.

[77] Sunohara JR, Ridgway ND, Cook HW, Byers DM. Regulation of MARCKS and MARCKS-related protein expression in BV-2 microglial cells in response to lipopolysaccharide. J Neurochem 2001;78:664-672.

[78] Brooks SF, Herget T, Broad S, Rozengurt E. The expression of 80K/MARCKS, a major substrate of protein kinase C (PKC), is down-regulated through both PKC-dependent and -independent pathways. Effects of bombesin, platelet-derived growth factor, and cAMP. J Biol Chem 1992;267:14212-14218.

[79] Brooks SF, Herget T, Erusalimsky JD, Rozengurt E. Protein kinase C activation potently down-regulates the expression of its major substrate, 80K, in Swiss 3T3 cells. EMBO J 1991;10:2497-2505.

[80] Wein G, Rossler M, Klug R, Herget T. The 3'-UTR of the mRNA coding for the major protein kinase C substrate MARCKS contains a novel CU-rich element interacting with the mRNA stabilizing factors HuD and HuR. Eur J Biochem 2003;270:350-365.

[81] Aderem A. The MARCKS brothers: a family of protein kinase C substrates. Cell 1992;71:713-716.

[82] Wang JK, Walaas SI, Sihra TS, Aderem A, Greengard P. Phosphorylation and associated translocation of the 87-kDa protein, a major protein kinase C substrate, in isolated nerve terminals. Proc Natl Acad Sci U S A 1989;86:2253-2256.

[83] Rosen A, Keenan KF, Thelen M, Nairn AC, Aderem A. Activation of protein kinase C results in the displacement of its myristoylated, alanine-rich substrate from punctate structures in macrophage filopodia. J Exp Med 1990;172:1211-1215.

[84] Spizz G, Blackshear PJ. Protein kinase C-mediated phosphorylation of the myristoylated alanine-rich C-kinase substrate protects it from specific proteolytic cleavage. J Biol Chem 1996;271:553-562.

[85] Spizz G, Blackshear PJ. Identification and characterization of cathepsin B as the cellular MARCKS cleaving enzyme. J Biol Chem 1997;272:23833-23842.

[86] Taniguchi H, Manenti S, Suzuki M, Titani K. Myristoylated alanine-rich C kinase substrate (MARCKS), a major protein kinase C substrate, is an in vivo substrate of proline-directed protein kinase(s). A mass spectroscopic analysis of the post-translational modifications. J Biol Chem 1994;269:18299-18302.

[87] Yamauchi E, Kiyonami R, Kanai M, Taniguchi H. Presence of conserved domains in the C-terminus of MARCKS, a major in vivo substrate of protein kinase C: application of ion trap mass spectrometry to the elucidation of protein structures. J Biochem 1998;123:760-765.

[88] Yamamoto H, Arakane F, Ono T, Tashima K, Okumura E, Yamada K*, et al.* Phosphorylation of myristoylated alanine-rich C kinase substrate (MARCKS) by proline-directed protein kinases and its dephosphorylation. J Neurochem 1995;65:802-809.

[89] Manenti S, Yamauchi E, Sorokine O, Knibiehler M, Van Dorsselaer A, Taniguchi H*, et al.* Phosphorylation of the myristoylated protein kinase C substrate MARCKS by the cyclin E-cyclin-dependent kinase 2 complex in vitro. Biochem J 1999;340 (Pt 3):775-782.

[90] Schonwasser DC, Palmer RH, Herget T, Parker PJ. p42 MAPK phosphorylates 80 kDa MARCKS at Ser-113. FEBS Lett 1996;395:1-5.

[91] Ohmitsu M, Fukunaga K, Yamamoto H, Miyamoto E. Phosphorylation of myristoylated alanine-rich protein kinase C substrate by mitogen-activated protein kinase in cultured rat hippocampal neurons following stimulation of glutamate receptors. J Biol Chem 1999;274:408-417.

[92] Hasegawa H, Nakai M, Tanimukai S, Taniguchi T, Terashima A, Kawamata T*, et al.* Microglial signaling by amyloid beta protein through mitogen-activated protein kinase mediating phosphorylation of MARCKS. Neuroreport 2001;12:2567-2571.

[93] Wolfman A, Wingrove TG, Blackshear PJ, Macara IG. Down-regulation of protein kinase C and of an endogenous 80-kDa substrate in transformed fibroblasts. J Biol Chem 1987;262:16546-16552.

[94] Wojtaszek PA, Stumpo DJ, Blackshear PJ, Macara IG. Severely decreased MARCKS expression correlates with ras reversion but not with mitogenic responsiveness. Oncogene 1993;8:755-760.

[95] Blackshear PJ, Lai WS, Tuttle JS, Stumpo DJ, Kennington E, Nairn AC*, et al.* Developmental expression of MARCKS and protein kinase C in mice in relation to the exencephaly resulting from MARCKS deficiency. Brain Res Dev Brain Res 1996;96:62-75.

[96] Shi Y, Sullivan SK, Pitterle DM, Kennington EA, Graff JM, Blackshear PJ. Mechanisms of MARCKS gene activation during Xenopus development. J Biol Chem 1997;272:29290-29300.

[97] Manenti S, Taniguchi H, Sorokine O, Van Dorsselaer A, Darbon JM. Specific proteolytic cleavage of the myristoylated alanine-rich C kinase substrate between Asn 147 and Glu 148 also occurs in brain. J Neurosci Res 1997;48:259-263.

[98] Braun T, McIlhinney RA, Vergeres G. Myristoylation-dependent N-terminal cleavage of the myristoylated alanine-rich C kinase substrate (MARCKS) by cellular extracts. Biochimie 2000;82:705-715.

[99] Matsubara M, Titani K, Taniguchi H, Hayashi N. Direct involvement of protein myristoylation in myristoylated alanine-rich C kinase substrate (MARCKS)-calmodulin interaction. J Biol Chem 2003;278:48898-48902.

[100] Dulong S, Goudenege S, Vuillier-Devillers K, Manenti S, Poussard S, Cottin P. Myristoylated alanine-rich C kinase substrate (MARCKS) is involved in myoblast fusion through its regulation by protein kinase Calpha and calpain proteolytic cleavage. Biochem J 2004;382:1015-1023.

[101] Kriegler M, Perez C, DeFay K, Albert I, Lu SD. A novel form of TNF/cachectin is a cell surface cytotoxic transmembrane protein: ramifications for the complex physiology of TNF. Cell 1988;53:45-53.

[102] Smith RA, Baglioni C. The active form of tumor necrosis factor is a trimer. J Biol Chem 1987;262:6951-6954.

[103] Hohmann HP, Remy R, Brockhaus M, van Loon AP. Two different cell types have different major receptors for human tumor necrosis factor (TNF alpha). J Biol Chem 1989;264:14927-14934.

[104] Wiegmann K, Schutze S, Kampen E, Himmler A, Machleidt T, Kronke M. Human 55-kDa receptor for tumor necrosis factor coupled to signal transduction cascades. J Biol Chem 1992;267:17997-18001.

[105] Neumann B, Machleidt T, Lifka A, Pfeffer K, Vestweber D, Mak TW*, et al.* Crucial role of 55-kilodalton TNF receptor in TNF-induced adhesion molecule expression and leukocyte organ infiltration. J Immunol 1996;156:1587-1593.

[106] Thomson AW, Lotze MT. The cytokine handbook. Amsterdam ; Boston: Academic Press, 2003.

[107] Cush J. Cytokine therapies. In: Hochberg MC SA, Smolen JS, Weinblatt ME, Weisman MH, ed. Rheumatology, 3rd ed. St. Louis, MO: MOSBY, 2003:461-484.

[108] Heller RA, Kronke M. Tumor necrosis factor receptor-mediated signaling pathways. J Cell Biol 1994;126:5-9.

[109] Goldblum SE, Ding X, Campbell-Washington J. TNF-alpha induces endothelial cell F-actin depolymerization, new actin synthesis, and barrier dysfunction. Am J Physiol 1993;264:C894-905.

[110] Raines EW, Ross R. Multiple growth factors are associated with lesions of atherosclerosis: specificity or redundancy? Bioessays 1996;18:271-282.

[111] Wojciak-Stothard B, Entwistle A, Garg R, Ridley AJ. Regulation of TNF-alpha-induced reorganization of the actin cytoskeleton and cell-cell junctions by Rho, Rac, and Cdc42 in human endothelial cells. J Cell Physiol 1998;176:150-165.

[112] Puls A, Eliopoulos AG, Nobes CD, Bridges T, Young LS, Hall A. Activation of the small GTPase Cdc42 by the inflammatory cytokines TNF(alpha) and IL-1, and by the Epstein-Barr virus transforming protein LMP1. J Cell Sci 1999;112 (Pt 17):2983-2992.

[113] Leibovich SJ, Polverini PJ, Shepard HM, Wiseman DM, Shively V, Nuseir N. Macrophage-induced angiogenesis is mediated by tumour necrosis factor-alpha. Nature 1987;329:630-632.

[114] Postlethwaite AE, Seyer JM. Stimulation of fibroblast chemotaxis by human recombinant tumor necrosis factor alpha (TNF-alpha) and a synthetic TNF-alpha 31-68 peptide. J Exp Med 1990;172:1749-1756.

[115] Cumberbatch M, Dearman RJ, Kimber I. Langerhans cells require signals from both tumour necrosis factor-alpha and interleukin-1 beta for migration. Immunology 1997;92:388-395.

[116] Banno T, Gazel A, Blumenberg M. Effects of tumor necrosis factor-alpha (TNF alpha) in epidermal keratinocytes revealed using global transcriptional profiling. J Biol Chem 2004;279:32633-32642.

[117] Lokuta MA, Huttenlocher A. TNF-alpha promotes a stop signal that inhibits neutrophil polarization and migration via a p38 MAPK pathway. J Leukoc Biol 2005;78:210-219.

[118] Koukouritaki SB, Vardaki EA, Papakonstanti EA, Lianos E, Stournaras C, Emmanouel DS. TNF-alpha induces actin cytoskeleton reorganization in glomerular epithelial cells involving tyrosine phosphorylation of paxillin and focal adhesion kinase. Mol Med 1999;5:382-392.

[119] Petrache I, Crow MT, Neuss M, Garcia JG. Central involvement of Rho family GTPases in TNF-alpha-mediated bovine pulmonary endothelial cell apoptosis. Biochem Biophys Res Commun 2003;306:244-249.

[120] Papakonstanti EA, Stournaras C. Tumor necrosis factor-alpha promotes survival of opossum kidney cells via Cdc42-induced phospholipase C-gamma1 activation and actin filament redistribution. Mol Biol Cell 2004;15:1273-1286.

[121] Koss M, Pfeiffer GR, 2nd, Wang Y, Thomas ST, Yerukhimovich M, Gaarde WA*, et al.* Ezrin/radixin/moesin proteins are phosphorylated by TNF-alpha and modulate permeability increases in human pulmonary microvascular endothelial cells. J Immunol 2006;176:1218-1227.

[122] Haubert D, Gharib N, Rivero F, Wiegmann K, Hosel M*, et al.* PtdIns(4,5)P-restricted plasma membrane localization of FAN is involved in TNF-induced actin reorganization. EMBO J 2007;26:3308-3321.

[123] Harris ED, Jr. Rheumatoid arthritis. Pathophysiology and implications for therapy. N Engl J Med 1990;322:1277-1289.

[124] Emery P, Salmon M. Early rheumatoid arthritis: time to aim for remission? Ann Rheum Dis 1995;54:944-947.

[125] Pincus T, Callahan LF, Sale WG, Brooks AL, Payne LE, Vaughn WK. Severe functional declines, work disability, and increased mortality in seventy-five rheumatoid arthritis patients studied over nine years. Arthritis Rheum 1984;27:864-872.

[126] Wolfe F. The natural history of rheumatoid arthritis. J Rheumatol Suppl 1996;44:13-22.

[127] Wolfe F, Mitchell DM, Sibley JT, Fries JF, Bloch DA, Williams CA*, et al.* The mortality of rheumatoid arthritis. Arthritis Rheum 1994;37:481-494.

[128] Fuchs HA, Kaye JJ, Callahan LF, Nance EP, Pincus T. Evidence of significant radiographic damage in rheumatoid arthritis within the first 2 years of disease. J Rheumatol 1989;16:585-591.

[129] van der Heijde DM, van Leeuwen MA, van Riel PL, van de Putte LB. Radiographic progression on radiographs of hands and feet during the first 3 years of rheumatoid arthritis measured according to Sharp's method (van der Heijde modification). J Rheumatol 1995;22:1792-1796.

[130] Cobb S, Anderson F, Bauer W. Length of life and cause of death in rheumatoid arthritis. N Engl J Med 1953;249:553-556.

[131] Koopman WJ, Gay S. Do nonimmunologically mediated pathways play a role in the pathogenesis of rheumatoid arthritis? Rheum Dis Clin North Am 1993;19:107-122.

[132] Panayi GS, Lanchbury JS, Kingsley GH. The importance of the T cell in initiating and maintaining the chronic synovitis of rheumatoid arthritis. Arthritis Rheum 1992;35:729-735.

[133] Feldmann M, Brennan FM, Maini RN. Role of cytokines in rheumatoid arthritis. Annu Rev Immunol 1996;14:397-440.

[134] Arnett FC, Edworthy SM, Bloch DA, McShane DJ, Fries JF, Cooper NS*, et al.* The American Rheumatism Association 1987 revised criteria for the classification of rheumatoid arthritis. Arthritis Rheum 1988;31:315-324.

[135] Calin A, Marks SH. The case against seronegative rheumatoid arthritis. Am J Med 1981;70:992-994.

[136] Sangha O. Epidemiology of rheumatic diseases. Rheumatology (Oxford) 2000;39 Suppl 2:3-12.

[137] Aho K, Heliovaara M, Maatela J, Tuomi T, Palosuo T. Rheumatoid factors antedating clinical rheumatoid arthritis. J Rheumatol 1991;18:1282-1284.

[138] Nielen MM, van Schaardenburg D, Reesink HW, van de Stadt RJ, van der Horst-Bruinsma IE, de Koning MH*, et al.* Specific autoantibodies precede the symptoms of rheumatoid arthritis: a study of serial measurements in blood donors. Arthritis Rheum 2004;50:380-386.

[139] Nielen MM, van Schaardenburg D, Reesink HW, Twisk JW, van de Stadt RJ, van der Horst-Bruinsma IE*, et al.* Increased levels of C-reactive protein in serum from blood donors before the onset of rheumatoid arthritis. Arthritis Rheum 2004;50:2423-2427.

[140] Padyukov L, Silva C, Stolt P, Alfredsson L, Klareskog L. A gene-environment interaction between smoking and shared epitope genes in HLA-DR provides a high risk of seropositive rheumatoid arthritis. Arthritis Rheum 2004;50:3085-3092.

[141] Stolt P, Bengtsson C, Nordmark B, Lindblad S, Lundberg I, Klareskog L*, et al.* Quantification of the influence of cigarette smoking on rheumatoid arthritis: results from a population based case-control study, using incident cases. Ann Rheum Dis 2003;62:835-841.

[142] Ostendorf B, Peters R, Dann P, Becker A, Scherer A, Wedekind F*, et al.* Magnetic resonance imaging and miniarthroscopy of metacarpophalangeal joints: sensitive detection of morphologic changes in rheumatoid arthritis. Arthritis Rheum 2001;44:2492-2502.

[143] Goupille P, Roulot B, Akoka S, Avimadje AM, Garaud P, Naccache L*, et al.* Magnetic resonance imaging: a valuable method for the detection of synovial inflammation in rheumatoid arthritis. J Rheumatol 2001;28:35-40.

[144] Karim Z, Wakefield RJ, Quinn M, Conaghan PG, Brown AK, Veale DJ*, et al.* Validation and reproducibility of ultrasonography in the detection of synovitis in the knee: a comparison with arthroscopy and clinical examination. Arthritis Rheum 2004;50:387-394.

[145] Devlin J, Gough A, Huissoon A, Perkins P, Holder R, Reece R*, et al.* The acute phase and function in early rheumatoid arthritis. C-reactive protein levels correlate with functional outcome. J Rheumatol 1997;24:9-13.

[146] Deodhar AA, Brabyn J, Jones PW, Davis MJ, Woolf AD. Longitudinal study of hand bone densitometry in rheumatoid arthritis. Arthritis Rheum 1995;38:1204-1210.

[147] Gough AK, Lilley J, Eyre S, Holder RL, Emery P. Generalised bone loss in patients with early rheumatoid arthritis. Lancet 1994;344:23-27.

[148] Hannonen P, Mottonen T, Hakola M, Oka M. Sulfasalazine in early rheumatoid arthritis. A 48-week double-blind, prospective, placebo-controlled study. Arthritis Rheum 1993;36:1501-1509.

[149] van der Horst-Bruinsma IE, Speyer I, Visser H, Breedveld FC, Hazes JM. Diagnosis and course of early-onset arthritis: results of a special early arthritis clinic compared to routine patient care. Br J Rheumatol 1998;37:1084-1088.

[150] McGonagle D, Conaghan PG, O'Connor P, Gibbon W, Green M, Wakefield R*, et al.* The relationship between synovitis and bone changes in early untreated rheumatoid arthritis: a controlled magnetic resonance imaging study. Arthritis Rheum 1999;42:1706-1711.

[151] Munro R, Hampson R, McEntegart A, Thomson EA, Madhok R, Capell H. Improved functional outcome in patients with early rheumatoid arthritis treated with intramuscular gold: results of a five year prospective study. Ann Rheum Dis 1998;57:88-93.

[152] Anderson JJ, Wells G, Verhoeven AC, Felson DT. Factors predicting response to treatment in rheumatoid arthritis: the importance of disease duration. Arthritis Rheum 2000;43:22-29.

[153] Symmons DP, Jones MA, Scott DL, Prior P. Longterm mortality outcome in patients with rheumatoid arthritis: early presenters continue to do well. J Rheumatol 1998;25:1072-1077.

[154] Quinn MA, Emery P. Window of opportunity in early rheumatoid arthritis: possibility of altering the disease process with early intervention. Clin Exp Rheumatol 2003;21:S154-157.

[155] Keystone EC, Kavanaugh AF, Sharp JT, Tannenbaum H, Hua Y, Teoh LS*, et al.* Radiographic, clinical, and functional outcomes of treatment with adalimumab (a human anti-tumor necrosis factor monoclonal antibody) in patients with active rheumatoid arthritis receiving concomitant methotrexate therapy: a randomized, placebo-controlled, 52-week trial. Arthritis Rheum 2004;50:1400-1411.

[156] Klareskog L, van der Heijde D, de Jager JP, Gough A, Kalden J, Malaise M*, et al.* Therapeutic effect of the combination of etanercept and methotrexate compared with each treatment alone in patients with rheumatoid arthritis: double-blind randomised controlled trial. Lancet 2004;363:675-681.

[157] Lipsky PE, van der Heijde DM, St Clair EW, Furst DE, Breedveld FC, Kalden JR*, et al.* Infliximab and methotrexate in the treatment of rheumatoid arthritis. Anti-Tumor Necrosis Factor Trial in Rheumatoid Arthritis with Concomitant Therapy Study Group. N Engl J Med 2000;343:1594-1602.

[158] Feldmann M, Maini RN. The role of cytokines in the pathogenesis of rheumatoid arthritis. Rheumatology (Oxford) 1999;38 Suppl 2:3-7.

[159] Brennan FM, Gibbons DL, Mitchell T, Cope AP, Maini RN, Feldmann M. Enhanced expression of tumor necrosis factor receptor mRNA and protein in mononuclear cells isolated from rheumatoid arthritis synovial joints. Eur J Immunol 1992;22:1907-1912.

[160] Chu CQ, Field M, Feldmann M, Maini RN. Localization of tumor necrosis factor alpha in synovial tissues and at the cartilage-pannus junction in patients with rheumatoid arthritis. Arthritis Rheum 1991;34:1125-1132.

[161] Brennan FM, Chantry D, Jackson A, Maini R, Feldmann M. Inhibitory effect of TNF alpha antibodies on synovial cell interleukin-1 production in rheumatoid arthritis. Lancet 1989;2:244-247.

[162] Keffer J, Probert L, Cazlaris H, Georgopoulos S, Kaslaris E, Kioussis D*, et al.* Transgenic mice expressing human tumour necrosis factor: a predictive genetic model of arthritis. EMBO J 1991;10:4025-4031.

[163] Williams RO, Feldmann M, Maini RN. Anti-tumor necrosis factor ameliorates joint disease in murine collagen-induced arthritis. Proc Natl Acad Sci U S A 1992;89:9784-9788.

[164] Feldman M, Taylor P, Paleolog E, Brennan FM, Maini RN. Anti-TNF alpha therapy is useful in rheumatoid arthritis and Crohn's disease: analysis of the mechanism of action predicts utility in other diseases. Transplant Proc 1998;30:4126-4127.

[165] Feldmann M, Brennan FM, Elliott MJ, Williams RO, Maini RN. TNF alpha is an effective therapeutic target for rheumatoid arthritis. Ann N Y Acad Sci 1995;766:272-278.

[166] Feldmann M, Brennan FM, Foxwell BM, Taylor PC, Williams RO, Maini RN. Anti-TNF therapy: where have we got to in 2005? J Autoimmun 2005;25 Suppl:26-28.

[167] Feldmann M, Charles P, Taylor P, Maini RN. Biological insights from clinical trials with anti-TNF therapy. Springer Semin Immunopathol 1998;20:211-228.

[168] Feldmann M, Maini RN. Anti-TNF alpha therapy of rheumatoid arthritis: what have we learned? Annu Rev Immunol 2001;19:163-196.

[169] Feldmann M, Maini RN. Discovery of TNF-alpha as a therapeutic target in rheumatoid arthritis: preclinical and clinical studies. Joint Bone Spine 2002;69:12-18.

[170] Taylor PC, Williams RO, Maini RN. Anti-TNF alpha therapy in rheumatoid arthritis--current and future directions. Curr Dir Autoimmun 2000;2:83-102.

[171] Landewe RB, Boers M, Verhoeven AC, Westhovens R, van de Laar MA, Markusse HM*, et al.* COBRA combination therapy in patients with early rheumatoid arthritis: long-term structural benefits of a brief intervention. Arthritis Rheum 2002;46:347-356.

[172] Egsmose C, Lund B, Borg G, Pettersson H, Berg E, Brodin U*, et al.* Patients with rheumatoid arthritis benefit from early 2nd line therapy: 5 year followup of a prospective double blind placebo controlled study. J Rheumatol 1995;22:2208-2213.

[173] Lard LR, Visser H, Speyer I, vander Horst-Bruinsma IE, Zwinderman AH, Breedveld FC*, et al.* Early versus delayed treatment in patients with recent-onset rheumatoid arthritis: comparison of two cohorts who received different treatment strategies. Am J Med 2001;111:446-451.

[174] Case JP. Old and new drugs used in rheumatoid arthritis: a historical perspective. Part 2: the newer drugs and drug strategies. Am J Ther 2001;8:163-179.

[175] Cush JJ. Safety overview of new disease-modifying antirheumatic drugs. Rheum Dis Clin North Am 2004;30:237-255, v.

[176] Ellis HM, Horvitz HR. Genetic control of programmed cell death in the nematode C. elegans. Cell 1986;44:817-829.

[177] Vaux DL, Cory S, Adams JM. Bcl-2 gene promotes haemopoietic cell survival and cooperates with c-myc to immortalize pre-B cells. Nature 1988;335:440-442.

[178] McDonnell TJ, Korsmeyer SJ. Progression from lymphoid hyperplasia to high-grade malignant lymphoma in mice transgenic for the t(14; 18). Nature 1991;349:254-256.

[179] Strasser A, Harris AW, Bath ML, Cory S. Novel primitive lymphoid tumours induced in transgenic mice by cooperation between myc and bcl-2. Nature 1990;348:331-333.

[180] Strasser A, Whittingham S, Vaux DL, Bath ML, Adams JM, Cory S*, et al.* Enforced BCL2 expression in B-lymphoid cells prolongs antibody responses and elicits autoimmune disease. Proc Natl Acad Sci U S A 1991;88:8661-8665.

[181] Watanabe-Fukunaga R, Brannan CI, Copeland NG, Jenkins NA, Nagata S. Lymphoproliferation disorder in mice explained by defects in Fas antigen that mediates apoptosis. Nature 1992;356:314-317.

[182] Barr PJ, Tomei LD. Apoptosis and its role in human disease. Biotechnology (N Y) 1994;12:487-493.

[183] Thompson CB. Apoptosis in the pathogenesis and treatment of disease. Science 1995;267:1456-1462.

[184] Natoli G, Costanzo A, Guido F, Moretti F, Levrero M. Apoptotic, non-apoptotic, and anti-apoptotic pathways of tumor necrosis factor signalling. Biochem Pharmacol 1998;56:915-920.

[185] Barnes PJ, Karin M. Nuclear factor-kappaB: a pivotal transcription factor in chronic inflammatory diseases. N Engl J Med 1997;336:1066-1071.

[186] Baud V, Karin M. Signal transduction by tumor necrosis factor and its relatives. Trends Cell Biol 2001;11:372-377.

[187] Bergmann MW, Loser P, Dietz R, von Harsdorf R. Effect of NF-kappa B Inhibition on TNF-alpha-induced apoptosis and downstream pathways in cardiomyocytes. J Mol Cell Cardiol 2001;33:1223-1232.

[188] Chang HY, Yang X. Proteases for cell suicide: functions and regulation of caspases. Microbiol Mol Biol Rev 2000;64:821-846.

[189] Idriss HT, Naismith JH. TNF alpha and the TNF receptor superfamily: structure-function relationship(s). Microsc Res Tech 2000;50:184-195.

[190] Vancurova I, Miskolci V, Davidson D. NF-kappa B activation in tumor necrosis factor alpha-stimulated neutrophils is mediated by protein kinase Cdelta. Correlation to nuclear Ikappa Balpha. J Biol Chem 2001;276:19746-19752.

[191] Madge LA, Pober JS. A phosphatidylinositol 3-kinase/Akt pathway, activated by tumor necrosis factor or interleukin-1, inhibits apoptosis but does not activate NFkappaB in human endothelial cells. J Biol Chem 2000;275:15458-15465.

[192] Pastorino JG, Tafani M, Farber JL. Tumor necrosis factor induces phosphorylation and translocation of BAD through a phosphatidylinositide-3-OH kinase-dependent pathway. J Biol Chem 1999;274:19411-19416.

[193] Ashkenazi A, Dixit VM. Death receptors: signaling and modulation. Science 1998;281:1305-1308.

[194] Nagata S. Apoptosis by death factor. Cell 1997;88:355-365.

[195] Wallach D, Kovalenko AV, Varfolomeev EE, Boldin MP. Death-inducing functions of ligands of the tumor necrosis factor family: a Sanhedrin verdict. Curr Opin Immunol 1998;10:279-288.

[196] Boldin MP, Varfolomeev EE, Pancer Z, Mett IL, Camonis JH, Wallach D. A novel protein that interacts with the death domain of Fas/APO1 contains a sequence motif related to the death domain. J Biol Chem 1995;270:7795-7798.

[197] Chinnaiyan AM, O'Rourke K, Tewari M, Dixit VM. FADD, a novel death domain-containing protein, interacts with the death domain of Fas and initiates apoptosis. Cell 1995;81:505-512.

[198] Medema JP, Scaffidi C, Kischkel FC, Shevchenko A, Mann M, Krammer PH*, et al.* FLICE is activated by association with the CD95 death-inducing signaling complex (DISC). EMBO J 1997;16:2794-2804.

[199] Nicholson DW, Thornberry NA. Caspases: killer proteases. Trends Biochem Sci 1997;22:299-306.

[200] Thornberry NA, Lazebnik Y. Caspases: enemies within. Science 1998;281:1312-1316.

[201] Rudel T, Bokoch GM. Membrane and morphological changes in apoptotic cells regulated by caspase-mediated activation of PAK2. Science 1997;276:1571-1574.

[202] Zhang HG, Hyde K, Page GP, Brand JP, Zhou J, Yu S*, et al.* Novel tumor necrosis factor alpha-regulated genes in rheumatoid arthritis. Arthritis Rheum 2004;50:420-431.

[203] Gallagher J, Howlin J, McCarthy C, Murphy EP, Bresnihan B, FitzGerald O*, et al.* Identification of Naf1/ABIN-1 among TNF-alpha-induced expressed genes in human synoviocytes using oligonucleotide microarrays. FEBS Lett 2003;551:8-12.

[204] Zhou A, Scoggin S, Gaynor RB, Williams NS. Identification of NF-kappa B-regulated genes induced by TNFalpha utilizing expression profiling and RNA interference. Oncogene 2003;22:2054-2064.

[205] Bandman O, Coleman RT, Loring JF, Seilhamer JJ, Cocks BG. Complexity of inflammatory responses in endothelial cells and vascular smooth muscle cells determined by microarray analysis. Ann N Y Acad Sci 2002;975:77-90.

[206] Tang Z, McGowan BS, Huber SA, McTiernan CF, Addya S, Surrey S*, et al.* Gene expression profiling during the transition to failure in TNF-alpha over-expressing mice demonstrates the development of autoimmune myocarditis. J Mol Cell Cardiol 2004;36:515-530.

[207] Zhao B, Stavchansky SA, Bowden RA, Bowman PD. Effect of interleukin-1beta and tumor necrosis factor-alpha on gene expression in human endothelial cells. Am J Physiol Cell Physiol 2003;284:C1577-1583.

[208] Aderem AA, Albert KA, Keum MM, Wang JK, Greengard P, Cohn ZA. Stimulus-dependent myristoylation of a major substrate for protein kinase C. Nature 1988;332:362-364.

[209] Albert KA, Nairn AC, Greengard P. The 87-kDa protein, a major specific substrate for protein kinase C: purification from bovine brain and characterization. Proc Natl Acad Sci U S A 1987;84:7046-7050.

[210] Tapp H, Al-Naggar IM, Yarmola EG, Harrison A, Shaw G, Edison AS*, et al.* MARCKS is a natively unfolded protein with an inaccessible actin-binding site: evidence for long-range intramolecular interactions. J Biol Chem 2005;280:9946-9956.

[211] Graceffa P, Jancso A, Mabuchi K. Modification of acidic residues normalizes sodium dodecyl sulfate-polyacrylamide gel electrophoresis of caldesmon and other proteins that migrate anomalously. Arch Biochem Biophys 1992;297:46-51.

[212] Timkovich R. Detection of the stable addition of carbodiimide to proteins. Anal Biochem 1977;79:135-143.

[213] Staros JV, Wright RW, Swingle DM. Enhancement by N-hydroxysulfosuccinimide of water-soluble carbodiimide-mediated coupling reactions. Anal Biochem 1986;156:220-222.

[214] Grabarek Z, Gergely J. Zero-length crosslinking procedure with the use of active esters. Anal Biochem 1990;185:131-135.

[215] Hillenkamp F, Karas M, Beavis RC, Chait BT. Matrix-assisted laser desorption/ionization mass spectrometry of biopolymers. Anal Chem 1991;63:1193A-1203A.

[216] Steiner V, Bornsen KO, Schar M, Gassmann E, Hoffstetter-Kuhn S, Rink H*, et al.* Analysis of synthetic peptides using matrix-assisted laser desorption ionization mass spectrometry. Pept Res 1992;5:25-29.

[217] Steiner V, Knecht R, Bornsen KO, Gassmann E, Stone SR, Raschdorf F*, et al.* Primary structure and function of novel O-glycosylated hirudins from the leech Hirudinaria manillensis. Biochemistry 1992;31:2294-2298.

[218] Fenn JB, Mann M, Meng CK, Wong SF, Whitehouse CM. Electrospray ionization for mass spectrometry of large biomolecules. Science 1989;246:64-71.

[219] Loo JA, Udseth HR, Smith RD. Peptide and protein analysis by electrospray ionization-mass spectrometry and capillary electrophoresis-mass spectrometry. Anal Biochem 1989;179:404-412.

[220] Shumate CB, Hill HH, Jr. Coronaspray nebulization and ionization of liquid samples for ion mobility spectrometry. Anal Chem 1989;61:601-606.

[221] Siu KW, Gardner GJ, Berman SS. Atmospheric pressure chemical ionization and electrospray mass spectrometry of some organoarsenic species. Rapid Commun Mass Spectrom 1988;2:69-71.

[222] Royer CA. Approaches to teaching fluorescence spectroscopy. Biophys J 1995;68:1191-1195.

[223] Royer CA. Fluorescence spectroscopy. Methods Mol Biol 1995;40:65-89.

[224] Yarmola EG, Parikh S, Bubb MR. Formation and implications of a ternary complex of profilin, thymosin beta 4, and actin. J Biol Chem 2001;276:45555-45563.

[225] Yarmola EG, Somasundaram T, Boring TA, Spector I, Bubb MR. Actin-latrunculin A structure and function. Differential modulation of actin-binding protein function by latrunculin A. J Biol Chem 2000;275:28120-28127.

[226] Hedrick JL, Smith AJ. Size and charge isomer separation and estimation of molecular weights of proteins by disc gel electrophoresis. Arch Biochem Biophys 1968;126:155-164.

[227] Ingram L, Tombs MP, Hurst A. Mobility-molecular weight relationships of small proteins and peptides in acrylamide-gel electrophoresis. Anal Biochem 1967;20:24-29.

[228] Raymond S, Nakamichi M. Electrophoresis in Synthetic Gels. Ii. Effect of Gel Concentration. Anal Biochem 1964;7:225-232.

[229] Tombs MP. An Electrophoretic Investigation of Groundnut Proteins: The Structure of Arachins a and B. Biochem J 1965;96:119-133.

[230] Schagger H, von Jagow G. Tricine-sodium dodecyl sulfate-polyacrylamide gel electrophoresis for the separation of proteins in the range from 1 to 100 kDa. Anal Biochem 1987;166:368-379.

[231] Kothakota S, Azuma T, Reinhard C, Klippel A, Tang J, Chu K*, et al.* Caspase-3-generated fragment of gelsolin: effector of morphological change in apoptosis. Science 1997;278:294-298.

[232] Coleman ML, Olson MF. Rho GTPase signalling pathways in the morphological changes associated with apoptosis. Cell Death Differ 2002;9:493-504.

[233] Bando M, Miyake Y, Shiina M, Wachi M, Nagai K, Kataoka T. Actin cytoskeleton is required for early apoptosis signaling induced by anti-Fas antibody but not Fas ligand in murine B lymphoma A20 cells. Biochem Biophys Res Commun 2002;290:268-274.

[234] Higuchi M, Aggarwal BB. TNF induces internalization of the p60 receptor and shedding of the p80 receptor. J Immunol 1994;152:3550-3558.

[235] Tsujimoto M, Yip YK, Vilcek J. Tumor necrosis factor: specific binding and internalization in sensitive and resistant cells. Proc Natl Acad Sci U S A 1985;82:7626-7630.

[236] Hyrich KL. Patients with suspected rheumatoid arthritis should be referred early to rheumatology. BMJ 2008;336:215-216.

[237] Cush JJ. Early rheumatoid arthritis -- is there a window of opportunity? J Rheumatol Suppl 2007;80:1-7.

[238] Ackermann C, Kavanaugh A. Tumor necrosis factor as a therapeutic target of rheumatologic disease. Expert Opin Ther Targets 2007;11:1369-1384.

[239] Bingham CO, 3rd, Miner MM. Treatment, management, and monitoring of established rheumatoid arthritis. J Fam Pract 2007;56:S1-7; quiz S8.

[240] Majithia V, Geraci SA. Rheumatoid arthritis: diagnosis and management. Am J Med 2007;120:936-939.

[241] Aderem A. Signal transduction and the actin cytoskeleton: the roles of MARCKS and profilin. Trends Biochem Sci 1992;17:438-443.

[242] Vasilopoulos Y, Gkretsi V, Armaka M, Aidinis V, Kollias G. Actin cytoskeleton dynamics linked to synovial fibroblast activation as a novel pathogenic principle in TNF-driven arthritis. Ann Rheum Dis 2007;66 Suppl 3:iii23-28.

[243] Metsios GS, Stavropoulos-Kalinoglou A, Veldhuijzen van Zanten JJ, Treharne GJ, Panoulas VF, Douglas KM*, et al.* Rheumatoid arthritis, cardiovascular disease and physical exercise: a systematic review. Rheumatology (Oxford) 2008;47:239-248.

[244] Engvall E, Jonsson K, Perlmann P. Enzyme-linked immunosorbent assay. II. Quantitative assay of protein antigen, immunoglobulin G, by means of enzyme-labelled antigen and antibody-coated tubes. Biochim Biophys Acta 1971;251:427-434.

[245] Engvall E, Perlman P. Enzyme-linked immunosorbent assay (ELISA). Quantitative assay of immunoglobulin G. Immunochemistry 1971;8:871-874.

[246] Palomaki P. Simultaneous use of poly- and monoclonal antibodies as enzyme tracers in a one-step enzyme immunoassay for the detection of hepatitis B surface antigen. J Immunol Methods 1991;145:55-63.

[247] Pope RM. Apoptosis as a therapeutic tool in rheumatoid arthritis. Nat Rev Immunol 2002;2:527-535.

[248] Firestein GS, Yeo M, Zvaifler NJ. Apoptosis in rheumatoid arthritis synovium. J Clin Invest 1995;96:1631-1638.

[249] Fraser A, Fearon U, Reece R, Emery P, Veale DJ. Matrix metalloproteinase 9, apoptosis, and vascular morphology in early arthritis. Arthritis Rheum 2001;44:2024-2028.

[250] Matsumoto S, Muller-Ladner U, Gay RE, Nishioka K, Gay S. Ultrastructural demonstration of apoptosis, Fas and Bcl-2 expression of rheumatoid synovial fibroblasts. J Rheumatol 1996;23:1345-1352.

[251] Nakajima T, Aono H, Hasunuma T, Yamamoto K, Shirai T, Hirohata K*, et al.* Apoptosis and functional Fas antigen in rheumatoid arthritis synoviocytes. Arthritis Rheum 1995;38:485-491.

[252] Sugiyama M, Tsukazaki T, Yonekura A, Matsuzaki S, Yamashita S, Iwasaki K. Localisation of apoptosis and expression of apoptosis related proteins in the synovium of patients with rheumatoid arthritis. Ann Rheum Dis 1996;55:442-449.

[253] Baier A, Meineckel I, Gay S, Pap T. Apoptosis in rheumatoid arthritis. Curr Opin Rheumatol 2003;15:274-279.

[254] Pap T, Cinski A, Baier A, Gay S, Meinecke I. Modulation of pathways regulating both the invasiveness and apoptosis in rheumatoid arthritis synovial fibroblasts. Joint Bone Spine 2003;70:477-479.

BIOGRAPHICAL SKETCH

Iman M. A. Al-Naggar was born on March 31st, 1981 to an Egyptian family living in Kuwait. She was Ashraf Al-Naggar's and Wafaa Badawy's first-born child, and eventually became the eldest of five. Iman started school at the age of three when she joined L'école Française, a French pre-K in Kuwait. Iman stayed in a French education system until the Ninth grade, when she received a French Brevet des collèges. She then joined the American School of Kuwait, where she stayed until graduation in June of 1998 with a High School Diploma. Iman had always known she loved Biology most, and two teachers in particular are to thank for it: Monsieur Jean Rocques in 6th grade and Miss Lisa Myhre in high school. In high school, Iman was an alto on the Honor Choir and performed solos in many school concerts. After graduating high school, Iman joined the Faculty of Science at Kuwait University where she majored in Molecular Biology and minored in Biochemistry. As an undergraduate student at Kuwait University, Iman joined the lab of Dr. Esmaeil Al-Saleh, where she did research on oil-degrading bacteria and really enjoyed the experience. She graduated in June of 2002 with honors. At Kuwait University, Iman also met her husband, Mr. Ahmad M. Mahmoud, and they married in January of 2002. In August 2002, they moved together to Gainesville, Florida where they both joined graduate programs at the University of Florida (She, the Interdisciplinary Program in Biomedical Sciences at the College of Medicine, He, the Department of Mechanical and Aerospace Engineering at the College of Engineering) and became avid Gator fans.

Iman has always loved Science, Biology in particular. Iman has always said that if she could go back in time and take only one thing with her from the future, it would be her Biology 101 book. She would just repeat all the brilliant experiments described and so be the discoverer of great things; more specifically, Iman would want to be the discoverer of Penicillin, which she believes to have been an extremely useful discovery. In fact, if Iman had to choose one person to

be, she would be Louis Pasteur! Iman carries her experiments each and every day in the lab with his famous quote "Chance favors the prepared mind" in mind.

During her years in graduate school, Iman made many friends and met special people. A few months before graduation, Iman and her husband were blessed with a beautiful baby girl, whom they named Salma Ahmad Mahmoud. Salma was born on September 12, 2007 at Shands Hospital at the University of Florida.